Localization and Coverage in Wireless Ad Hoc Networks

by

Jeremy Gribben

Thesis submitted to the

Faculty of Graduate and Postdoctoral Studies

In partial fulfillment of the requirements

For the MCS degree in

Computer Science

School of Information Technology and Engineering

Faculty of Engineering

University of Ottawa

Abstract

Localization and coverage are two important and closely related problems in wireless ad hoc networks. Localization aims to determine the physical locations of devices in a network, while coverage determines if a region of interest is sufficiently monitored by devices. Localization systems require a high degree of coverage for correct functioning, while coverage schemes typically require accurate location information. This thesis investigates the relationship between localization and coverage such that new schemes can be devised which integrate approaches found in each of these well studied problems. This work begins with a thorough review of the current literature on the subjects of localization and coverage. The localization scheduling problem is then introduced with the goal to allow as many devices as possible to enter deep sleep states to conserve energy and reduce message overhead, while maintaining sufficient network coverage for high localization accuracy. Initially this sufficient coverage level for localization is simply a minimum connectivity condition. An analytical method is then proposed to estimate the amount of localization error within a certain probability based on the theoretical lower bounds of location estimation. Error estimates can then be integrated into location dependent schemes to improve on their robustness to localization error. Location error estimation is then used by an improved scheduling scheme to determine the minimum number of reference devices required for accurate localization. Finally, an optimal coverage preserving sleep scheduling scheme is proposed which is robust to localization error, a condition which is ignored by most existing solutions. Simulation results show that with localization scheduling network lifetimes can be increased by several times and message overhead is reduced while maintaining negligible differences in localization error. Furthermore, results show that the proposed coverage preserving sleep scheduling scheme results in fewer active devices and coverage holes under the presence of localization error.

Acknowledgements

I would like to thank my research supervisor, Dr. Azzedine Boukerche, for his guidance and creative insights while working on this thesis project. I would also like to acknowledge my colleagues at the PARADISE Research Laboratory for their positive feedback and constructive criticisms of this work. Finally, I cannot fully express my gratitude towards my parents, Jim and Heather, for their ongoing encouragement and support throughout my studies.

Contents

List of Tables

List of Figures

Chapter 1

Introduction

Wireless ad hoc networks are becoming increasingly important with growing uses which include wireless sensor networks (WSN), personal area networks (PAN) and vehicular ad hoc networks (VANets), in which a centralized infrastructure is not desirable. This work investigates for the first time the localization and coverage problems in wireless ad hoc networks in a unified way, such that novel solutions to each of these problems can be obtained which would not have been previously possible by considering them independently.

1.1 Objectives

Localization systems aim to determine the physical locations (coordinates) of all nodes in a network, where the locations of wireless devices can be estimated when sufficient range (or angle) measurements between them are available. Coverage protocols on the other hand aim to determine if all points in a region of interest are monitored or within range of a sufficient number of wireless devices.

It is clear that localization and coverage very closely related problems in wireless ad

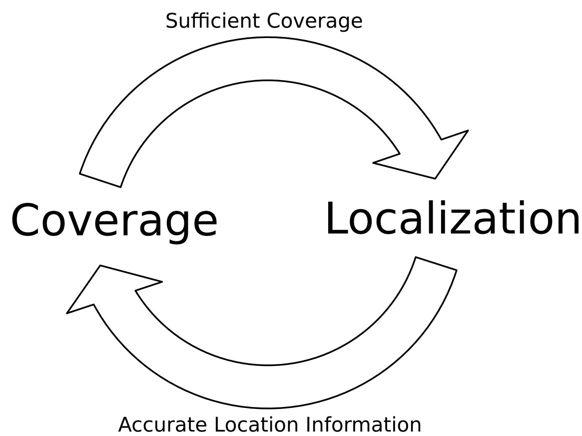

Figure 1.1: Relationship between localization and coverage. Localization requires a high degree of coverage for accurate results, while coverage relies on having accurate location information available.

hoc and sensor networks. Due to measurement noise in ranging information used by localization schemes, redundant range measurements are required in order to reduce error and allow for sufficiently accurate location estimation. In other words, localization systems require a high degree of *coverage* to satisfy accurate results. Conversely, protocols which calculate the coverage of a region evaluate the overlapping areas of coverage of individual devices in that region. To do this successfully however, accurate knowledge of the *locations* of devices must be derived *a priori*. This cyclic relationship between localization and coverage, demonstrated by Figure 1.1, is the principal problem under investigation in this thesis. The aim of this this is to answer questions about the relationship between localization and coverage, and whether approaches used in solving one of these two problems can be applied to the other in novel ways in order to improve on localization and coverage in wireless ad hoc networks. Specifically, this thesis aims to answer the questions of how can coverage be used to improve on localization systems, and how can localization be used to improve on the calculation of coverage?

1.1.1 Improving Localization with Coverage

To answer the first question of how to improve localization with coverage, we observe a limitation with current localization systems which is that although localization schemes benefit from having as many redundant measurements as possible to reduce error, these additional measurements increase the communication overhead and energy usage of wireless devices. To balance these two conflicting requirements of maintaining high localization accuracy while minimizing communication and energy usage, the idea of coverage preserving sleep scheduling is used, which aims to minimize the number of active devices to conserve energy while maintaining a minimimum quality of service (QoS) in the network. The first contribution of this thesis is therefore a way of measuring the QoS of localization in a network given a group of reference devices which enable unlocalized devices to learn their positions [48]. The second contribution of this thesis is then a sleep scheduling scheme, which schedules as many devices in a network as possible into a deep sleep mode to reduce communication and energy usage, while maintaining a sufficiently high localization QoS for new and mobile devices in a network which need to compute their positions [49, 50].

1.1.2 Improving Coverage with Localization

To answer the second question of how to improve coverage using properties of localization systems, we observe that current approaches to computing the coverage of sensors in a wireless sensor network make the impractical assumption that all sensors have exact location information. However, when error is present in the positions of sensors associated errors appear with the coverage calculation resulting in additional energy usage due to more sensors than are required to cover an area, or coverage holes due to not enough deployed sensors. To alleviate such problems, the third contribution of this thesis is a coverage preserving sleep scheduling scheme which is robust to localization error [47]. This is accomplished by estimating the amount of localization error from the localization system [48], then correcting for this error while computing the coverage of devices.

1.2 Organization of Thesis

The remainder of this thesis will be organized as follows. In Chapter 2, preliminary details are described which give a foundation for the remainder of the thesis. Here the system model and the localization problem will be formally described. In Chapter 3, work related to this thesis will be outlined, which cover areas which include localization systems, localization analysis techniques, and coverage. In Chapter 4 an initial scheme which solves the localization scheduling problem is introduced, which maintains minimum connectivity for sufficiently accurate localization while scheduling overly redundant nodes to sleep. In Chapter 5 a method to estimate the amount of location error within a certain probability is proposed which can give a measure of the overall quality of localization. In Chapter 6 an improved localization scheduling scheme is proposed which uses a more analytical reference node selection mechanism based on the location error estimation method from Chapter 5. In Chapter 7 the inverse problem is investigated; that is, an optimal coverage preserving sleep scheduling scheme is introduced which is robust to localization error by using the location error estimation method from Chapter 5. Finally, this work is concluded in Chapter 8, along with insights into future research directions.

Chapter 2

Preliminaries

In this chapter, the system model of the networks which will be studied in this thesis is presented, along with notations which will be used throughout the rest of this work. The system model follows from years of well established experimental and theoretical research in wireless networks [123, 116] and on estimation theory [77]. In addition, similar notations in this work are found throughout the literature in the area of localization systems [13, 14, 38, 116].

2.1 System Model

In this work, a wireless network is considered which is composed of n randomly deployed nodes in set $\mathcal{N}$, consisting of *unknown* nodes in $\mathcal{U} \subset \mathcal{N}$ which do not know their positions, *settled* nodes in $\mathcal{S} \subset \mathcal{N}$ which were originally in $\mathcal{U}$ but discovered their positions using a localization system, and *beacon* nodes in $\mathcal{B} \subset \mathcal{N}$ which know their positions *a priori*. All devices have a communication range of r units, and are distributed in a two-dimensional squared sensor field $Q = [0, s] \times [0, s]$.

Each node $i \in \mathcal{N}$ has Cartesian coordinates $\mathbf{z}_i = (x_i, y_i) \in \mathbf{R}^2$, which represents the location of the node i in Q. For simplicity, only two dimensions are considered in this work, but the methods here explained can be easily extended to three dimensions.

The true distance between two nodes i and j is $d_{i,j} = \|\mathbf{z}_i - \mathbf{z}_j\| = \sqrt{(x_i - x_j)^2 + (y_i - y_j)^2}$. The neighbours of node i are denoted by $N(i) = \{j \in \mathcal{N} | d_{i,j} \leq r\}$, which are the nodes within communication range of i. For simplicity, symmetric communication links are considered, i.e. if $j \in N(i)$, then $i \in N(j)$.

Nodes are equipped with radio frequency (RF) transceivers for communication. Using the RSS or TOA of radio signals, i can estimate the distance to any $j \in N(i)$, denoted $\tilde{d}_{i,j}$. Accuracy of distance estimates are limited, as RSS and TOA measurements are highly prone to error.

When RSS is used log-normal shadowing describes the relationship between received signal strength and distances, where distance measurements are a function of the received power at $\mathbf{z}_i$ transmitted by j, $P_{i,j}$. $P_{i,j}$ is Gaussian with mean power $\bar{P}_{i,j}$ and variance σ_{dB}^2 in decibel milliwatts, given by

$$P_{i,j} \sim \mathcal{N}(\bar{P}_{i,j}, \sigma_{dB}^2), \tag{2.1}$$

$$\bar{P}_{i,j} = P_0 - 10 n_p log_{10}(d_{i,j}/d_0)$$

where P_0 is the received power at distance d_0 as calculated by the free-space path loss formula, n_p is the path loss exponent and σ_{dB} is the standard deviation of the shadowing, which are measured from the environment. The estimated distance between nodes i and j is then given by

$$\tilde{d}_{i,j} = d_0 \left(P_0/P_{i,j}\right)^{\frac{1}{n_p}} \tag{2.2}$$

In the TOA case, the measured time of arrival between i and j is assumed to be

Gaussian distributed with mean time $d_{i,j}/c$ and variance σ_T^2,

$$T_{i,j} \sim \mathcal{N}(d_{i,j}/c, \sigma_T^2), \tag{2.3}$$

where c is the speed of light and σ_T^2 is measured from the environment and is independent of $d_{i,j}$. The estimated distance between i and j is therefore $\tilde{d}_{i,j} = c \cdot T_{i,j}$. This ranging model is described in detail and verified experimentally in [116].

The selection of the environmental parameters used in the simulations for this thesis are those which were measured experimentally in [116] to match the model in equations (2.1) and (2.3). These are $n_p = 2.30$, $\sigma_{dB} = 3.92$ dB, and $d_0 = 1$ m for RSS measurements, and $\sigma_T = 6.1$ ns for TOA measurements.

2.2 Localization

With three or more distance measurements to nodes $j \in \mathcal{S} \cup \mathcal{B}$ with known positions, a node is able to estimate its own position, $\hat{\mathbf{z}}_i = (\hat{x}_i, \hat{y}_i)$. The CRLB places a lower bound on the variance of any unbiased estimator $\hat{\boldsymbol{\theta}}$ of a parameter $\boldsymbol{\theta}$ [77], and is given by inverse of the Fisher information matrix (FIM) $\mathbf{I}(\boldsymbol{\theta})$. That is, $\mathbf{C}(\hat{\boldsymbol{\theta}}) \geq \mathbf{I}^{-1}(\boldsymbol{\theta})$, where $\mathbf{C}(\hat{\boldsymbol{\theta}})$ is the covariance matrix of $\hat{\boldsymbol{\theta}}$. The ijth element of the FIM is given as

$$[\mathbf{I}(\boldsymbol{\theta})]_{ij} = -E\left[\frac{\partial^2 \ln\, p(\mathbf{x}; \boldsymbol{\theta})}{\partial\theta_i \partial\theta_j}\right] \tag{2.4}$$

where $p(\mathbf{x}; \boldsymbol{\theta})$ is the pdf of the measurement data, and $\mathbf{x}$ is a random measurement taken at the true value of $\boldsymbol{\theta}$. The CRLB was derived for position estimation in [116], where the parameter vector $\boldsymbol{\theta}$ is the set of node locations, $\mathbf{z}_i$, and $p(\mathbf{x}; \boldsymbol{\theta})$ is given by the statistical model of distance measurements for RSS or TOA using log-normal shadowing or Gaussian noise, respectively. The minimum variance of the estimated position of a node i, with reference nodes $\mathcal{R} \subseteq \{\mathcal{S} \cap N(i)\}$, is given by equations (2.5) and (3.5) for RSS and TOA, respectively [116],

$$\sigma^2_{i,RSS} = \left(\frac{10n_p}{\sigma_{dB}\log 10}\right)^{-2} \frac{\sum_{j\in\mathcal{R}} d_{i,j}^{-2}}{\sum_{j\in\mathcal{R}} \sum_{k\in\mathcal{R},k\neq j} \left(\frac{d_{i\perp j,k} d_{j,k}}{d_{i,j} d_{i,k}}\right)^2} \tag{2.5}$$

$$\sigma^2_{i,TOA} = c^2\sigma_T^2|\mathcal{R}| \left[\sum_{j\in\mathcal{R}} \sum_{k\in\mathcal{R},k\neq j} \left(\frac{d_{i\perp j,k} d_{j,k}}{d_{i,j} d_{i,k}}\right)^2\right]^{-1} \tag{2.6}$$

where $d_{i\perp j,k}$ is the shortest distance of node i to the line intersecting nodes j and k. For the remainder of this thesis the RSS and TOA subscripts will be dropped, and denote the CRLB simply by σ_i^2.

In practice, localization systems do not typically achieve the lower bounds in equations (2.5) and (3.5), and have error slightly higher. Trilateration based methods represent the position and distance of a beacon node j to node i with the circle equation $(\hat{x}_i - x_j) + (\hat{y}_i - y_j) = \tilde{d}_{i,j}$. When three or more distance and position measurements are available, these equations can be solved for $(\hat{x}_i, \hat{y}_i)$ using a least squares method. This linearization simplifies computation and gives a good position estimate, but information is lost in the process and so these estimators do not achieve minimum variance. The nonlinear maximum-likelihood estimators (MLE) in [116] give improved accuracy and are asymptotically optimal. The bias-reduced MLE used for RSS for a node i with reference nodes $\mathcal{R}$ is

$$\hat{\mathbf{z}}_i = \arg\min_{\{\mathbf{z_i}\}} \sum_{j\in\mathcal{R}} \left(\ln \frac{\tilde{d}_{i,j}/C^2}{d^2(\mathbf{z}_i, \mathbf{z}_j)}\right)^2, \tag{2.7}$$

$$C = \exp\left[\frac{1}{2}\left(\frac{\ln(10)}{10}\frac{\sigma_{dB}}{n_p}\right)^2\right]$$

while the MLE for the TOA case is

$$\hat{\mathbf{z}}_i = \arg\min_{\{\mathbf{z_i}\}} \sum_{j \in \mathcal{R}} \left(cT_{i,j} - d(\mathbf{z}_i, \mathbf{z}_j)\right)^2 . \tag{2.8}$$

In this thesis, it is assumed that the position estimators in (2.7) and (2.8) are unbiased. In the case of TOA, the bias is assumed to be known for environments of interest and can be subtracted out from distance measurements, resulting in an unbiased estimator. One of the fundamental drawbacks of the RSS signal metric, however, is that there remains residual bias even with the bias-reduced estimator in (2.7). Therefore, one would expect greater location error in actual deployments, necessitating higher node densities and signal to noise.

With this network model, the localization error estimation problem can be stated as follows.

Definition (Localization Problem): Given a network with a set $\mathcal{N}$ of nodes, where n are unknown nodes in $\mathcal{U} \subset \mathcal{N}$ with unknown positions $\{\mathbf{z}_1, ..., \mathbf{z}_n\}$, m are beacon nodes in $\mathcal{B} \subset \mathcal{N}$ with known positions $\{\mathbf{z}_{n+1}, ..., \mathbf{z}_{n+m}\}$, and noisy range measurements $\tilde{d}_{i,j}$ between neighbouring pairs of nodes i and j are available, estimate the positions $\hat{\mathbf{z}}_i$ of unknown nodes $i \in \mathcal{U}$ as close as possible to their true positions $\mathbf{z}_i$, minimizing the estimation error $\boldsymbol{\varepsilon_i} = \mathbf{z_i} - \hat{\mathbf{z}}_{\boldsymbol{i}}$.

Chapter 3

Related Work

In this chapter a detailed survey of related work is provided for this thesis. This related work includes the variety of available localization systems, localization analysis techniques which evaluate these systems, and coverage schemes which calculate the level of coverage in a network.

3.1 Localization Systems

Localization systems typically use some form of ranging metric to measure the distances between nodes (devices), which can in turn be used to estimate node locations provided that sufficient such measurements are available. However, due to the noisy nature of distance measurements, there is often a significant amount of positioning error associated with even the best localization systems [27], motivating ongoing research into increasingly more sophisticated localization schemes with improved accuracy and reliability [25, 46, 94].

There are a number recent surveys available on localization systems in wireless ad hoc networks, including several pertaining to WSN [13, 98, 82, 142, 92], localization in VANets

[16], indoor localization systems [91, 51], and secure localization [154]. In this section a survey of recent localization schemes is presented, organized by range measurement techniques, single-hop techniques where unknown nodes are within one hop of beacons, multi-hop techniques where beacons are several hops away from unknown nodes, and centralized approaches where positions are computed at a central location.

3.1.1 Range Measurement Techniques

Fundamental to location estimation is range measurement between two wireless devices, typically sensed from the received waveforms of propagating radio signals. A commonly used ranging metric used is the received signal strength of wireless signals [27]. Propagation models indicate that received signal strength attenuates logarithmically with distance, plus an additional noise factor [123]. This model is known as log-normal shadowing, where distance measurements are a Gaussian distributed function of the received power at the receiver.

Another commonly used ranging metric is the time of arrival (TOA) of wireless signals [52, 152]. Here the time of flight of a wireless signal from sender to receiver is measured (or similarly, the round trip time of flight), and is to related to the distance by the radio propagation speed, c. The time of arrival between two nodes has been shown to be Gaussian distributed with mean value as the ratio of the distance between the nodes and c [116].

A number of other range measurement techniques have been used in practice, although RSS and TOA are by far the most popular due to their low cost and relative ease of implementation. The time difference of arrival (TDOA) of two signals moving at different propagation speeds, such as radio and ultrasound pulses, can be used to achieve accuracy to within a few centimeters [120], but suffers from line-of-sight (LOS) requirements and additional hardware cost. Alternatively, the angle of arrival (AOA) can be estimated by using an antenna array and measuring the time difference of arrival signals across the arrays, from which angles between nodes can be derived. Interestingly, it was shown in [133] that the AOA metric provides no additional information from TOA with multiple antennas. In addition, with the recent introduction of the 802.15.4a standard a great deal of localization research is currently taking place based on the additional physical layer of ultra-wideband (UWB) which is capable of very high bandwidth at lower energy levels [119], which gives a high signal-to-noise ratio (SNR) for very accurate ranging, but only at shorter distances making it ideal for localization in ad hoc networks [70, 4, 36, 157].

3.1.2 Single-Hop Localization

The most well known single-hop localization system is the Global Positioning System (GPS), which consists of 24 to 32 satellites in Earth orbit which act as beacons at known positions, broadcasting TOA signals to GPS receivers which compute their locations using trilateration [114]. However, open access services such as GPS are often unfeasible due to cost, energy usage, imprecision, and unavailability [114]. Other shorter-range single-hop localization technologies have been developed which avoid some of the drawbacks of GPS. The Cricket location-support system [120] consists of reference nodes spread throughout a building which transmit their position information periodically, while listeners receive and analyze this information to learn their locations. The GPS-less system in [19] is similar, with reference devices set up in a grid pattern. Fingerprinting is a different approach commonly found in indoor localization systems such as RADAR [10] and MoteTrack [93], in which a radio transceiver measures the received signal strength of transmitting reference nodes at known positions, and stores the received radio signatures in a database. Unlocalized devices then determine their own coordinates by comparing their RSSI observations with this *a priori* measurement data. Despite the drawback of requiring substantial effort to generate an initial database of signal signatures, fingerprinting remains a viable option for localization [18, 22] due to its potential for improved accuracy as compared to trilateration-based techniques [28].

3.1.3 Multi-hop Localization

When reference nodes are not within radio range of unknown nodes, multi-hop localization techniques must be used. Multi-hop localization systems can be classified as either range-based or range-free. Range-based systems estimate inter node distances using some form of range measurement technology, such as those shown in the previous section. Range-free systems on the other hand do not depend on any specific ranging technique, but instead regard two nodes which are connected (within communication range of one another) as being one distance unit apart.

The range-based DV-Distance scheme in the Ad Hoc Positioning System (APS) [35] extends the concept of GPS in WSN by broadcasting beacon positions over multiple hops, where the number of hops and average hop size are calculated to allow estimation of the distances to beacon nodes without requiring direct communication. APS has three main phases, shown in Figure 3.1 a-c. Initially all beacon nodes which know their positions *a priori* flood their positions throughout the network so that all devices are aware of all beacon nodes. As positions are being forwarded, the current hop count of the message from the source is also sent. When a beacon node receives the position of another beacon, it computes the average distance per hop which is taken as the ratio of the distance between it and the source beacon, and the total number of hops separating them. Next, the average distance per hop is propagated to unknown devices in the network, which store the first received hop distance as the average distance per hop, and the lowest number of hops between itself and a given beacon node as the number of hops to that beacon. The distance to a beacon multiple hops away can then be estimated as the number of hops to the beacon multiplied by the average distance per hop, thus allowing nodes to estimate their positions using beacon devices which are multiple hops away.

An iterative refinement phase was introduced to APS in [126], where after obtaining initial position estimates from a DV-Distance scheme, nodes exchange position estimates with their one-hop neighbours, and treat these neighbours as intermediary reference devices, shown in Figure 3.1 d. Nodes continually update their positions using the new positions of ones neighbours, until each device eventually converges on a solution. The refinement phase in [128] takes place in a consistent sequence across collaborative sub-trees, preventing local oscillations between small numbers of nodes which would have resulted in erroneous local minima. In the confidence-based iterative localization (CIL) scheme [148] each node is assigned a confidence value indicating its localization accuracy based on a Quality of Trilateration (QoT) metric, so that in the refinement phase reference nodes with higher confidence values are preferentially selected to limit error propagation.

DV-Hop is the range-free equivalent of DV-Distance in the APS [35]. The hop-count-based neighbour partition (HCNP) algorithm [94] improves upon the accuracy of DV-Hop by additionally considering the number of hops that ones neighbouring nodes are away from anchors. Region-based localization (RBL) is another approach to range-free localization, popularized by the APIT scheme [53] where unknown nodes estimate their locations as the center of gravity of triangles formed between anchors in which a node resides. In [5] unknown nodes are restricted to lie in the sorted order-K Voronoi

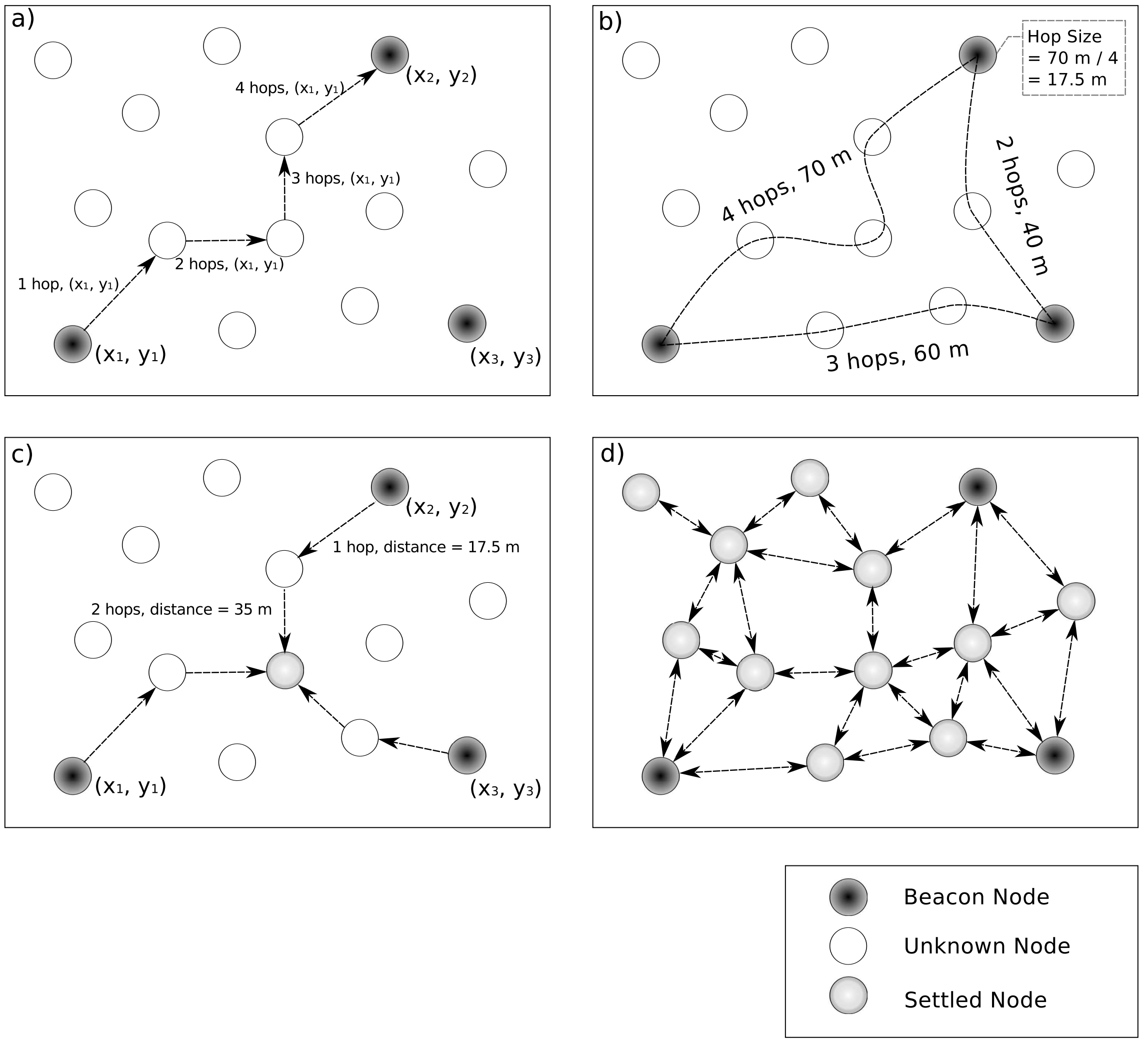

Figure 3.1: Example and phases of the APS multi-hop localization algorithm: (a) Beacon nodes begin the multi-hop localization algorithm by flooding their positions, (b) beacon nodes calculate the average distance per hop as the distance between beacons divided by the number of hops, (c) average hop distances are propagated to unknown nodes along with the number of hops to each beacon node, allowing unknown nodes to calculate their positions and become settled nodes, (d) refinement phase added to the initial APS algorithm where settled nodes exchange position estimates to further refine their own locations.

cell of its reference nodes, which is a generalization of the Voronoi cell. A cost function based on these Voronoi cells is derived which allows localization without the use of an energy decay model that rivals maximum-likelihood estimators which do have access to such a model.

A number of recent works make use of the probabilistic framework of Bayesian estimators [45], which merge multiple sources of information to provide position estimates. For example, when ranging or position information is available at multiple time intervals, or when positioning information from multiple sensing modalities is available, Bayesian estimators can be used to fuse such information together along with the current observation state [58, 108]. Kalman filters and extended Kalman filters are the most widely used Bayes filters, where current estimates combined with prior information and are corrected based on the Kalman gain matrix [108, 131, 46]. Particle filters provide another implementation for Bayes filters, which are not as computationally efficient as Kalman filters, but do not depend on a Gaussian distribution of samples and so are more robust [45]. Probabilities are represented by a number of random samples, called particles. Over time, additional samples increase the weight of particles, so that there is a greater probability in locations with the highest particle concentration [108, 63]. Particle filtering has proved to be an extremely effective tool and is receiving a great deal of attention in localization of mobile networks [60, 9], including VANets [15, 104, 130].

3.1.4 Centralized Approaches

Centralized localization schemes can provide more accuracy than distributed systems, at the cost of additional computation and communication overhead. Maximum-likelihood (ML) methods [117] to determine the most likely configuration of sensor nodes via nonlinear optimization of a cost function. Multidimensional scaling (MDS) [132, 67] computes the coordinates of a nodes by singular value decomposition, which gives the least squares approximation by eigen-decomposition. Weighted MDS as opposed to classical MDS is used in [34] and [24] which assigns higher weights to more accurate range measurements using a distance model. In general, ML estimators (MLE) achieve better accuracy while MDS is more computationally efficient. Therefore, MDS can be used as an initialization method for ML so that the benefits of both techniques are obtained [87].

Convex position estimation in [41] formulates localization as a semi-definite program (SDP) with convex constraints, which is solved with a centralized computer. In [11] the SDP is broken down into multiple components which can be solved with a distributed method by partitioning the network. The recent work in [112] derives a non convex estimator to approximate the ML estimator, which can then be solved by SDP. The estimates of the SDP can then be used as a starting point for the MLE, which gives the accuracy of MLE with greater computational efficiency. Simulated annealing (SA) is another technique for solving optimization problems which has been used for localization [75]. A cost function based on inter node distances was optimized with SA, using a temperature control parameter, T, to anneal the problem until a good solution is "frozen". Simulation results showed that the SA approach achieved greater accuracy that SDP [75].

3.2 Localization Error Analysis

Being able to analyze the behavior of localization systems under a variety of scenarios is extremely useful in practice. While message, time and computational complexity are important factors to consider when designing localization schemes, usually more important to consider are the accuracy and precision of the provided position estimates [26]. Limits on the achievable positioning accuracy with different system parameters have been proposed [116, 127], providing a benchmark with which we can compare the performance of localization schemes. Furthermore, theoretical analysis of the error characteristics of location error gives a better understanding into how localization systems work so that improved schemes can be devised [148]. In this section we will evaluate localization analysis tools based on information theory, with the majority of material looking at the Cramér-Rao Lower Bound (CRLB) and its variants. In addition, localization analysis based on probabilistic frameworks will be evaluated, as well as techniques established from graph theory.

3.2.1 Information Theory Approaches

Uncertainty Ellipses

A simple measure of localization accuracy is the circular error probable (CEP) [140], which is a circle defined with its centre at the mean value of the location estimate, with a radius containing half of all estimates, which is a measure of the uncertainty of the estimator relative to its mean. Uncertainty ellipses determine the probability P that a random realization of a location estimate will fall within an ellipse described by the following equation [113]

$$P = P\left\{ \frac{1}{1-\rho^2} \left[\frac{x-\mu_x}{\sigma_x^2} - 2\rho \frac{(x-\mu_x)(y-\mu_y)}{\sigma_x^2 \sigma_y^2} \frac{y-\mu_y}{\sigma_y^2} \right] \leq c^2 \right\} \tag{3.1}$$

where μ_x and μ_y are the mean values and σ_x^2 and σ_y^2 are the variances of the location estimator in the x and y directions, respectively, as shown in Figure 3.2, and ρ the correlation coefficient. Here c is a constant which expresses the desired probability, P. Despite the availability of more sophisticated accuracy measures, uncertainty ellipses re-

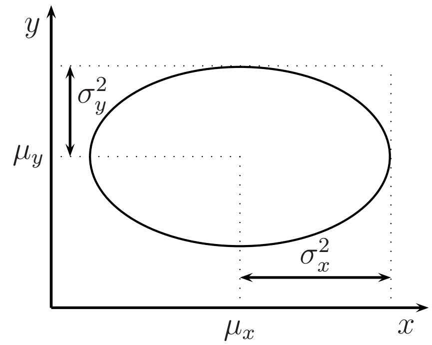

Figure 3.2: Example of an uncertainty ellipse.

main in practical use today for their intuitive geometrical perspective on varying anchor configurations [6, 40].

GDOP

The Geometric Dilution of Precision (GDOP) [150] is a widely used metric by the GPS community to quantify the difficulty of specific geometries for localization, by essentially relating position accuracy to measurement accuracy. It is defined as the ratio of the root-mean-square (RMS) position error to the RMS ranging error [140], where the ranging error is common to all measurements and is typically dependent on the environment, while the position error depends on the specific geometry of the available reference sensors, given by [140, 150, 85]

$$GDOP = \frac{\sqrt{\sigma_x^2 + \sigma_y^2}}{\sigma_R} \tag{3.2}$$

where σ_R is the RMS ranging error which typically follows a zero mean Gaussian distribution, and σ_x^2 and σ_y^2 are the RMS position errors in the x and y directions. The important observations from the derivation of σ_x^2 and σ_y^2 in [150, 85] are that a lower (better) GDOP is achieved when reference devices are equally spaced apart and are equidistant from the unknown device, and the GDOP decreases with an increasing number of references, with an optimum value of $2/\sqrt{N}$, where N is the number of reference nodes [85].

Cramér-Rao Lower Bound

The CRLB is a well known result from information theory which places a lower bound on the variance of any unbiased estimator $\hat{\boldsymbol{\theta}}$ of a parameter $\boldsymbol{\theta}$ [77], and is given by inverse of the Fisher information matrix (FIM) $\mathbf{I}(\boldsymbol{\theta})$. That is, $\mathbf{C}(\hat{\boldsymbol{\theta}}) \geq \mathbf{I}^{-1}(\boldsymbol{\theta})$, where $\mathbf{C}(\hat{\boldsymbol{\theta}})$ is the covariance matrix of $\hat{\boldsymbol{\theta}}$. The ijth element of the FIM is given as

$$[\mathbf{I}(\boldsymbol{\theta})]_{i,j} = -E\left[\frac{\partial^2 \ln\, p(\mathbf{x};\boldsymbol{\theta})}{\partial\theta_i \partial\theta_j}\right] \tag{3.3}$$

where $p(\mathbf{x};\boldsymbol{\theta})$ is the pdf of the measurement data, and $\mathbf{x}$ is a random measurement taken at the true value of $\boldsymbol{\theta}$. The FIM essentially gives calculates the curvature of the log-liklihood function [115]. In Figure 3.3 the log-liklihood function in b) has a higher curvature and is more tightly distributed than the log-liklihood function in a); therefore the FIM would be larger in b) resulting in a lower CRLB. For 2-D position estimation, the parameter vector is the 2-D vector $\boldsymbol{\theta} = [\boldsymbol{\theta}_x, \boldsymbol{\theta}_y]$, where $\boldsymbol{\theta}_x = [x_1, ..., x_n]$ is the set of x coordinates of all nodes and $\boldsymbol{\theta}_x = [x_1, ..., x_n]$ the set of y coordinates [116]. The pdf $p(\mathbf{x};\boldsymbol{\theta})$ is given by the statistical model for distance or angle measurements, such as RSS with log-normal shadowing in equation (2.1) or TOA with Gaussian noise in equation (2.3). The corresponding entries in the FIM can then be readily computed by taking the partial derivatives of (2.1) or (2.3) [116, 127]. The location variance of node i is defined as the sum of variances in the x and y directions, $\sigma_i^2 = \mathrm{Var}_{\theta_x}(\hat{x}_i) + \mathrm{Var}_{\theta_y}(\hat{y}_i)$, where $\hat{z}_i = [\hat{x}_i, \hat{y}_i]$ is an estimator of z_i. Therefore, the CRLB determines that σ_i^2 is lower bounded by [115]

$$\sigma_i^2 \geq [\mathbf{I}^{-1}(\boldsymbol{\theta})]_{i,i} + [\mathbf{I}^{-1}(\boldsymbol{\theta})]_{i+n,i+n} \tag{3.4}$$

where the diagonal entries i, i and $i+n, i+n$ in the FIM correspond to the values associated with node i in the x and y directions, respectively.

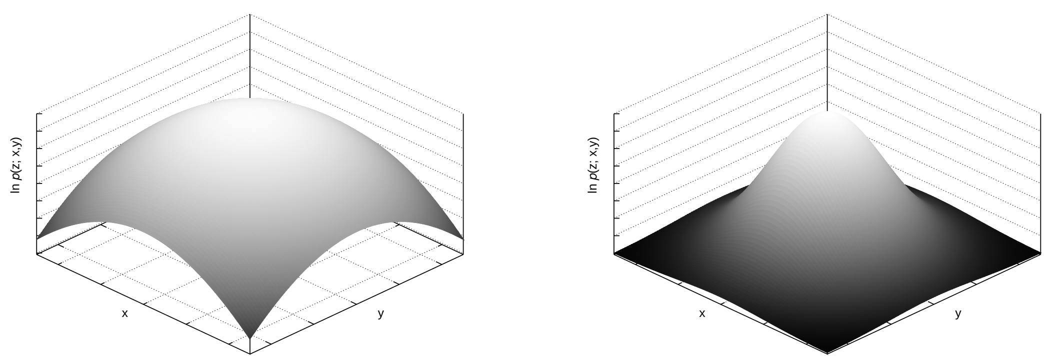

(a) (b)

Figure 3.3: Example of the log-liklihood function for two different probability density functions. The CRLB will be less with the distribution in b) since it has a tighter distribution than a).

The CRLB for the most simple case of a single unknown node u with measurements to reference devices $[1, ..., m]$ with known positions was derived for RSS and TOA in [116], given for TOA by

$$\sigma_u^2 = c^2 \sigma_T^2 m \left[\sum_{i=1}^{m-1} \sum_{j=i+1}^{m} \left(\frac{d_{u\perp i,j} d_{i,j}}{d_{u,i} d_{u,j}} \right)^2 \right]^{-1} \tag{3.5}$$

where $d_{u\perp i,j}$ is the shortest distance of node u to the line intersecting nodes i and j. Similar derivations for the CRLB can be found in the literature for TOA [116, 115, 84, 106], for RSS [116, 115, 21], for AOA [115, 106, 7, 127] and for TDOA [21]. It has been shown that the GDOP is in fact a special case of the CRLB with a single unknown node having Gaussian distributed range measurements to beacon nodes, which becomes

$GDOP = \sigma_u^2/\sigma_R^2$ [23]. In the single hop TOA case, $\sigma_R = c\sigma_T$ [116].

The CRLB was derived when there is uncertainty associated beacon positions in [127], where beacon positions are modeled with a Gaussian distribution with a prior pdf. The FIM associated with the prior pdf of beacon uncertainties is $\mathbf{I}_0(\boldsymbol{\theta})$, so that CRLB becomes [127]

$$\mathbf{C}(\hat{\boldsymbol{\theta}}) \geq \frac{1}{\mathbf{I}(\boldsymbol{\theta}) + \mathbf{I}_0(\boldsymbol{\theta})} \tag{3.6}$$

A CRLB for range-free positioning such as DV-Hop [35] is derived in [111], making assumptions that the node deployment follows a Poisson distribution with rate λ, and the expected value and variance of the hop distance correction (estimated distance per hop), denoted $E(\bar{x})$ and $V(\bar{x})$, are approximated with a Beta distribution. Given that the fraction of beacon nodes is f, and the TTL value for beacon broadcasts (whether or not a beacon position is heard) is h, nodes are able to contact on average n beacon nodes in the circle enclosing $hE(\bar{x})$, where $n = \pi(hE(\bar{x}))^2 f\lambda$. Let I_2 be the 2×2 identity matrix. The DV-Hop CRLB is then derived as [111]

$$\mathbf{C}(\hat{\boldsymbol{\theta}}) \geq \frac{V(\bar{x})}{\pi h E(\bar{x}) f \lambda} I_2 \tag{3.7}$$

The CRLB has further been derived for other types of localization systems which were discussed in Section III. Bounds were provided for a fingerprinting-based localization scheme in [59], and for a centralized SDP scheme in [112]. These CRLBs were derived using the FIM in equation (3.3) with different pdf models for range measurements. The posterior Cramér-Rao bound (PCRB) for mobile target tracking scenarios is an area of ongoing research [56, 55, 57]. Estimators typically make use of Bayes filters such as Kalman or particle filters, which take advantage of position estimates at prior time steps to obtain the posterior pdf for location estimation. The PCRB has been challenging as bounds have been in many cases overly optimistic [124]. The essential strategy in calculating the PCRB in [57] is to initially determine bounds which are conditional on the sequence of available measurements, after which an unconditional bound is generated by taking a weighted average of the conditional bounds.

When beacon nodes do not exist, schemes must rely on a relative coordinate system for localization rather than absolute coordinates [20, 117]. Difficulties arise when deriving the CRLB for this anchor-free scenario, as it has been shown that the FIM is singular, meaning that the CRLB is not directly available according to equation (3.3) [29, 6, 151]. Since there are no fixed references nodes positions have 3 degrees of freedom: rotation and x-y translation; thus it was proved that the rank of the FIM is deficient by at least 3 [29]. Simply selecting a group of nodes to act as fixed references, as was done in [20], does not suffice since the bounds change depending on the selection of reference nodes [29]. It was shown in [6] that inter node measurements are only able to estimate $\boldsymbol{\theta}$ up to its equivalence class $S(\boldsymbol{\theta})$, which is the class of all rigid transformations, rotations and scalings of $\boldsymbol{\theta}$. In other words, inter node measurements do not provide any information about these transformation vectors, so that the FIM will be singular. It is therefore required for additional information to be supplied, which in [6] come in the form of parametric constraints. Localization error bounds are then separated in terms of constrained error, $\mathit{\Sigma}_c$, and relative error due to inter node measurements, $\mathit{\Sigma}_r$, from which an upper bound is derived as $\mathit{\Sigma}_r \leq \mathbf{I}(\boldsymbol{\theta})^\dagger$, where $\mathbf{I}(\boldsymbol{\theta})^\dagger$ is the Moore-Penrose pseudoinverse of the FIM. From this, weaker bounds on a minimally constrained system have been derived showing that additional constraints can only lower the relative error [6].

The CRLB derivation in [110] includes path-loss effects, in which the SNR between nodes i and j is modeled as proportional to $d_{i,j}^{-\alpha}$, where α is the path-loss exponent. When *a priori* knowledge on the path-loss covariance model is available it is added into the CRLB terms resulting in a lower value; otherwise the CRLB reduces to that familiar one in [116].

There are a number of scenarios in which 3-D localization is required, including aviation systems and underwater WSN. The CRLB for 3-D localization was derived in [153], where the localization problem is extended to 3 dimensions with error modeled as Gaussian noise and the FIM is derived in a straightforward fashion according to equation (3.3).

CRLB Challenges

A number of random phenomena in the wireless medium affect the received waveforms and thus localization accuracy, such as fading, shadowing, multipath and nonline-of-sight (NLOS) propagation [133], which cause bias in the signal metrics. The CRLB is intended to provide a lower bound on the variance of unbiased estimators; therefore, consideration must be taken when determining localization bounds in biased scenarios.

NLOS signals are those that are affected by obstructions between the sender and receiver preventing a direct line of sight between them, resulting in a reduced signal strength and increased propagation times. It was shown that NLOS signals do not contribute to localization accuracy unless prior statistics on their error contribution are available [121, 122, 70, 133]. When prior NLOS statistics are available, the generalized CRLB (G-CRB) is used in [122], given by

$$\mathbf{C}(\hat{\boldsymbol{\theta}}) \geq \mathbf{I}_D^{-1}(\boldsymbol{\theta}) + \mathbf{I}_P^{-1}(\boldsymbol{\theta}) \tag{3.8}$$

where $\mathbf{I}_D(\boldsymbol{\theta})$ is the data information matrix associated with LOS measurements which is essentially that given by equation (3.3), and $\mathbf{I}_P(\boldsymbol{\theta})$ is the prior information matrix pertaining to NLOS signals in such a case that a probability distribution for these measurements is available (from statistical scattering models for example [66].) A similar derivation for the G-CRB is obtained in [4] which uses the data information, $\mathbf{I}_D(\boldsymbol{\theta})$, and prior information, $\mathbf{I}_P(\boldsymbol{\theta})$, where the prior information includes statistics for NLOS propagation delay, multipath bias, and additive bias characterizing blockage from obstacles. The pdfs used follow from extensive UWB measurements in various environments [3].

When nodes are not synchronized in time with one another and there is a clock bias present, the information matrix must be modified to take into account these biases [84]. In the case of symmetric communication links (i.e. if $j \in N(i)$ then $i \in N(j)$) then synchronization is not relevant since round-trip TOA can be used. Otherwise the FIM is augmented to include a column containing variances from clock bias to give a lower bound on clock bias estimates [84].

Position Error Bounds

Further to the G-CRB with biases, the fundamental limits on localization accuracy for an UWB system operating in dense cluttered environments, called the position error bound (PEB), was derived in [70]. The measured distance between nodes i and j is expressed by

$$\tilde{d}_{i,j} = d_{i,j} + b_{i,j} + \epsilon_{i,j} \tag{3.9}$$

where $b_{i,j}$ is the NLOS bias term caused by obstacles and $\epsilon_{i,j}$ is Gaussian measurement noise. This model easily incorporates real data for $b_{i,j}$ from range measurement campaigns [71], or can assume any distribution (e.g. uniform) in the absence of such measured data. The pdf of $b_{i,j}$ is expressed as a histogram function with $K^{i,j}$ bars denoted

$\beta_1^{i,j}, ..., \beta_K^{i,j}$, where each bar has a measured weight $w_k^{i,j}$, given by

$$f_{b_{i,j}}(b) = \sum_{k=1}^{K^{i,j}} w_k^{i,j} u_{\{\beta_{k-1}^{i,j}, \beta_k^{i,j}\}}(b) \tag{3.10}$$

where $u_{\{\beta_{k-1}^{i,j}, \beta_k^{i,j}\}} = 1$ when $\beta_{k-1}^{i,j} \leq b \leq \beta_k^{i,j}$ and 0 otherwise. The bias term is combined with the measurement noise so that one has $\tilde{\nu}_{i,j} = b_{i,j} + \epsilon_{i,j}$ and its corresponding pdf,

$$f_{\tilde{\nu}_{i,j}} = \int_{-\infty}^{\infty} f_{b_{i,j}}(x) f_{\epsilon_{i,j}}(\tilde{\nu}_{i,j} - x) dx \tag{3.11}$$

In order to obtain an unbiased estimator of the range measurement, the average value of $\tilde{\nu}_{i,j}$, denoted $m_{i,j}$ is subtracted from range measurement $\tilde{d}_{i,j}$, giving unbiased range measurements $\tilde{d}_{i,j} = d_{i,j} + \tilde{\nu}_{i,j} - m_{i,j}$ and their associated probability distributions $f_{i,j}(\tilde{d}_{i,j}|\mathbf{z}_i)$ which are derived by expanding equation (3.11) into the Gaussian range measurements. The Cramér-Rao Lower Bound is the inverse of the FIM, $\mathbf{C}(\hat{\boldsymbol{\theta}}) \geq \mathbf{I}^{-1}(\boldsymbol{\theta})$, from which the PEB is defined as

$$PEB(x_i, y_i) \triangleq \sqrt{\text{tr}\{\mathbf{I}^{-1}\}} \tag{3.12}$$

The elements in the FIM in equation (3.12) are of the same form as equation (3.3), but using the pdf in (3.11). The derivation of the FIM obtained for an unknown node u with m reference devices labeled $\{1, ..., m\}$ is then

$$\mathbf{I}^{-1} = \sum_{i=1}^{m} A(\boldsymbol{\beta}^{u,i}, d_{u,i}) M(\phi) \tag{3.13}$$

The term $M(\phi)$ in equation (3.13) contains the geometric information of u relative to the reference devices, while $A(\boldsymbol{\beta}^{u,i}, d_{u,i})$ gives weight to the geometric information based on the bias information $\boldsymbol{\beta}^{u,i} = \beta_1^{u,i}, ..., \beta_K^{u,i}$ and the relative distances $d_{u,i}$ [70]).

A performance measure called the squared position error bound (SPEB) was derived in [133] which quantifies the limits of wideband localization in the presence of nonline-of-sight (NLOS) and multipath propagation, by analyzing the received waveforms themselves rather than the signal metrics such as TOA or RSS.

$$\boldsymbol{\theta} = [\boldsymbol{z}^{\boldsymbol{T}} \boldsymbol{\kappa}_{\boldsymbol{1}}^{\boldsymbol{T}} \ \boldsymbol{\kappa}_{\boldsymbol{2}}^{\boldsymbol{T}} \ \cdots \ \boldsymbol{\kappa}_{\boldsymbol{m}}^{\boldsymbol{T}}] \tag{3.14}$$

where z is the position of the unknown node, and $\boldsymbol{\kappa}_i$ are the multipath parameters associated with reference node i, which consist of the signal amplitude, α_j, and the range bias, b_j. The derivations of the limits of the SPEB are involved and are beyond the scope of this thesis, andthe reader is therefore referred to [133]. However, the main observations resulting from the derivations in [133] can be summarized as follows:

- When no *a priori* information is available, NLOS signals do not provide additional information for position estimation. When *a priori* channel knowledge exists, NLOS contribute to a lower SPEB.

- For LOS signals, only the first path provides localization information; other multipath components can be eliminated.

- AOA obtained from antenna arrays does not increase position accuracy beyond TOA. AOA is equivalent to multiple TOA measurements.

- Localization with a clock asynchronism always results in a higher SPEB than when clocks are synchronized or when there is a known offset.

The framework in [133] was further extended in [134] to include cooperative multi-hop localization.

3.2.2 Probability Theory Approaches

There are a number of situations where information theory results such as the Cramér-Rao Lower Bound are not ideal, and so alternative methods of analyzing localization behavior are needed in such situations. The probabilistic method provides one alternative means of localization analysis by determining error probabilities based on network properties such as node distribution, radio coverage, and average node density.

Resolution Limit

In range-free localization schemes such as DV-Hop [35] a measure called the *resolution limit* was introduced in [107]. The resolution limit gives the expected distance z that a node can move without changing the connectivity of the underlying sensor graph. This is demonstrated in Figure 3.4, where a node which is initially at point p can move a distance z to point p' without changing the connectivity graph if there are no nodes in regions A or A', which are the areas affected by the movement. From the point of view of localization schemes which are based only on connectivity information, position estimates will always remain the same as long as nodes are not moved by more than the resolution limit. The expected distance z that a sensor can be moved without changing the connectivity graph is given by [107, 95, 60]

$$E(z) = \frac{1}{4r\lambda} \tag{3.15}$$

where λ is the expected node density which is the ratio of the total number of nodes n to the total network area Q. It was shown in [95] that the resolution limit in equation (3.15) is overly optimistic and a more accurate limit is possible by noting that the maximum that a node can move in *any* direction must be taken into account, not just the amount that a node can be moved in one *given* direction in a deployment. The improved resolution

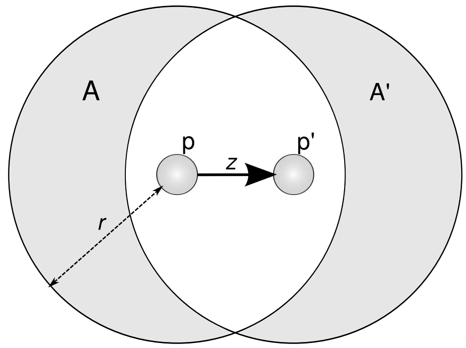

Figure 3.4: The resolution limit is the distance z that a node can move without changing connectivity information, which occurs when no sensors are in areas A and A'.

limit is given as follows.

$$E(z) = \frac{1}{4\pi r\lambda}\left[1 - \frac{4\pi r^2\lambda e^{-4\pi r^2\lambda}}{1 - e^{-4\pi r^2\lambda}}\right] \tag{3.16}$$

Hop-Count Progress

A number of papers have worked on deriving the pdf of the distance between two nodes conditioned on the number of hops between, $p(d|h)$ [32], from which the conditional expectation $E(d|h)$ can be derived to estimate the value of d for localization [141]. The derivations for $p(d|h)$ exist for 1-D networks, but have not yet been extended to 2-D networks.

The expected hop progress describes the expected distance that a message travels towards its destination at a given hop along its path [79, 81, 144], which can be used to estimate the distance between two nodes given the number of hops between them. In a uniformly distributed network with average node density λ, the expected hop progress was derived as [79]

$$\bar{z} = r\left[1 + e^{-\lambda\pi r^2} - \int_{-1}^{1} e^{-\lambda r^2(cos^{-1}(t) - t\sqrt{1-t^2})}dt\right] \tag{3.17}$$

The expected hop progress was applied to the hop-count based localization problem in [80] by observing the difference between the expected hop progress $\bar{z}$ to the actual hop progress z, normalized by the transmission radius, denoted by

$$\delta = \left|\frac{z - \bar{z}}{a}\right| \tag{3.18}$$

The larger the value of δ, the more inaccurate the hop progress estimation, resulting in higher position error. The general hop progress expectation results from [79] were further utilized by the localization scheme in [94] to prove that more accurate position estimation is achieved when the hop distances between neighbouring nodes and anchors are used in addition to the hop distances to ones own anchors alone. Furthermore, a lower bound on the minimum node density required to achieve localization accuracy of at least ϵ was derived based on the total size of the network area and the number of hops.

Probability of Localization

Lower bounds on the probability of unknown nodes failing to become localized are derived in [37]. With the assumption of a uniform deployment of n nodes, m of which are anchors, over a circular region of radius R and radio range r, the localization failure probability is lower bounded by

$$
\begin{aligned}
P_F \geq & \left[1-(1-a)\cdot b^2\right]^{n-3} \\
& \cdot \left[1+b^2(1-a)(n-3)\right. \\
& \left. +b^4(1-a)^2\frac{(n-1)(n-2)}{2}\right]
\end{aligned} \tag{3.19}
$$

where $a = (1 - \frac{m}{n})$ is the fraction of unknown nodes and $b = \frac{r}{R}$ is the fraction of coverage of a given node to the network region. The result in equation (3.19) was further expanded to incorporate the log-normal shadowing model which is affected by the receiver detection threshold and path loss exponent. Beyond the obvious requirement of having three or more measurements to anchors, threshold conditions for localization failure were investigated based on a and b [37].

The probability of triangulation is calculated in [86], which is closely related to the coverage problem [101] and is simply the probability that any point is covered by at least three nodes. Nodes are assumed to be Poisson distributed with density λ and have unit distance communication radius ($r = 1$). The probability of a specific point being triangulated is derived by integrating the circular areas in which reference nodes must lie in order to satisfy triangle constraints based on the average node density and communication range.

The quality of trilateration (QoT) metric [148] moves beyond the binary metric of whether or not a node can be localized, and evaluates the probability that the estimated position of a given node i, $\hat{\mathbf{z}}_i$, is within a disk area with radius R centered at the true position of i, $\mathbf{z}_i$. For a given node i with distance measurements to reference devices j, k and l, where each measurement follows some probability distribution $f_{i,j}(x)$ which is known *a priori*, the QoT of a trilateration t is calculated as

$$Q(t) = \int_{\mathbf{p}} f_{i,j}(d_{\mathbf{p},h}) f_{i,k}(d_{\mathbf{p},k}) f_{i,l}(d_{\mathbf{p},l}) d\mathbf{p} \tag{3.20}$$

where the integral in equation (3.20) is taken over the set of points $\mathbf{p}$ in the disk of radius R surrounding $\mathbf{z}_i$, where the value of R is application specific.

Probabilistic Analysis for Other Localization Schemes

The probabilistic method is used to analyze other types of localization systems which do not follow the trilateration approach common to many schemes. Accuracy analysis for region-based localization (RBL) algorithms such as APIT [53] were investigated in [156]. Given a uniform deployment region Q with area S which is partitioned into sub regions $P = \{Q_1, ..., Q_k\}$ by a RBL scheme, each with respective size s_i, the probability of a single node u with position (x_u, y_u) being located within region Q_i is $p(u \in Q_i) = \frac{s_i}{S}$. The expected localization error ε of u when u is in Q_i is then [156]

$$E[\varepsilon] = \sum_{i=1}^{k} \frac{1}{S} \int \int_{Q_i} \sqrt{(x - x_i^c)^2 + (y - y_i^c)^2} dxdy \tag{3.21}$$

where (x_i^c, y_i^c) is the centroid of region Q_i. The difficulty in evaluating (3.21) then becomes determining what area to integrate Q_i over. The position, size and shape of the Q_i have varying degrees of impact on $E[\varepsilon^2]$. It was finally shown that the worse case localization error of u in a RBL algorithm is lower bounded by $\sqrt{\frac{S}{k}\frac{2}{\sqrt{\pi}}}$ [156].

For fingerprint-based localization schemes such as RADAR [10], the probability of selecting the correct position from a RSS fingerprint database is investigated in [73, 136]. The analysis begins with the simple case of selecting the correct location when only two possible fingerprints are available in the database. This is referred to as the pairwise correct probability (PCP) (or conversely, the pairwise error probability). This result is expanded to the case of a set of many available location fingerprints by comparing the difference of the distance between the sampled RSS to the correct fingerprint and the incorrect fingerprints, given by $C_k = ||\tilde{P}_i - P_i|| - ||\tilde{P}_k - P_i||$, where $\tilde{P}_i$ is the correct fingerprint, $\tilde{P}_k$ is an incorrect fingerprint with index k, and P_i is the sampled RSS.. The probability of a correct decision is then [73]

$$\begin{aligned} Pr\{\text{Correct Decision}\} &= P\{C_1 \leq 0, ..., C_K \leq 0\} \\ &\approx \prod_{k=1;k\neq i}^{K} Pr\{C_k \leq 0\} \end{aligned} \tag{3.22}$$

where there are K available fingerprints in the database. The probability distributions in (3.22) are approximated by proximity graphs [136], which are variants on Voronoi diagrams relating neighbouring fingerprints, giving the probability of selecting a given fingerprint, rather than the mathematically more difficult expression of determining the probability of a correct decision.

3.2.3 Graph Theory Approaches

Graph theory provides useful tools in the analysis of localization systems whereby the network is represented by a graph $G = (V, E)$ with wireless devices as vertices and edges between vertices exist where distance measurements are available. This representation allows one to look at the overall connectivity information of the network to determine if all nodes can be uniquely localized based on given data.

Localizability

Determining if each node can be uniquely localized is known as the localizability problem, which has been investigated in several works using graph theory [8, 149, 68].

In the most simple case, trilateration [35, 128] can determine if a given node is localizable; however, trilateration can easily assign wrong positions to nodes which cannot be localized or fail to locate nodes which can be localized by using information from several multiple hops away [149].

Graph rigidity theory has been used for the investigation of localizability, where a graph is rigid if its set of nodes cannot be continuously moved while still maintaining a set of distance constraints between them [83]. A graph is globally rigid if there exists a unique embedding of the vertices in a plane while still satisfying the distance constraints [33]. The graph in Figure 3.5 a) is rigid, but can be deformed to the formation in b) without modifying distances between nodes. The formation in c), however, is globally rigid as it cannot be deformed. It was shown in [8] that a graph is uniquely localizable if and only if it is globally rigid, assuming that at least three anchor nodes do not all lie in a straight line. Furthermore, a graph is generically globally rigid in $\mathbb{R}^2$ if and only if it is 3-connected and generically redundantly rigid [64], where generic in this sense means that the result holds not only for a specific set of distance measurements, but also for perturbed yet consistent data. k-connected graphs remain connected upon the removal of any k edges, while redundant rigidity implies that the graph remains rigid even after one of the edges is removed. A efficient polynomial time centralized algorithm for testing global rigidity, and thus localizability, was described in [65] by simply verifying 3-connectivity and redundant rigidity.

Distributed localizability testing is however much more difficult to implement, as full verification of 3-connectivity and redundant rigidity can require knowledge of edges which are multiple hops away. An efficient polynomial time algorithm to identify all nodes which are one-hop localizable (nodes which can be localized using only information from one-hop neighbours) was described in [149]. Trilateration is in fact the simplest case of the wheel graph W_4 consisting of a central vertex connected to 3 rim vertices, which are

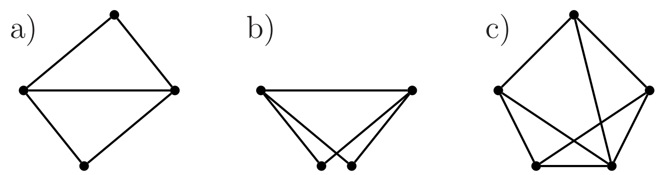

Figure 3.5: a) and b) have the same distance values between nodes, but different realizations. c) Globally rigid formation which cannot be deformed without varying distance values.

each connected to each other. Wheel graphs were shown to be globally rigid [8] and thus localizable; therefore the algorithm in [149] iteratively determines if nodes are contained within cycles of wheel graphs of previously localized nodes, beginning with anchors. The algorithm was able to identify many more localizable nodes by considering larger wheel graphs, W_d, up to degree d, than by simply considering trilateration alone. The largest degree of wheel graphs is bounded by the constant d, as realizing nodes in general wheel graphs is NP-hard [129].

Flip Ambiguities

Flip ambiguities are a specific phenomenon which prevent unique localizability, in which the positions of nodes can be reflected about the line connecting neighbouring reference devices without changing relative distances [43]. Such flip ambiguities can result in significant localization errors and are especially prominent in perimeter nodes of the network, and additionally these errors have strong potential to be propagated to other nodes in iterative localization schemes, resulting in increased overall error [105, 74].

To deal with the flip ambiguity problem, a localization scheme based on robust quadrilaterals was introduced in [105]. Robust quadrilaterals are sets of four nodes which are fully connected and well spaced such that even in the presence of noise they remain uniquely localized relative to one another. Specifically, robust quads are defined as fully connected quadrilaterals of nodes A, B, C, D which are composed of sub-triangles $\triangle ABC$, $\triangle ABD$, $\triangle ACD$, $\triangle BCD$, where each sub-triangle must satisfy

$$b \sin^2\theta = d_{\text{min}} \tag{3.23}$$

where b is the shortest side and θ the smallest angle of such triangles, and d_{min} is a threshold value based on the measurement noise [105]. Localization then proceeds iteratively, performing trilateration on nodes which are members of robust quadrilaterals, thus avoiding flip ambiguities.

Improvements on the quadrilateral robustness criteria were proposed in [135, 74]. The quad robustness test introduced in [135] combines partial robustness tests from all 12 of the sub-triangles formed by A, B, C, D and uses a second threshold value in $[0, 1)$. Extensive geometric analysis on flip ambiguities were carried out in [74], leading to a new quad robustness criteria to quantify such phenomena. A measure called $(\bar{\epsilon}, \delta_S)$-robustness is introduced, where $\bar{\epsilon}$ is the upper bound threshold on distance measurement errors (e.g. $\bar{\epsilon}$ can be chosen as 3σ, where measurements are Gaussian distributed with standard deviation σ) and δ_S is a predefined accuracy level within which all nodes must be uniquely localized. A quadrilateral with points A, B, C, D is then determined to be $(\bar{\epsilon}, \delta_S)$-robust if it satisfies

$$\begin{aligned} &\min_{\hat{D}} \tfrac{1}{2} \Big| |C\hat{D}| - |C\hat{D}'| \Big| > \bar{\epsilon}, \\ &\text{when} |\hat{D}\hat{D}'| > \delta_S \end{aligned} \tag{3.24}$$

where $\hat{D}$ and $\hat{D}'$ are the possible positions of D pending a flip, and distances $d_{A,D}$ and $d_{B,D}$ are available. Essentially, (3.24) determines flip ambiguities that are substantial ($|\hat{D}\hat{D}'| > \delta_S$) and that are larger than the distance measurement threshold $\bar{\epsilon}$.

3.2.4 Summary

We have seen several different methods for analyzing localization error, including approaches rooted in information theory, in probability theory, and in graph theory. An overview of the various analytical techniques which have been described is shown in Figure 3.6.

3.3 Applications of Localization Error Analysis

In the previous section a number localization analysis techniques based on several different approaches have been seen. In this section practical applications are described which utilize localization analysis to various ends. These applications include providing benchmarks with which to compare new localization schemes, optimizing the positions and/or selection of beacon nodes, estimating the amount of localization error, location refinement schemes, and improving energy efficiency of localization schemes.

3.3.1 Localization Performance Evaluation

The most natural use for localization analysis is in the evaluation of the performance of new localization schemes with respect to their accuracy, with the most prevalent measure being the CRLB. The CRLB is derived based on the system model with which the localization scheme is evaluated. The CRLB is a lower bound on the location error variance, therefore the localization scheme in question is run multiple times for statistical significance, and the root mean squared error (RMSE) of the scheme is obtained based on the results. The RMSE can the be plotted next to the CRLB to determine the optimality of the scheme with respect to the CRLB. An example is shown in Figure 4.1, where the RMSE of an MLE location estimator with RSS range measurements is plotted next to the

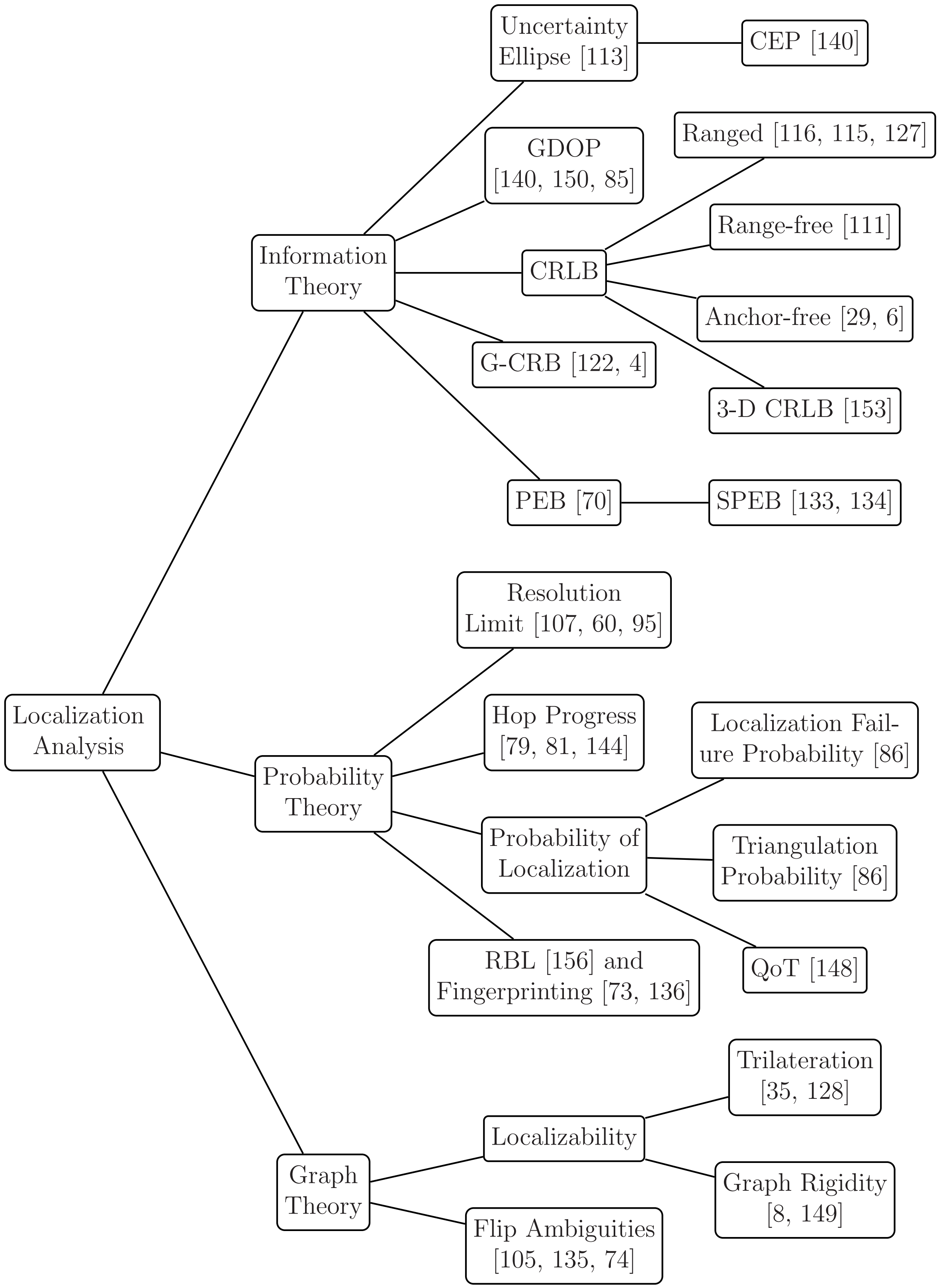

Figure 3.6: Overview of available localization analysis techniques, showing the overall hierarchy of the different methods.

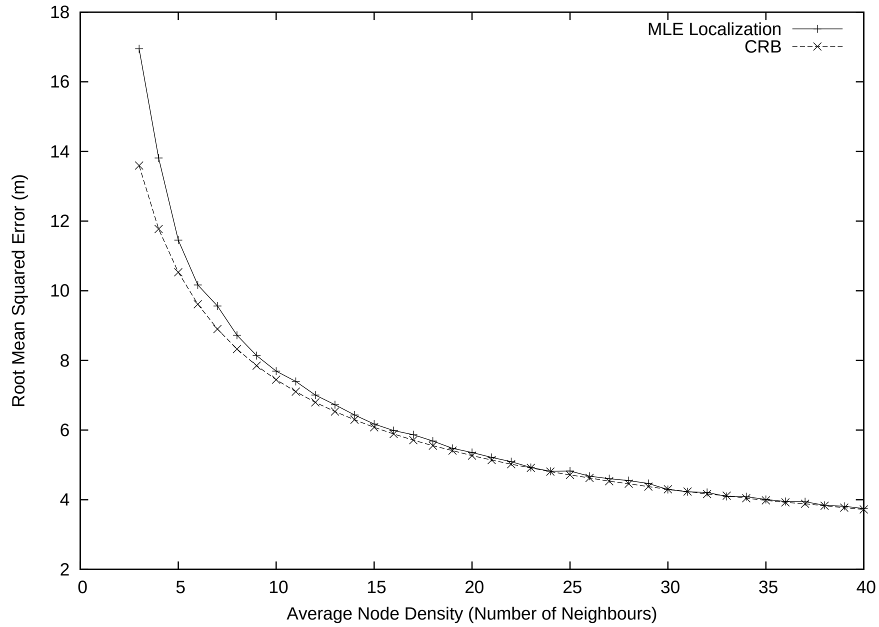

Figure 3.7: RMSE of MLE and its CRLB for RSS localization, with increasing node densities. The MLE asymptotically reaches the CRLB with sufficient data samples.

CRLB with increasing node densities, showing that the MLE achieves the CRLB with node densities at and above 15. Numerous recent examples of this standard approach exist in the literature to whichthe reader is referred [128, 103, 146, 40, 78, 145, 157].

3.3.2 Beacon Optimization

When beacon nodes are mobile or can be deployed to specific locations, one topic of research is the optimal placement of beacon nodes for localization. As with any optimization problem a suitable cost function must be derived which is to be optimized. In the case of beacon placement, this cost function will typically make use of the localization analysis methodology found in the previous section. The optimal placement of sensors for passive source localization, where signals from a radiating source are detected by a cooperating array of sensors for localization, is investigated in [1, 42, 109]. A geometric interpretation of the CRLB is used in [1], and the positions of the sensors are arranged in order to minimize the CRLB. Optimization of antennas on linear antenna arrays for passive source localization is achieved again by minimizing the CRLB in [42]. An alternate cost function was derived in [109] which does not rely on the CRLB, but instead derived an upper bound on the estimation error of a linear least squares based location estimator and an iterative estimator with which to gauge localization accuracy. A distributed scheme for optimizing the positions and coordinating motion of sensors for target tracking is studied in [99], where the determinant of the FIM for ultrasound based location estimation is used as the objective function for sensor position optimization. Critical points are identified which maximize its value, resulting in an optimal configuration of sensors uniformly distributed around the target. An integer linear programming approach to sensor placement for triangulation based localization was presented in [138] which involves a generic uncertainty function for angle measurements based on the geometry of of devices. An iterative algorithm called RELOCATE was proposed in [72] to optimally place sensors to guarantee good localization. The scheme acts to reposition beacon devices to minimize the Position Error Bound (PEB). Pioneering work was carried out to not only optimize beacon positions for high quality range measurement across a wide area, but also to extend the results to more realistic environments which include obstacles, where range measurements do not all carry equal weight.

Selecting a subset of available range measurements from beacon nodes is useful for reducing computational overhead and energy usage due to localization in constrained devices [118, 96] and for reducing error associated with less accurate beacon measurements [89]. Optimal selection of the three beacon nodes which minimize localization error is referred to as sub-optimal trilateration [96]. The three beacon devices which minimize the GDOP are selected for trilateration in [96], which reduces computational complexity while achieving almost the same degree of accuracy as when all measurements are used, and significantly reduced error as compared to when three beacons are randomly selected. Similarly, the GDOP is used to select the optimum n out of m GPS satellites [118]. An efficient recursive method was derived for determining the minimum GDOP using the revolving door method, allowing an overall reduction in computational resources for localization [118]. A subset of beacon nodes for multi-hop localization is selected in [88], with the goal of reducing resource usage while maintaining localization accuracy. The subset of beacon nodes is selected by considering whether or not adding additional beacon nodes as references will reduce the CRLB by a non-negligible amount. This approach is further extended in [89] where a DV-Hop based localization scheme is modified to have beacon nodes broadcast their positions with a probability based on the CRLB, such that the probability is higher for unknown nodes to receive position information from beacons which give a lower CRLB, effectively reducing location error along with overhead. A similar objective function to [99] involving the determinant of the FIM with acoustic AoA information is used in [76] to select a subset of active sensors for localization of a mobile target. Finally, a sleep scheduling scheme for reference nodes is described in [50] to save energy and reduce communication overhead, while maintaining sufficiently high localization accuracy by ensuring that the CRLB in a reference device's immediate neighbourhood is above a given threshold before entering into deep sleep state. This problem will be further examined in this thesis in Chapters 4 and 6. A further overview of target tracking based sensor selection schemes can be found in the recent survey of [125].

3.3.3 Error Detection and Estimation

The detection and estimation of localization error has many important uses, including the removal of outlier measurements to reduce error [68, 155], location verification for wireless security [2, 90, 154], and developing location-dependent applications and protocols which are resilient to localization error [48, 50].

The scheme in [68] uses graph rigidity theory to detect outlier range measurements. Outlier edges are determined to be those that are within redundantly rigid components but are not embeddable. An algorithm was derived to mark all edges which are not parts of bilateration generic cycles as outliers, indicating that a certain level of redundancy is required. The Dixon test is a statistical test to detect and reject outliers in a data set, and is used in [155] remove outlier range measurements which are uncharacteristic of the other measurements.

The approach in [48] is for nodes to estimate the amount of error present in their derived positions with a certain probability. The variance of localization error variance is modeled with a function based on the CRLB. Probabilistic methods then use this variance model to estimate upper bounds on localization error, which are computed locally by wireless devices. Location with estimated error over a certain limit can then be dealt with appropriately at the application level. In later chapters throughout this thesis this approach will be studied.

3.4 Coverage

In this thesis the coverage problem and its interaction with localization systems is further explored. Coverage is a fundamental issue in wireless networks, and is described as a measure of the quality of service of a network [101]. In wireless sensor networks, one may be interested in the level of sensor coverage, which is the observable area by its sensors. In other wireless networks, one may also be interested in radio coverage, which is the area within radio range of at least one device in the network. Common uses of coverage include finding weak points in networks where coverage is low to help strengthen future deployments [101], and finding redundancy within networks where multiple devices cover the same area [12, 61, 143].

Meguerdichian et al. in [101, 102] used Voronoi diagrams to show the path with the worst possible coverage between two points, called the *maximal breach path*, and Daulaunay triangulation to show the path with best possible coverage between two points, called the *maximal support path*. These algorithms can be used to find strengths and weakness in the coverage of a network, and can then assist in future deployments of devices in order to further strengthen the coverage level.

A problem of particular interest in this thesis the optimal sleep scheduling problem, where schemes aim to limit density by scheduling certain nodes to enter a deep sleep mode to conserve energy while maintaining the minimum level of coverage in the network. The *k-coverage* problem is studied in [61, 62], where a point is *k-covered* if it is within range of at least k devices, and we can determine whether an entire area is *k-covered* with $O(nd\log(d))$ complexity, where n is the number of devices in the network, and d is the maximum node density [61]. The scheme presented in [62] finds the minimum subset of active devices which simultaneously ensure that the entire network area is both k-covered and k-connected, and schedules devices into sleep mode and adjusts radio transmission ranges to reduce energy consumption while maintaining coverage and connectivity. Coverage is determined by ensuring that all devices are k-perimeter-covered; a condition for coverage which was derived in [61]. Figure 3.8 shows an example of a central node i which is perimeter covered by its neighbours, which can be computed easily by calculating the

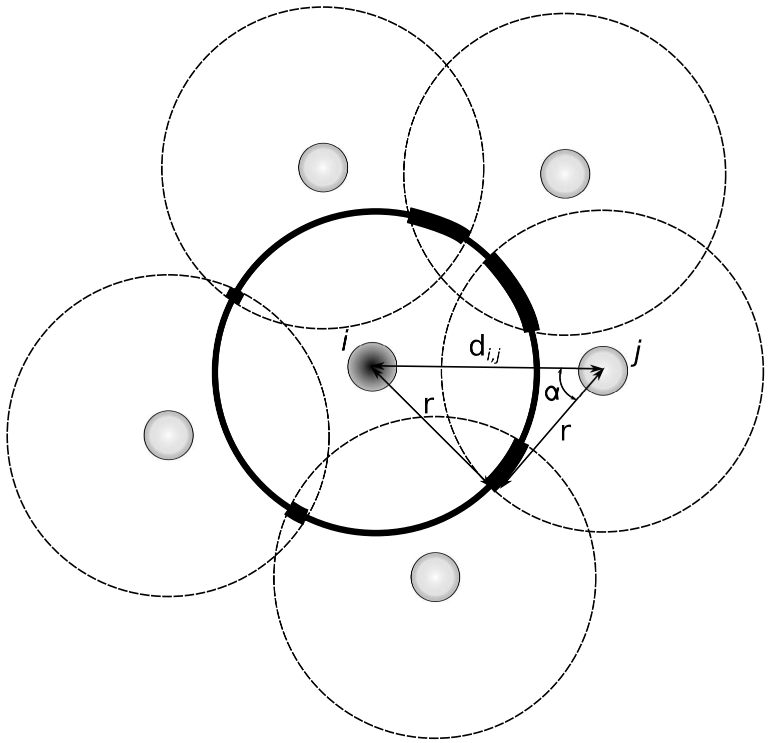

Figure 3.8: Example showing the perimeter coverage of a central node by its neighbours.

arch of i with each of its neighbours j, given by $\alpha = \arccos(\frac{d_{i,j}}{2r})$, and verifying that the perimeters cover the entire range $[0, 2\pi]$.

In [139], coverage is calculated by nodes evaluating the central angles between intersection points of overlapping sensing regions of neighbours. When the union of central angles is the entire 360 degrees of a node's sensing region, it is considered covered, so is eligible to enter sleep mode to conserve energy. Both schemes in [62] and [139] depend on a random backoff delay to decide on which nodes will be selected for deep sleep in a distributed algorithm. The protocol presented in [12] uses the central angle method in [139] to locally compute coverage but avoids the non-determinism of a random backoff delay by selecting active nodes which are covering the largest number of neighbouring devices, which effectively minimizes the number of active nodes.

For purposes of routing in ad hoc networks, not all devices along a path from source A to destination B need to be actively transmitting the given information. Many scenarios only require the minimum number of active devices along the path to transmit the information, thus reducing energy usage and message collision probabilities. Two significant scheduling algorithms include GAF [147], and Span [30]. GAF splits the network into virtual grids, such that nodes within adjacent grids can communicate with each other. Thus, from the point of view of routing, all nodes within a single grid behave the same, and so only one node in a grid needs to be active at a time. An example is shown in Figure 3.9, where a virtual grid is formed with cells of size s which must be less than the nominal radio range r. Then nodes within the same cell are equivalent for routing purposes, so only a single node per cell needs to remain active, denoted by the dark nodes in Figure 3.9. Span has similar goals to GAF in reducing energy consumption while maintaining sufficient connectivity for routing, but doesn't require node positions to be known beforehand. Instead, Span uses only local connectivity information to determine which nodes must remain active for routing. These active devices are known as coordinators. Devices which discover that two of their neighbours cannot reach each other directly are eligible to become coordinators, and are selected to become coordinators after a random backoff delay to avoid multiple devices from becoming active simultaneously.

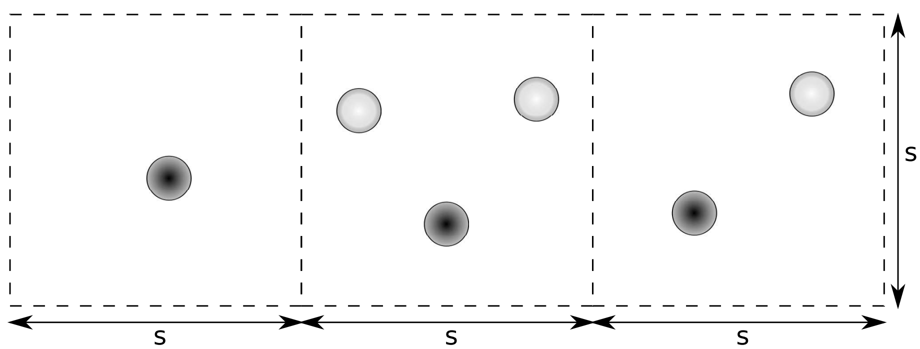

Figure 3.9: In the GAF protocol, the network is separated into virtual grids, and only one device per cell needs to be active for routing (dark nodes).

Chapter 4

Scheduling for Scalable Energy-Efficient Localization

4.1 Introduction

In this chapter, a scheme is presented to improve the scalability and energy efficiency of localization in mobile ad hoc networks based on a recently published peer-reviewed conference paper [49]. Unlike static networks where nodes need only to compute their locations once, in mobile networks when a localized node moves its position becomes unknown again. It must therefore recompute its position by observing position and range measurements from its new neighbours, necessitating a high communication and computational overhead.

Existing localization schemes ignore scalability as the number of available reference nodes increases. Current schemes utilize measurements from all available reference devices in order to improve on position accuracy. However, simulation results in this chapter show that when reference devices are sufficiently dense, new distance measurements become redundant and do not have a significant impact on estimation accuracy. Instead, an increasing number of localization messages will be exchanged, which increases the likelihood of collisions, net energy consumption, and the time for computing a solution, further increasing error.

The scalability and energy-efficiency of node localization are improved upon by limiting the number of active reference devices participating in localization, while maintaining sufficient coverage to ensure acceptable location error. To achieve this result, the level of coverage which is sufficient for the desired accuracy is determined. When a node discovers that one or more of its neighbours is not sufficiently connected, it is eligible to become a reference node. To avoid excessive reference nodes from becoming available, eligible nodes wait for a random amount of time before announcing that they will become references. All computation is performed using only local information broadcasted by the immediate neighbours of a node, thus it scales well and requires minimal extra messaging. Furthermore, no assumptions are made about the specific localization algorithm used, only that inaccurate ranges and positions of reference devices are observed. Simulations show that in sufficiently dense networks we can achieve network lifetimes with localization scheduling which more than double those without it, while localization accuracy is only marginally affected.

4.2 Methods

4.2.1 Problem Statement

When mobility is possible and settled nodes move they will again have unknown positions, and must receive position updates from their new neighbours in order to recompute their coordinates. This results in high communication costs when uncontrolled, and so we aim to reduce this overhead by solving the following localization scheduling problem.

Definition (Localization Scheduling Problem): Given a network with unknown nodes $\mathcal{U}$, settled nodes $\mathcal{S}$, and beacon nodes $\mathcal{B}$, where nodes can join $\mathcal{U}$ at any time, either from leaving $\mathcal{S}$ due to node movement, or by new nodes joining the network, select a set of *reference* nodes $\mathcal{R} \subseteq \mathcal{S} \cup \mathcal{B}$, such that only nodes in $\mathcal{R}$ are used in estimating the positions $\hat{\mathbf{z}}_i$ of nodes in $i \in \mathcal{U}$, while the estimation error $\boldsymbol{\varepsilon_i} = \mathbf{z_i} - \hat{\mathbf{z}}_{\boldsymbol{i}}$ remains sufficiently low.

The next section will describe the conditions required for sufficient localization accuracy in the localization scheduling problem.

4.2.2 Conditions for Localization

The effects of node density on localization accuracy were investigated by looking at the theoretical lower bound of localization accuracy given by the CRLB compared with two different location estimators commonly used in practice, namely trilateration and MLE. The minimum connectivity required for sufficient localization accuracy were observed, which will need to be met by the network before allowing nodes to be scheduled for sleep, which effectively reduces node density.

Monte Carlo simulations were run to evaluate the effect of changing node density on the CRLB in equation (2.5), and the trilateration and MLE location estimators shown in Chapter 2. Figure 4.1 shows the error of these estimators compared to the CRLB when an unknown node i is located in the centre of a group of known nodes $N(i)$, which are all at an equal distance, d_i, away from i, and are equally spaced apart from one another. For the trilateration and MLE estimators, 5000 simulations were run at each node density from 3 to 100 neighbours based on the wireless model described in Chapter 2, and the mean squared error (MSE) was computed as a function of node density.

As can be seen in Figure 4.1, initially when a node has very few neighbours, its

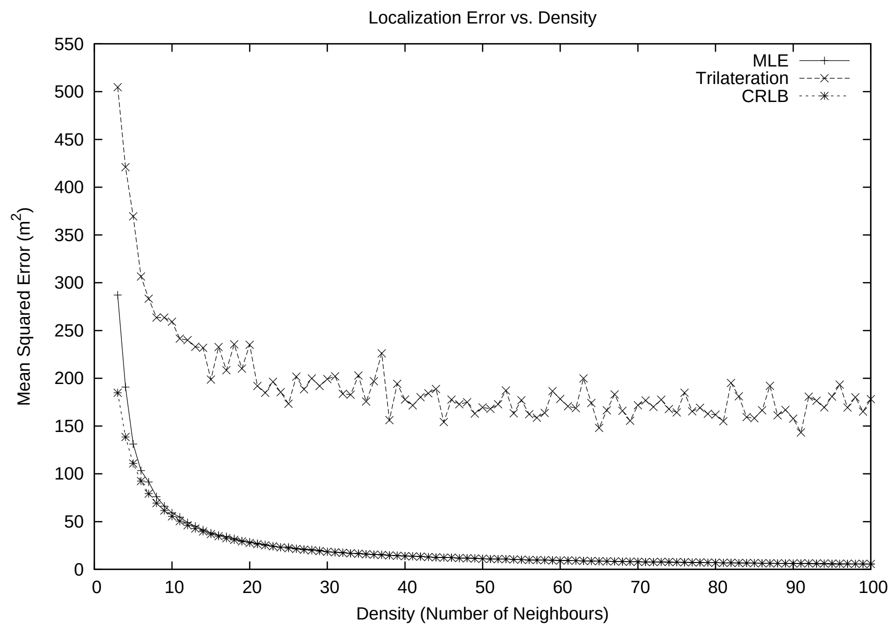

Figure 4.1: MSE of MLE and trilateration estimators, and CRLB of RSS localization, with changing node densities.

localization error will be very high. However, as the number of neighbours increases, its position error decreases exponentially, until eventually increasing density has relatively little effect on error. It is noted in Figure 4.1 that when around 15 observations are available the estimation becomes much more stable. This number is consistent with other simulations in the literature [69, 126, 128]. Using these results, we can select an appropriate minimum node density, χ, which can ensure reliable localization. The selection of χ will be investigated further in the evaluations section in this chapter.

4.2.3 Localization Scheduling Algorithm

In this section the proposed localization scheduling algorithm is described. Connectivity information is exchanged between neighbouring nodes and is used to make local decisions as to which devices are required for accurate localization. Eligible reference nodes wait for a randomized period of time before announcing that they are references to limit needless active nodes. Devices which are not selected as reference nodes sleep for an extended duration, then wake up to participate in another election round in order to rotate the set reference nodes, ensuring that energy is used evenly throughout the network.

Reference Node Decision

In the initial phase of the proposed scheme, a DV-Hop based algorithm [126] is run so that all nodes are in $\mathcal{S} \cup \mathcal{B}$. In this multihop positioning algorithm, beacons flood two messages throughout the network: their positions, and a corrected hop distance. To avoid the need for additional communication, each node stores a list of their one-hop neighbours, and transmits this list during the second localization flood message, so that all nodes know the connectivity information of their two-hop neighbours.

Once connectivity information is known for ones neighbours, a node is able to determine if it is eligible to become a reference node. If there are single-hop neighbours which are not sufficiently covered by existing reference nodes, then a given node is eligible to become a reference, by the following rule.

Definition (Reference Node Eligibility Rule): A settled node $s \in \mathcal{S}$ or beacon node $b \in \mathcal{B}$ is eligible to become a reference node $r \in \mathcal{R}$ if it is connected to less than χ neighbours, or if one of its neighbours is connected to less than χ neighbours, where χ is a design parameter describing the average density required to ensure sufficiently localization accuracy with high probability.

Nodes store a list of reference nodes to which they are currently connected. To avoid the over wake-up problem, where multiple nodes become references simultaneously, eligible nodes wait for a randomized delay time before announcing their decision to their neighbours. When this delay has passed, a node checks its eligibility; if it can, it becomes

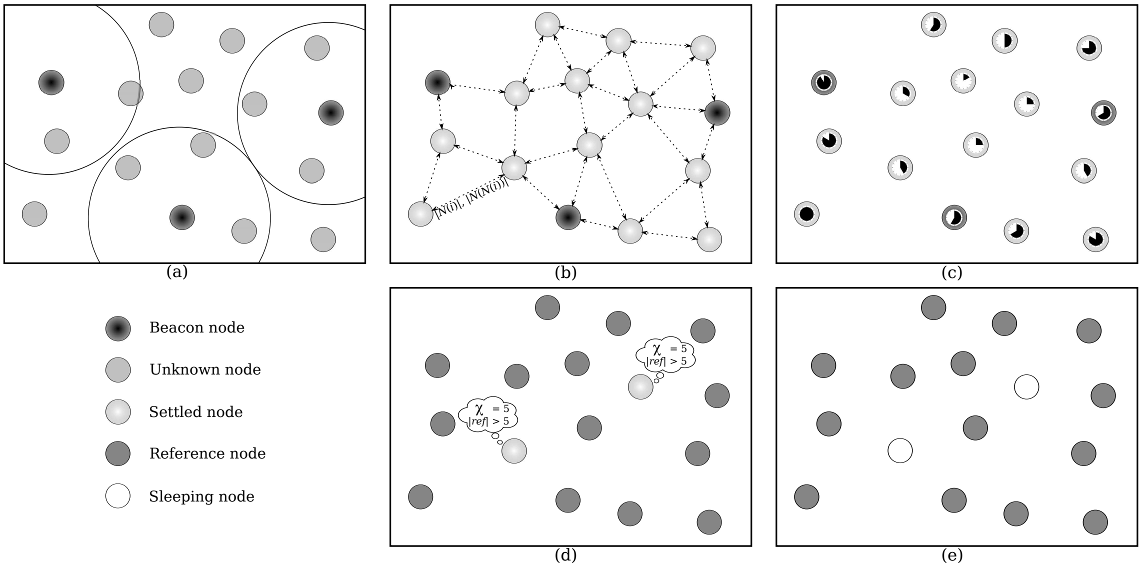

Figure 4.2: Example and phases of the localization scheduling algorithm: (a) Beacon nodes begin the multi-hop localization algorithm, (b) nodes exchange connectivity information with their neighbours, (c) localized nodes wait for a random delay time, (d) nodes check their eligibility to become references, (e) ineligible nodes enter sleep mode for a period of time.

a reference node and announces its state to its neighbours. Otherwise, ineligible nodes are scheduled to sleep for a period of time to conserve energy, since they will not be participating in localization. The phases of this scheme are shown in the example of Figure 4.2.

Nodes which wait for a shorter delay time are more likely to become references than those with longer delays. Poorly connected nodes will be more likely to become references since they have fewer neighbours in contention. Therefore, one would like nodes with more neighbours to have shorter delays, to ensure a more uniform density. One would also want nodes with more energy to become references so that energy consumption is spread out evenly across the network, and certain devices do not become depleted much faster than others. The delay function is similar to that found in Span [30], and is given as follows.

$$delay = \left[\left[1 - \frac{|N(i)|}{\underset{\{j \in N(i)\}}{\arg\max} |N(j)|} \right] + \left[1 - \frac{E_r}{E_t} \right] + R \right] \times T \tag{4.1}$$

The first term in (4.1) looks at the connectivity of node i relative to its neighbours $N(i)$, and tends to zero when i has the highest connectivity compared to all of its neighbours, so that heavily connected nodes have shorter delays. The second term uses the ratio of the remaining energy of a device, E_r, to the total energy available to that device at time 0, E_t, which is smallest when $E_r = E_t$, ensuring that nodes with more energy have shorter delays so that they are more likely to become references. Finally, R is a pseudo-random number in the range (0, 1], and T is an upper bound on the time for a typical message transmission.

Reference Rotation

To achieve accurate localization for as long as possible, the active set of reference nodes must be periodically rotated so that no devices are depleted too quickly, creating coverage holes. After running the initial reference node decision algorithm once, all nodes start a timer T_R at the time of the last received reference decision message. When T_R expires, sleeping nodes wake-up, and active reference nodes become tentative references, which still participate in localization, but are considered non-reference nodes for the next selection round. To account for neighbours which may have moved out of range and for new neighbours which have come into range, nodes exchange their 2-hop neighbour information, requiring an additional 2 messages per node. This could alternatively be done by piggybacking on existing localization messages to avoid message overhead. Nodes then run the reference node decision algorithm as outlined in the previous section.

The complete localization scheduling algorithm is given in Algorithm 4.1. There are two types of messages used by the scheme: *HELLO* messages (lines 1-7) which are used to exchange connectivity information between neighbours, and *REFERENCE* messages (lines 8-15) which distribute information regarding the current reference nodes. Nodes wait for the delay given by (4.1) (lines 20-22), then check their eligibility to become references (lines 24, 38-42). Eligible nodes then remain active, while all others go to sleep (line 32). Reference nodes remain active for T_R seconds, after which all devices wake up so that new references can be selected (lines 33-37). For brevity pseudo-code is omitted for localization as it is well described in other literature.

4.3 Evaluation and Results

Implementation and evaluations of the proposed algorithm are done using the network simulator *ns-2* version 2.33. Further details of the simulation environment are given in Appendix A. Energy settings are based on the XBow IRIS XM2110CA [137]. 1000 network devices are deployed uniformly over a square area of size 300 m $\times$ 300 m. To keep network topology consistent between simulation runs, node density is varied by modifying the receiving threshold of wireless devices which effectively controls their communication range.

The implementation follows the pseudo-code in Algorithm 4.1. Twenty beacon nodes are selected at random which know their positions at all times. The beacon nodes initiate localization of the unknown nodes by performing a refinement-based localization scheme similar to to that of Savarese et al. [126]. When all nodes become settled and have estimated their positions, nodes begin to move randomly throughout the network. For simplicity, a single mobile node is simulated, moving at a constant speed of 10 m/s, which updates its position once per minute by requesting position information from its

Algorithm 4.1 - Localization Scheduling Algorithm

▷ **Input:**
INITIATOR **or** $msg_i = HELLO$(neighbours).
▷ **Action:**
$neighbours_i \leftarrow neighbours_i \cup$ **sender**;
$neighbours_{i,\mathbf{sender}} \leftarrow msg_i$.neighbours;
if $sentHello_i =$ **false then**
  $sentHello_i \leftarrow$ **true**;
  Send $HELLO$ to $N(i)$;
[Re]Start $timer_i(0, delay_{max})$

▷ **Input:**
$msg_i = REFERENCE$(isReference,references).
▷ **Action:**
$references_{i,j} \leftarrow msg_i$.references;
if msg_i.isReference **then**
  $references_i \leftarrow references_i \cup$ **sender**;
  if $|references_i| \geq \chi$ **and** $hasMinimum_i =$ **false then**
    $hasMinimum_i =$ **true**;
    Send $REFERENCE(isReference_i, references_i)$ to $N(i)$;

▷ **Input:**
$timer_i$(ID,time) timeout.
▷ **Action:**
if $timer_i$.ID $= 0$ **then**
  Send $HELLO(neighbours_i)$ to $N(i)$;
  [Re]Start $timer_i(1, delay_{max})$
else if $timer_i$.ID $= 1$ **then**
  $delay_i \leftarrow \left[\left[1 - \frac{|neighbours_i|}{max(\forall |neighbours_{i,j}|)}\right] + \left[1 - \frac{E_r}{E_t}\right] + R\right] T;$
  [Re]Start $timer_i(2, delay_i)$
else if $timer_i$.ID $= 2$ **then**
  if $isEligible()$ **then**
    $isReference_i \leftarrow$ **true**;
    Send $REFERENCE(isReference_i)$ to $N(i)$;
  [Re]Start $timer_i(3, delay_{max})$
else if $timer_i$.ID $= 3$ **then**
  $neighbours_i, \forall neighbours_{i,j} \leftarrow \emptyset$
  $hasMinimum_i, sentHello_i \leftarrow$ **false**;
  [Re]Start $timer_i(4, T_R)$
  if $isReference_i =$ **false then** go to sleep;
else if $timer_i$.ID $= 4$ **then**
  wake up;
  $isReference_i \leftarrow$ **false**; $sentHello_i \leftarrow$ **true**;
  Send $HELLO$ to $N(i)$;
  [Re]Start $timer_i(0, delay_{max})$

▷ **Input:**
PROCEDURE *isEligible()*.
▷ **Action:**
if $|references_i| \leq \chi$ **then return true**;
for each $references_{i,j}$ **do**
  if $|references_{i,j}| \leq \chi$ **then return true**;
return false;

current neighbours. With this scenario, we measure the number of localization messages transmitted, localization error of the mobile node, and energy expended by the network with and without localization scheduling.

4.3.1 Message Overhead Comparison

My first experiment compares the messaging overhead of repeated position estimation with and without the use of localization scheduling. For this experiment, we compare the number of messages exchanged as a single mobile node moves through the network recomputing its position, using information broadcasted by localized neighbours. Figure 4.3 shows the average number of messages sent per localization as average node density is varied from 10 neighbours to 100. Different values of χ are used, and are plotted together in Figure 4.3, along with running without localization scheduling. With low node density, scheduling has minimal impact on message overhead. However, as the density is increased, with a lower χ value (a lower minimum connectivity) the message overhead is increasingly improved.

4.3.2 Localization Accuracy

The average localization error over several thousand position updates of a mobile device is plotted in Figure 4.4 for increasing node densities and different minimum densities, χ. With low network density, the accuracy is very similar with and without localization scheduling since nearly all nodes must remain active to maintain the minimum density. As average node density is increased, error is reduced slightly when localization scheduling is not used, while error remains fairly constant when scheduling is used, since node density is more constant. However, the error difference is less than 10% even when the network has an average density of 100 and many more positions estimates are available

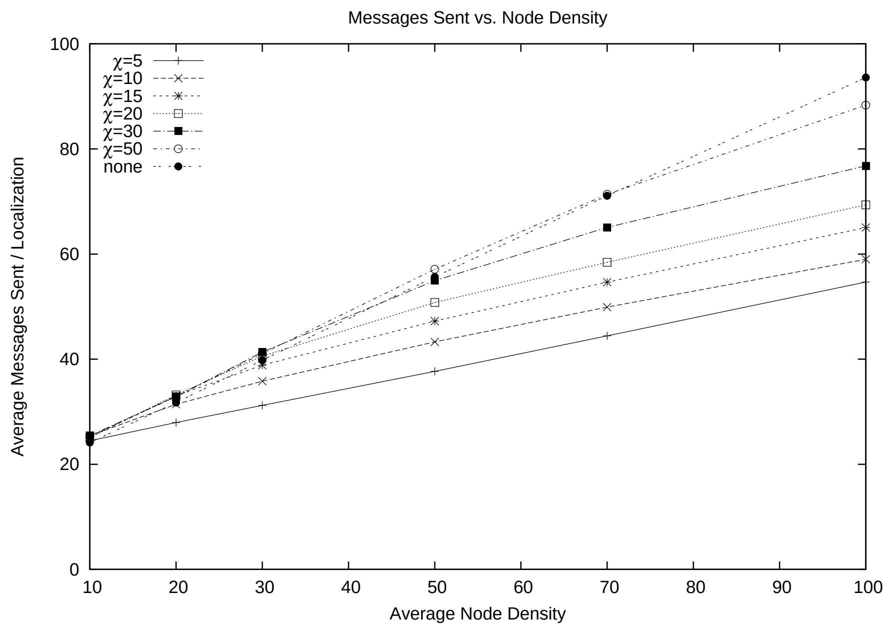

Figure 4.3: Messages sent with and without localization scheduling with varying average node densities.

to the mobile node without localization scheduling.

Although accuracy is better for unknown nodes initially when scheduling is not used, it comes at the cost of increased net energy usage by reference nodes. Figure 4.5 shows localization accuracy of the mobile node over an extended period of time, for different χ values. As will be seen in the next section, reference nodes all run out of energy at the same time when sleep scheduling is not used. However, with localization scheduling the moving target can be localized for much longer, and nodes run out of energy much more gradually. With $\chi = 5$, the highest accuracy is maintained for the longest period of time, since the network lifetime is significantly longer.

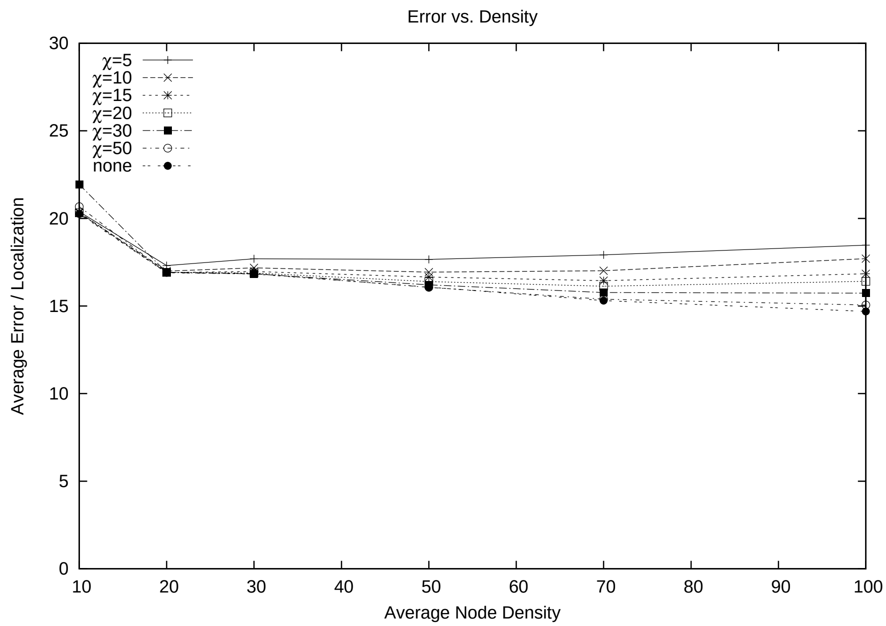

Figure 4.4: Localization error with and without localization scheduling with varying average node densities.

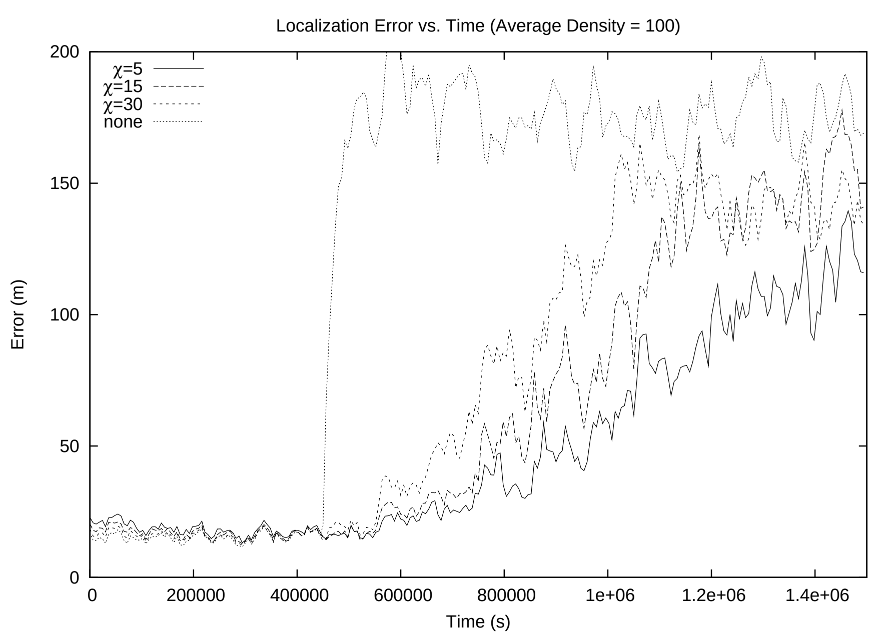

Figure 4.5: Localization error over time with and without localization scheduling. Average node density is 100.

4.3.3 Network Lifetime

When all nodes remain active, devices can be accurately localized; however, if all nodes run out of energy at once the network is useless, as was previously shown. When nodes alternate between active and sleeping states, however, mobile agents can be localized accurately for a much longer period of time, and the network remains useful much longer than it would have otherwise been without localization-scheduling. As seen in Figure 4.6, all nodes run out of energy within a very short window of time when all nodes remain active. However, when nodes are scheduled between active and sleeping modes, the network lifetime is significantly increased. When a lower minimum density is used, active nodes remain in the network for much longer to localize a moving target. In Figure 4.6, nodes run out of energy in groups at approximately each 100,000 seconds. This is due to the choice of the rotation time for reference nodes, which was selected to be 100,000 seconds in order to limit the number of times that the election algorithm needs to be run. If a smaller rotation interval were selected, we would notice smooth exponential decay as expected.

4.3.4 Localization Latency and Accuracy

As the number of nodes increase, the amount of computation time required by location estimators increases. By limiting node density with the proposed scheme, the amount of computation is limited which improves the rate at which an accurate solution is derived. In the mobile case, convergence latency is of utmost importance, as slow position estimates will be out of date the moment that they are computed, resulting in increased error. By limiting node density in a controlled way, we reduce the amount of information used to compute one's position to only the minimal necessary amount. Therefore, solving for one's current position using only a limited number of distance and position

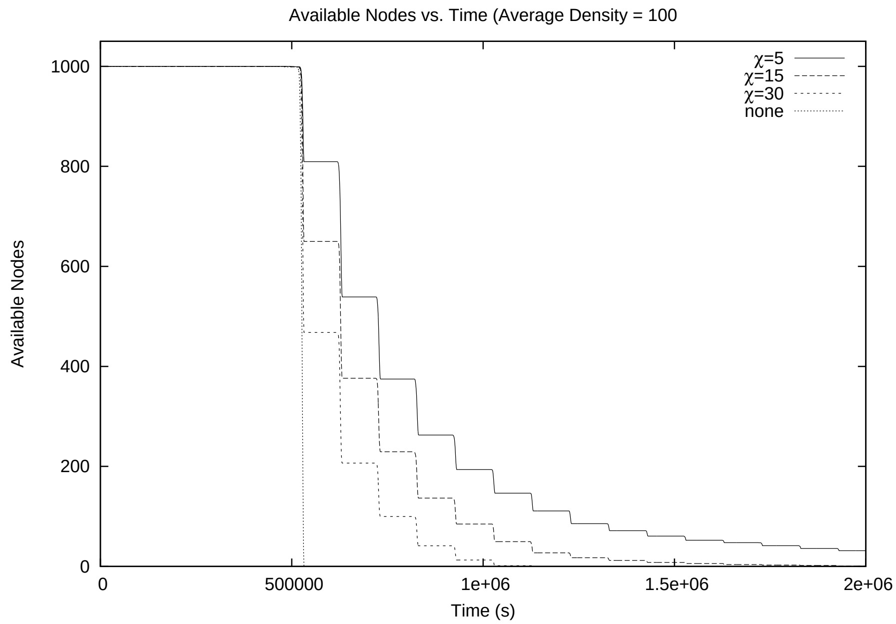

Figure 4.6: Remaining nodes with energy over time with and without localization scheduling. Average node density is 100.

measurements significantly reduces the computation time.

To show the effect that node density has on computation time, both MLE and trilateration computation with varying node densities on different hardware platforms were timed. To benchmark the localization overhead, random node locations and distance measurements were passed to the core localization algorithms, and system clock readings with microsecond accuracy were taken before and after the localization procedures. In Figure 4.7 we plot the average localization computation time on two different IA-32 processors, running at 3.0 GHz and 550 MHz, respectively, and on an XBow Imote2 sensor node with an Intel PXA271 processor running at 13 MHz. These three platforms have similar capabilities to a wide range of existing mobile hardware, including notebook computers, personal digital assistants (PDAs), and sensor nodes (motes), respectively. Due to system limitations, only the trilateration estimator was evaluated on the Imote2.

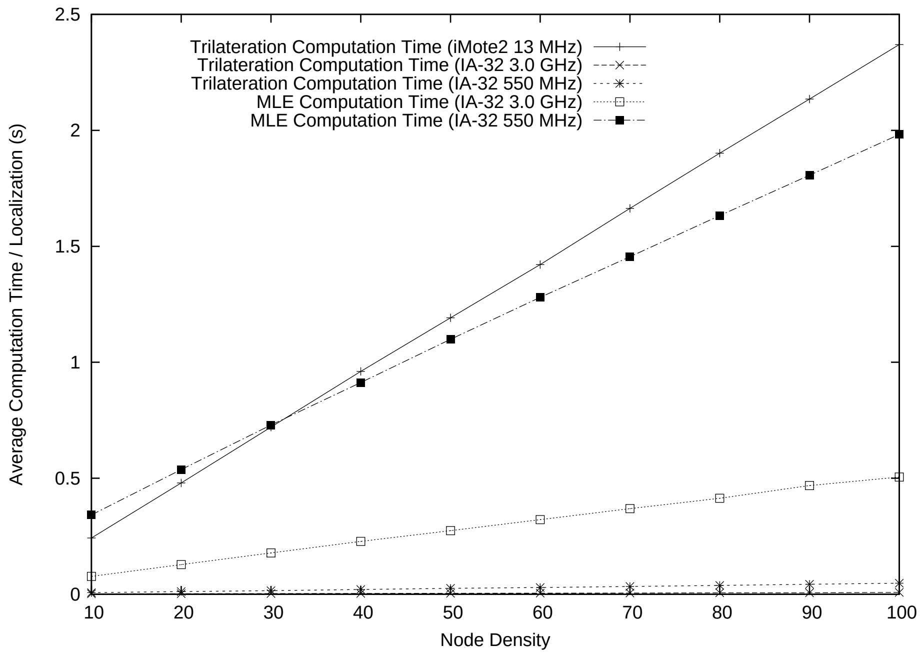

Figure 4.7: Average computation time for localization with varying node densities and computation platforms.

The important observation from Figure 4.7 is the linear increase in computation time as node density is increased, which will be present regardless of hardware architecture used. Also important is that trilateration is an order of magnitude faster to compute than the MLE, but is much less accurate (as was seen in Figure 4.1). Limiting node density therefore makes MLE much more accessible on mobile hardware, which will in turn help to reduce position error.

We simulate the scenario of a mobile node moving at various speeds between 5 m/s and 35 m/s, updating its location once per minute. When the mobile node computes its position there will now be a delay given by Figure 4.7 (the data from the IA-32 550 MHz system is used), which results in increasing error with computation time. Figure 4.8 shows the average error of the MLE and trilateration estimators with and without localization scheduling with an average node density of 100. At lower speeds (< 15 m/s)

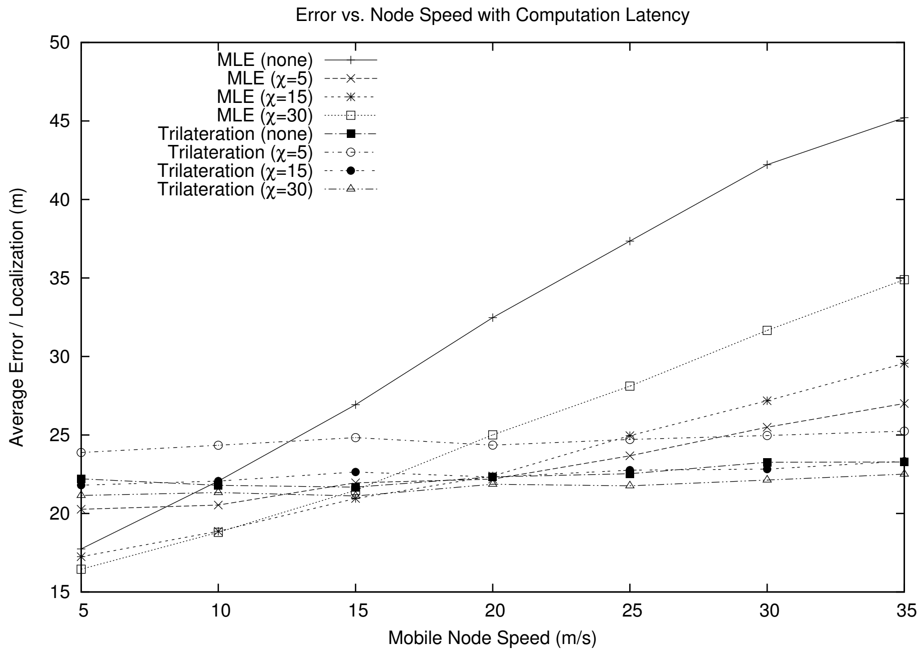

Figure 4.8: Localization error with MLE and trilateration estimators at varying speeds, with error contribution from computation latency. Average node density is 100.

better accuracy is achieved with the MLE estimator than with trilateration when node density is reduced using localization scheduling. At higher speeds, the MLE computation time increases error quickly, and so trilateration is more accurate. However, with both estimators we are able to reduce position error by adjusting the minimum number of active nodes, χ, accordingly.

4.4 Discussions

Existing localization schemes in wireless ad hoc networks rely on redundant measurements from multiple devices with known positions in order to reduce error. However, when node density is high this can result in excessive localization messages with minimal improvement on position accuracy. In this work a scheduling algorithm was presented to select a subset of active reference nodes to be used in localization, which has the effect of reducing message overhead, increasing network lifetime, and improving localization accuracy in dense mobile networks. We investigated the Cramér-Rao Lower Bound (CRLB) and existing single-hop localization techniques to determine the optimal average node density to ensure sufficient estimation accuracy. The correctness and effectiveness of the proposed scheme were evaluated through extensive simulation results, which showed that in dense networks localization messages were greatly reduced and network lifetimes were more than doubled, while maintaining high estimation accuracy. Furthermore, computational time of localization algorithms was reduced, which effectively decreases accumulated error due to computation latency when locating a mobile device.

Chapter 5

Location Error Estimation

5.1 Introduction

Many applications and protocols associated with ad hoc networks require precise location information as a precursor to their functioning, such as data mining in WSN, coverage, and routing. However, there is often a significant amount of positioning error associated with even the best localization systems [13], which can have a significant impact on the accuracy and efficacy of location-dependent applications. In this chapter a means for wireless devices to probabilistically determine the amount of error present in their estimated positions for a given localization system is provided, which can be incorporated into location sensitive applications to improve on their robustness and overall effectiveness. Work in this chapter is based on a recently published peer-reviewed conference paper [48].

A typical scenario for WSN consists of randomly deployed sensors collecting data and transmitting it to a base station for analysis [97]. If accurate location information is necessary for the proper interpretation of measured data, then inaccuracies of node positions can lead to false observations. By predicting the degree of localization error, one can assign a lower confidence or even reject sensed events associated with low position accuracy. Another fundamental problem in WSN is coverage, where we want to know if all points in a region are monitored by one or more sensors [101], so that additional sensors can be deployed to inadequately covered areas, or sensors can enter sleep mode to conserve energy in overly covered areas [62]. Most of these schemes assume that precise location information is available for calculation of coverage. However, in the presence of localization errors, additional coverage holes or overly redundant sensor deployment can occur. With estimates on the amount of localization error, overly covered or under covered regions can be avoided. Location information is also useful for geographic routing [100], where data is routed based on geographic locations instead of network addresses. With localization error estimation, nodes with larger position errors can be less used to avoid potentially inefficient paths. Location verification in secure localization schemes is an area of open research which aims to differentiate between errors due to malicious nodes and error inherent to the localization system itself [2, 90, 154], the latter of which can be characterized by a suitable error estimation method. Finally, when it is possible for nodes to estimate the amount of localization error in their neighbours, these estimates can be used in the localization scheduling problem which was seen in the previous chapter to decide on which regions can be localized with sufficiently low error so that that redundant reference devices can enter sleep mode.

There are two key contributions which are made to the localization problem in wireless ad hoc networks in this chapter. First, a model for location error variance in localization systems is proposed which wireless devices can use to estimate their true location error. The model is based on the observation that localization error variance behaves similarly to the theoretical lower bound on the variance of location estimators, given by the CRLB. The CRLB is easily computed locally, and is used in the location error variance model along with the number of available beacon nodes. The second contribution is a fully distributed scheme for nodes to determine the amount of error in their position estimates with a given probability, p, where p is an input thresholding parameter to the system. The scheme uses the proposed model of error variance and the cumulative distribution function (cdf) of localization error to probabilistically determine the amount of error in nodes' location estimates. Once known, nodes can compensate for this error in future applications which rely on location information.

5.2 Methods

5.2.1 Problem Statement

The problem under investigation in this chapter is referred to as the localization error estimation problem and can be stated as follows.

Definition (Localization Error Estimation Problem (1)): For a given wireless node $i \in \mathcal{N}$, and probability p, $0 < p < 1$, determine the minimum distance, d'_i, such that the amount of location error, $|\boldsymbol{\varepsilon}_i| = |\mathbf{z}_i - \hat{\mathbf{z}}_i|$, of i is less than or equal to d'_i with probability greater than or equal to p. This is given as follows.

$$d'_i(p) = \arg\min_{z} \left[\Pr\{|\boldsymbol{\varepsilon}_i| \leq z\} \geq p \right] \tag{5.1}$$

Solving (5.1) allows applications to have a certain level of confidence in how much localization error to expect, which in turn enables one to design more robust, fault tolerant systems where localization error can be handled accordingly. Rearranging (5.1), one obtains an alternate form of the localization error bound prediction problem.

Definition (Localization Error Estimation Problem (2)): For a given wireless node $i \in \mathcal{N}$, and distance d'_i, determine the minimum probability, p, such that the location error, $|\boldsymbol{\varepsilon}_i|$, of i is less than or equal to d'_i with probability greater than or equal to p. This is given as follows.

$$p(d'_i) = \Pr\{|\boldsymbol{\varepsilon}_i| \leq d'_i\} \tag{5.2}$$

This alternate form given by equation (5.2) allows applications to determine the probability at which the localization error is less than some specific value. For example, a sensing application may be interested in whether or not the localization error of a node is less than or equal to its sensing range to validate the accuracy of its sensed data.

5.2.2 Location Error Estimation

The solution to the localization error estimation problem will now be presented. The main contributing factors to localization error in ad hoc wireless networks are first presented. Based on these error inducing parameters, a model of localization error is then derived which is designed to estimate the true variance of localization systems based only on information which is locally collected by wireless devices during the course of a multi-hop localization run. This model of location error variance is then used by probabilistic methods at each node to estimate the minimum amount of localization error with a given probability, or alternatively, the probability of localization error being less than a given amount.

Error Inducing Parameters in Localization

There are a number of potential sources for localization error in wireless networks, which can be categorized as extrinsic and intrinsic [127]. Extrinsic error pertains to physical effects on the propagation environment, including fading caused by obstacles and Doppler shift due to movement. Intrinsic error is related to flaws within the hardware and software of wireless devices, preventing location estimators from achieving minimum variance.

In this work only intrinsic error sources are considered. Of these, the system parameters of interest are the number of nodes, $|\mathcal{N}|$, the number of beacons, $|\mathcal{B}|$, the average node density, ρ, and the average number of hops to beacon nodes. As was found in my own simulations and in the work of others [39, 69, 127], the most important intrinsic factors for localization error are the number of beacons and node density; therefore, we adopt a model of localization error based on these parameters.

Localization Error Model

From the asymptotic properties of the MLE, the estimators in equations (2.7) and (2.8) are asymptotically distributed according to $\hat{\mathbf{z}}_i \sim \mathcal{N}(\mathbf{z}_i, \sigma_i^2)$ for sufficiently large data records [77]. That is, with a sufficient number of RSS or TOA measurements, the estimator $\hat{\mathbf{z}}_i$ has a Gaussian distribution with mean $\mathbf{z}_i$, and variance equal to the CRLB, σ_i^2, evaluated at the true position of $\mathbf{z}_i$. In practice, however, the CRLB is overly optimistic so that localization systems do not exactly match it, and so the following model for localization variance is introduced which behaves closer to the actual variance of location estimation than the CRLB.

$$\varphi_i^2(\sigma_i^2, |\mathcal{B}|) = a\sigma_i^2 + b|\mathcal{B}| + c \tag{5.3}$$

The function in equation (5.3) takes the CRLB computed by node i, σ_i^2, given by equations (2.5) and (3.5), and the number of beacon nodes, $|\mathcal{B}|$, and scales it using the constants a, b and c.

The values of a, b and c are determined with the Monte Carlo method, where extensive localization simulations are performed prior to physical deployment of devices in order to obtain statistical data on the performance of the localization system to be used. A least squares estimator is then used to choose a, b and c to minimize the difference between the error model, φ_i^2, and the observed data from simulations. The steps for data generation for the Monte Carlo simulations are as follows.

1. Generate X independent network topologies, with nodes in $\mathcal{N} = \{\mathcal{N}_1 ... \mathcal{N}_X\}$, and varying numbers of beacon nodes.

2. Run the localization simulation Y times for each of the generated topologies to yield Y realizations of $\hat{\mathbf{z}}_i$ for each node $i \in \mathcal{N}$, where the jth realization of $\hat{\mathbf{z}}_i$ is denoted $\hat{\mathbf{z}}_{i,j}$.

3. For each node i, compute σ_i^2, and estimate the mean, $\widehat{E(\hat{\mathbf{z}}_i)}$, and mean squared error, $\widehat{\mathrm{MSE}(\hat{\mathbf{z}}_i)}$, of $\mathbf{z}_i$, given by

$$\widehat{E(\hat{\mathbf{z}}_i)} = \frac{1}{Y} \sum_{j=1}^{Y} \hat{\mathbf{z}}_{i,j} \tag{5.4}$$

$$\widehat{\mathrm{MSE}(\hat{\mathbf{z}}_i)} = \frac{1}{Y} \sum_{j=1}^{Y} (\hat{\mathbf{z}}_{i,j} - \widehat{E(\hat{\mathbf{z}}_i)})^2 \tag{5.5}$$

Results from the simulation runs are then used as data for a least squares estimator of a, b and c which minimizes the squared error between the variance model, φ_i^2, and the actual mean squared error of the location estimator, $\widehat{\mathrm{MSE}(\hat{\mathbf{z}}_i)}$, given by

$$\hat{\boldsymbol{\theta}} = [a\ b\ c]^T = \arg\min_{a,b,c} \sum_{i \in \mathcal{N}} (\widehat{\mathrm{MSE}(\hat{\mathbf{z}}_i)} - (a\sigma_i^2 + b|\mathcal{B}| + c))^2 \tag{5.6}$$

The solution to the least squares estimator in equation (5.6) is given by,

$$\hat{\boldsymbol{\theta}} = (\mathbf{H}^T\mathbf{H})^{-1}\mathbf{H}^T\mathbf{x} \tag{5.7}$$

where,

$$\mathbf{H} = \begin{bmatrix} \sigma_1^2 & |\mathcal{B}|_1 & 1 \\ \sigma_2^2 & |\mathcal{B}|_2 & 1 \\ \vdots & \vdots & \vdots \\ \sigma_{|\mathcal{N}|}^2 & |\mathcal{B}|_{|\mathcal{N}|} & 1 \end{bmatrix}, \mathbf{x} = \begin{bmatrix} \widehat{\mathrm{MSE}(\hat{\mathbf{z}}_1)} \\ \widehat{\mathrm{MSE}(\hat{\mathbf{z}}_2)} \\ \vdots \\ \widehat{\mathrm{MSE}(\hat{\mathbf{z}}_{|\mathcal{N}|})} \end{bmatrix} \tag{5.8}$$

Here, the calculated CRLB, the number of available beacon nodes and the mean squared localization error of a given node $i \in \mathcal{N}$ are given by σ_i^2, $|\mathcal{B}|_i$ and $\widehat{\mathrm{MSE}(\hat{\mathbf{z}}_i)}$, respectively.

The localization error variance of a particular node i is then estimated to be φ_i^2, requiring only knowledge of the estimated locations of the neighbours of i, $N(i)$, in order to compute σ_i^2, the number of beacons nodes in the system, $|\mathcal{B}|$, and values for the constants a, b and c, which are determined *a priori* to physical deployment of the network via localization simulation performed in the intended environment.

5.2.3 Location Error Estimation Method

In the given network model it is assumed that position estimates are unbiased, meaning that $E(\hat{\mathbf{z}}_i) = \mathbf{z}_i$. Therefore, the mean localization error $\boldsymbol{\varepsilon}_i$ is equal to zero, since

$$E(\boldsymbol{\varepsilon}_i) = E(\mathbf{z}_i - \hat{\mathbf{z}}_i) = \mathbf{z}_i - \mathbf{z}_i = \mathbf{0} \tag{5.9}$$

For the localization error estimation problem one must determine the minimum probability, p, such that $Pr(|\boldsymbol{\varepsilon}_i| \leq d) \geq p$ holds, for a given distance, d_i'. As $\hat{\mathbf{z}}_i$ is asymptotically Gaussian distributed according to $\mathcal{N}(\mathbf{z}_i, \varphi_i^2)$, $\boldsymbol{\varepsilon}_i$ is also Gaussian, with $\mathbf{0}$ mean and variance φ_i^2, given by $\mathcal{N}(\mathbf{0}, \varphi_i^2)$. For the problem at hand only the error distance is of interest, not direction. The magnitude (distance) of the error $|\boldsymbol{\varepsilon}_i|$ then follows the half-normal distribution. Therefore, the probability of a node i being localized with error less than or equal to d is computed using the cdf of the half-normal distribution.

$$\Pr\{|\boldsymbol{\varepsilon}_i| \leq d\} = \frac{1}{\varphi_i}\sqrt{\frac{2}{\pi}}\int_0^d \exp\left(-\frac{u^2}{2\varphi_i^2}\right)du \tag{5.10}$$

Substituting equation (5.10) into equations (5.1) and (5.2), solutions are obtained for both forms of the localization error bound prediction problem in equations (5.11) and (5.12) respectively.

$$d_i'(p) = \underset{0\leq z\leq s}{\arg\min}\left[\frac{1}{\varphi_i}\sqrt{\frac{2}{\pi}}\int_0^z \exp\left(-\frac{u^2}{2\varphi_i^2}\right)du \geq p\right] \tag{5.11}$$

$$p(d_i') = \frac{1}{\varphi_i}\sqrt{\frac{2}{\pi}}\int_0^{d_i'} \exp\left(-\frac{u^2}{2\varphi_i^2}\right)du \tag{5.12}$$

The minimization problem in equation (5.11) can be solved trivially since we restrict the search to less than the size of the network area, s (otherwise position estimates would not be useful). These equations can be computed locally by wireless devices by computing φ_i^2 from equation (5.3), where a, b, c are known, and only position estimates of one's single hop neighbours and the number of beacons are required. When run in conjunction with a localization scheme, this information can be obtained without requiring additional communication.

As an example, the cdf from equations (5.11) and (5.12) is shown in Figure 5.1 with the value of φ_i set to 5.0 and 10.0. If we set $p = 0.7$, we see that with $\varphi_i = 5.0$ the minimum distance such that the error is less than that distance is $d_i'(p) = 5.2$, whereas when $\varphi_i = 10.0$ the minimum distance increases to $d_i'(p) = 10.4$. In general, the higher the values of φ_i^2 and p, the higher the value of $d_i'(p)$.

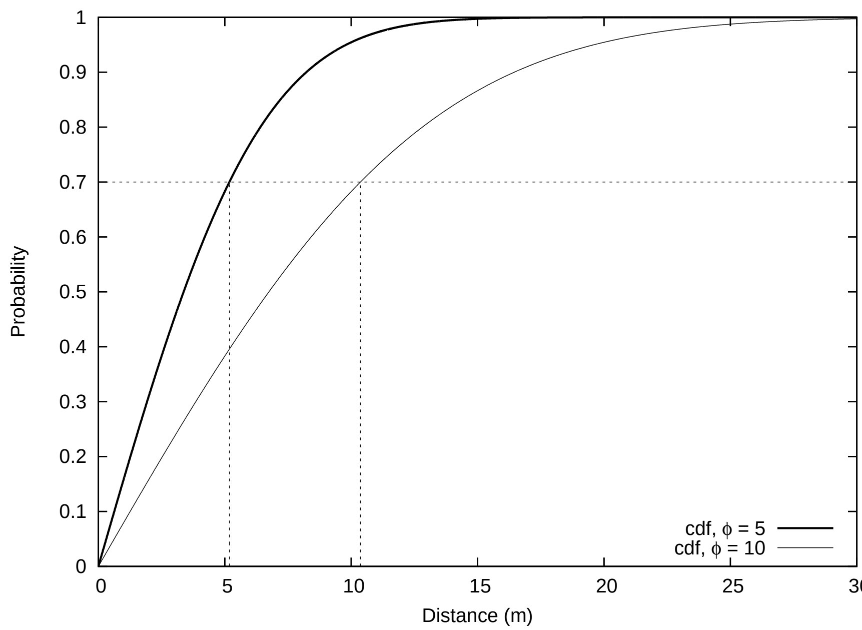

Figure 5.1: cdf of half-normal distribution with $\varphi = 5$ and $\varphi = 10$ and the system parameter $p = 0.7$.

5.3 Results

In this section simulation results are presented which verify the correctness of the presented localization error estimation algorithm. Implementation is done using the network simulator *ns-2* version 2.33. An implementation of a localization scheme similar to that in [126] was used, in which all unknown nodes initially estimate their locations using the positions and number of hops to available beacon nodes, followed by an iterative refinement phase where initial positions of neighbouring nodes are used as intermediary reference devices to improve accuracy. It should be noted however that the methods derived in this paper do not depend on any specific localization scheme, but only on the limitations of the underlying measurement model, and so the selected localization implementation is of secondary importance.

Nodes each have a radio range of 50 m [137] and are deployed randomly with a uniform distribution over a squared area of size $[0, s] \times [0, s]$, where node density is controlled by varying s. Differing percentages of beacon nodes, which know their positions at all times, are randomly selected from variable sized node populations.

5.3.1 Error Variance Model Fitting

The steps outlined in the previous section for data generation for Monte Carlo simulation are used to find values for the constants a, b and c which best fit the variance model given by equation (5.3).

The total number of nodes in the network is varied at 200, 300, 400 and 500 nodes, the percentage of beacon nodes is set to 5%, 10%, 15%, 20% and 25% of the total nodes, average node density is set to 15, 30, 45, 70 and 85 nodes, and a random seed value which affects node deployment topology is varied from 1 to 10. This results in the generation of X independent network topologies with varying properties, where $|X| = 4{\cdot}5{\cdot}5{\cdot}10 = 1000$.

For each of the X independent topologies, $Y = 32$ runs of the implemented localization simulation are executed, and we store for each node i its estimated position, $\hat{\mathbf{z}}_i$, its calculated CRLB value, σ_i^2, and its number of available beacon nodes, $|\mathcal{B}|_i$. From the Y realizations of $\hat{\mathbf{z}}_i$, the MSE is calculated according to equation (5.5). Finally, all data are used by the least squares estimator given by equation (5.7), yielding values for a, b and c.

Obtained results for the model fit are summarized in Table 5.1. It is noticed that the scaling parameters are significantly larger when RSS is used as compared with TOA, and that b and c are almost negligible in the TOA situation. This indicates that the error variance approaches the CRLB much more closely with TOA and that there is very little dependance on the number of available beacon nodes in this modality.

The average MSE of nodes with varying node densities across the given X topologies

	a	b	c
RSS	4.7681	-0.8787	85.1189
TOA	1.4595	-0.0016	-0.0014

Table 5.1: Computed values of a, b and c

is shown in Figures 5.2 and 5.3 for the RSS and TOA cases, respectively. Alongside the MSE curves are the average computed values from the proposed error model, φ_i^2, using the obtained values of a, b and c. These graphs clearly show that the error model closely matches the measured mean squared localization error across a range of average node densities. However, it is noticed for the TOA case that MSE increases by a much higher amount at lower node densities than does the error model, but the two follow each other extremely closely when the average node density is greater than 30. This is due to the presence of outliers at lower node densities in which unknown devices, which are typically located close to the extremities of the network area, are poorly connected to beacon devices resulting in degenerate configurations with high localization error, skewing the average MSE. These degenerate configurations are not present when node density is sufficient, and are not as noticeable when RSS is used since error is much higher, so that these effects are relatively negligible. The outlier detection problem, which aims to detect and reject the small number of outliers that can significantly degrate overall localization accuracy, is an area of ongoing research [68].

The closeness of fit of the proposed error model is tested by using the values of a, b and c obtained from the initial X topologies in Z newly generated topologies which differ from the initial set of X topologies by varying the deployment seed value from 11 to 20 (so that $|Z| = 1000$). This simulates the scenario of generating an initial set of training data in the intended environment of interest in order to determine the fit parameters a, b, c, followed by the actual deployment which is completely independent, and makes

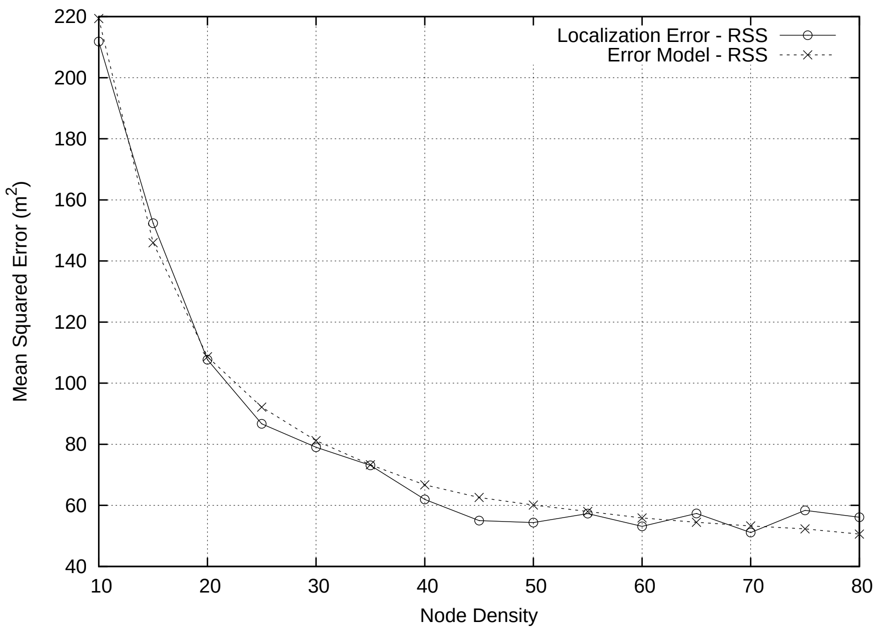

Figure 5.2: Localization error compared with estimated error from model - RSS.

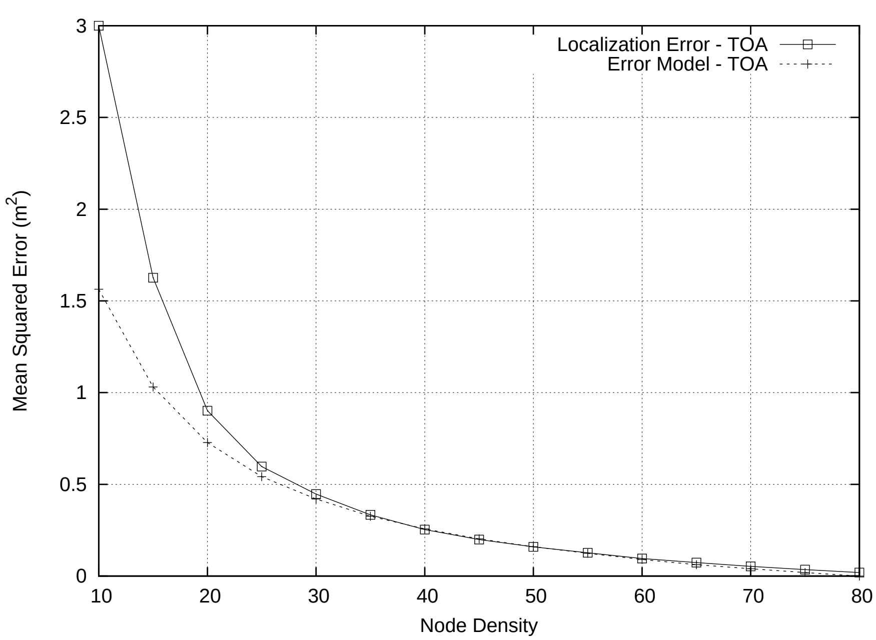

Figure 5.3: Localization error compared with estimated error from model - TOA.

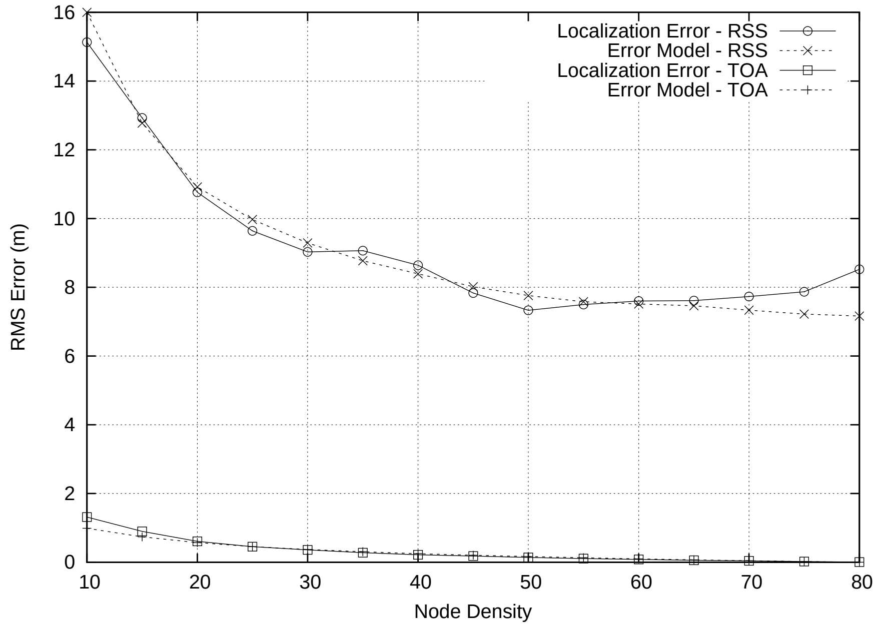

Figure 5.4: Localization error compared with estimated error from model with new network topologies.

use of the parameters found through the training set to estimate the error variance. Figure 5.4 shows the average RMSE of localization error compared with the proposed error model for both the RSS and TOA measurement modes in the Z new topologies. With this it can be seen that the error model successfully estimates localization error deviation in an independent set of deployments, which shows the feasibility of estimating localization error variance in real-world environments, provided that the system model and deployment strategy of the training simulations describe the real world scenario with sufficient accuracy.

5.3.2 Localization Error Estimation

The next set of experiments evaluate the effectiveness of the localization error estimation methods described by equations (5.11) and (5.12). Graphs with 300, 400 and 500 nodes are simulated, average node densities of 30, 45 and 70, and percentages of beacon nodes of 10% and 20%, with 10 random deployment seeds per configuration.

For each of the $3 \cdot 3 \cdot 2 \cdot 10 = 180$ independent topologies we begin by running the localization scheme, followed by computing the minimum distance, d_i', such that the amount of location error, $|\boldsymbol{\varepsilon}_i|$, is less than or equal to d_i' with probability greater than or equal to p using equation (5.11), for $p = 0.1, 0.2, ..., 0.9, 0.95, 0.99$. The average results of computing d_i' over given node densities at the different values for p are shown in Figure 5.5 for the TOA case. We can observe that at lower node densities the minimum distance at which localization error is bounded increases rapidly, especially when a higher probability of localization is desired. This means that we require higher node densities in order to obtain a high probability of localization within tight distance bounds. Similarly, when a high probability of localization is required, the distance at which localization error is bounded at that probability increases, and increases more rapidly as p approaches 1. The results with RSS show a similar trend, but with the computed distances being higher due to the higher error associated with RSS range measurements.

Next, the localization simulation is run 1000 times on each of the generated topologies for statistical averaging. The amount of error in the estimated positions is stored for each run, as well as the estimated variance given by the proposed error model. For each node i, the histogram of its localization error is generated, yielding its estimated pdf. The cdf for each node can then be estimated from the histogram by integrating all error values less than or equal to the desired distance. To test the effectiveness of the localization error estimation solution we then take the estimated cdf evaluated at the computed value of $d_i(p)'$ (i.e. the total number of location estimates $\leq d_i(p)'$) for a given probability p, where $d_i(p)'$ is computed from equation (5.11) (as was shown in Figure 5.5), and compare the result with p. This gives the actual probability of the

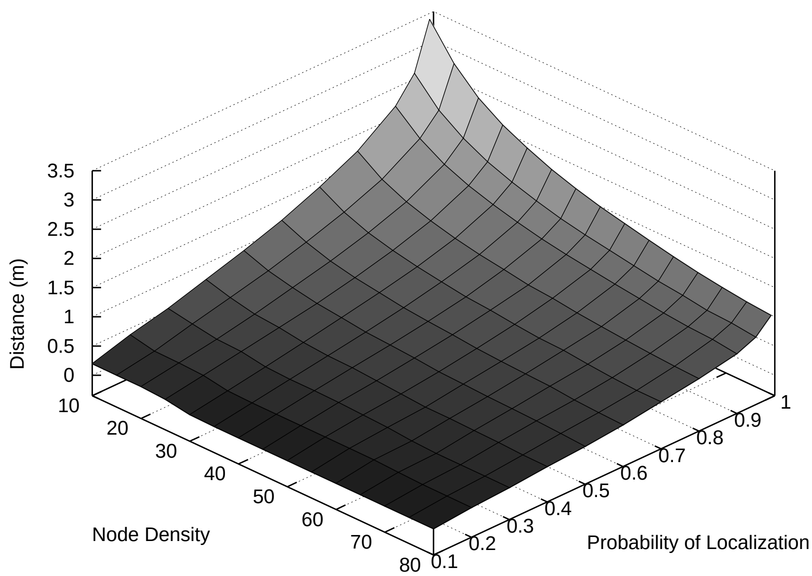

Figure 5.5: Estimated localization error at given probabilities - TOA.

localization error being less than or equal to $d_i(p)'$ which is obtained from the cdf of the 1000 localization runs, as compared to the selected probability p. Figures 5.6 and 5.7 show the actual probability of localization error being less than or equal to $d_i(p)'$ versus the chosen probability, p, averaged over the given node densities for the RSS and TOA cases, respectively. With a perfect error estimator, the chosen probability would match exactly the actual probability of localization within that error. Notice that with RSS the error bound tends to be slightly over-estimated in that there is a higher probability than p of the error being less than $d_i(p)'$, indicating that $d_i(p)'$ should have been chosen to be smaller. The opposite is the case when TOA is used, in that error bound is slightly under-estimated. In addition, there is a slight tendancy of increasing probability of localization compared with the chosen probably with increasing node densities in the RSS, while the probability decreases with density with TOA. In spite of this however, good correlation is found between the actual and selected probabilites across the range of node densities,

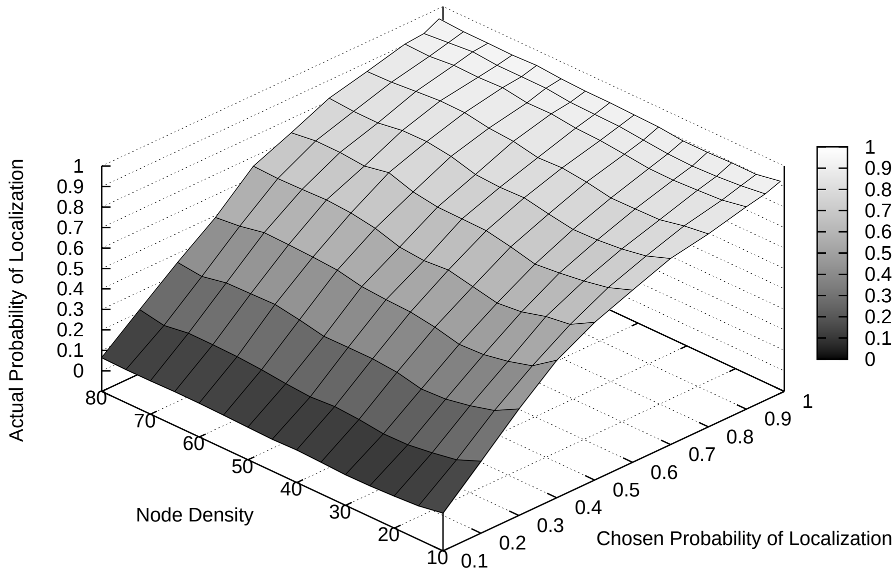

Figure 5.6: Actual probability of localization error less than estimated localization error, d_i', for different node densities - RSS.

especially considering the dramatic variation of MSE across node densities as was seen previously in Figures 5.2 and 5.3,

The average over all node densities is shown in Figure 5.8, which demonstrates that although there is some discrepency between chosen and actual probabilities over the different node densities, on average a good fit is obtained. This is a limitation of the least squares fitting procedure used, in that the values found for a, b, c are an average best fit for all possible configurations, but do not work perfectly over the entire range. It is also observed in the RSS case that when a higher probability of localization within $d_i(p)'$ is desired the chosen and actual probabilities do not match as well due to the inherent randomness of localization which prevents the actual probability from reaching unity. With TOA on the other hand, error estimation appears to be more effective at higher probabilities. Overall it is observed that the estimated error at the chosen probabilities

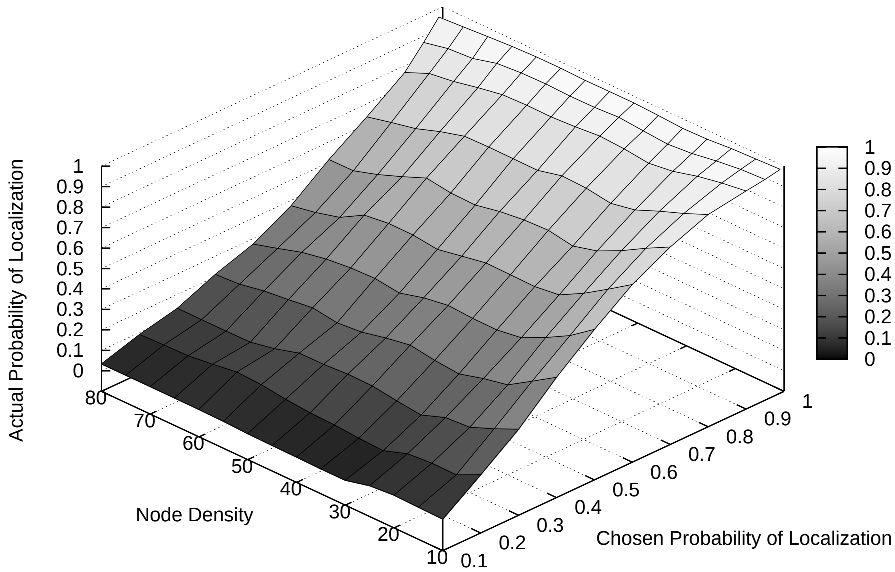

Figure 5.7: Actual probability of localization error less than estimated localization error, d_i', for different node densities - TOA.

appear to match the actual probabilities on average within ± 0.1, and slightly better when using TOA, which should be acceptable for use in location dependent applications.

We next evaluate the effectiveness of the alternate form of the location error estimation problem which takes as input a given distance, d_i', and determines the minimum probability, $p(d_i')$, such that localization error is less than or equal to that distance, given by equation (5.12). d_i' is varied from 2 m to 44 m at 2 m intervals in the RSS case, and from 0.2 m to 4 m at 0.2 m intervals with TOA, and computed the average value of $p(d_i')$ over the given node densities, shown in Figure 5.9 for RSS (TOA shows similar behavior). It is observed that at the same distance there is a higher probability of localization error being less than that distance the higher the node density is. For example, there is a 0.9 probability of being localized within 15 m when the node density is 30, while the probability is as low as 0.7 on average with only 10 neighbours. These estimated

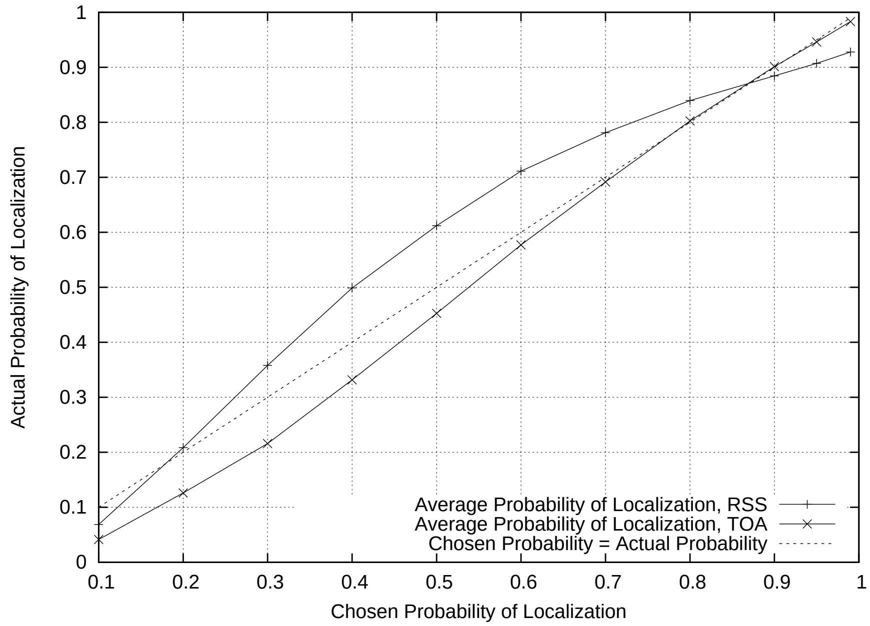

Figure 5.8: Actual probability of localization error less than estimated localization error, d_i', averaged over all node densities.

probabilities are then compared with the actual probabilities of error less than or equal to d_i' as measured from the 1000 localization runs averaged over all node densities, shown in Figures 5.10 and 5.11 for both RSS and TOA measurement modes, respectively. When TOA is used very accurate results are achieved, with the estimated and actual probabilities being almost identical. With RSS measurements, results are not quite as accurate as we underestimate the probability of localization within shorter distances ($d_i' \leq 15$) and observe that the estimated probability increases at a rate greater than the actual probability, showing an imperfect fit with the proposed error model. This should be expected, however, due to the significantly larger error present in RSS based localization systems, and is therefore still acceptable for location dependent applications since errors in the location error estimation scale relative to the magnitude of overall location error. Also important to note with both measurement modes is the fact that initially when the

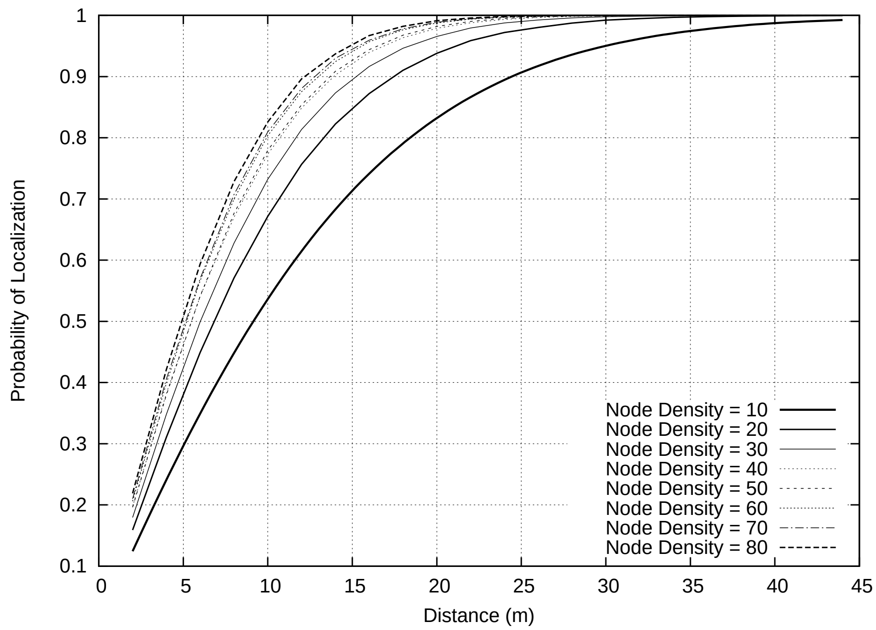

Figure 5.9: Estimated probability of localization error less than given distances - RSS.

desired error bound is set very small, the probability of localization within that bound is relatively low. The probability increases rapidly at first with increasing error distance, then reaches asymptotic behavior as $p(d_i')$ approaches 1. This may provide a good starting point for the selection of the system parameters p and d_i' from equations (5.11) and (5.12), respectively, for use in future applications. Specifically, based on the asymptotic conditions seen in Figures 5.10 and 5.11, selecting p below 0.9, and likewise d_i' below 15 m for RSS, or 1.25 m for TOA, would be good choices, since there is diminishing value in exceeding these ranges.

5.4 Discussions

Many ad hoc network applications rely on nodes having accurate knowledge of their geographic locations. However, inherent in all localization systems is a degree of error in

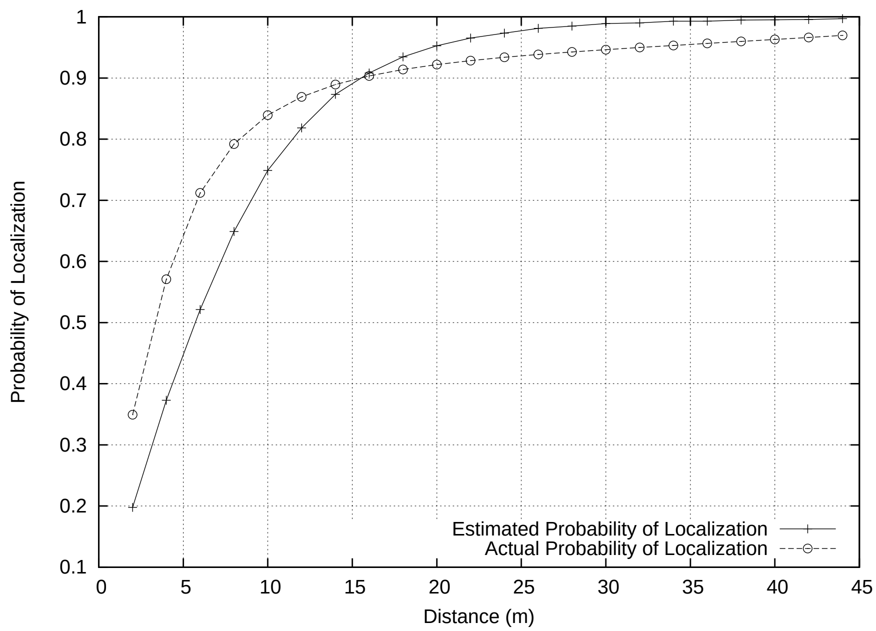

Figure 5.10: Actual probability of localization error being less than distance given by localization error estimate, compared with estimated probability - RSS.

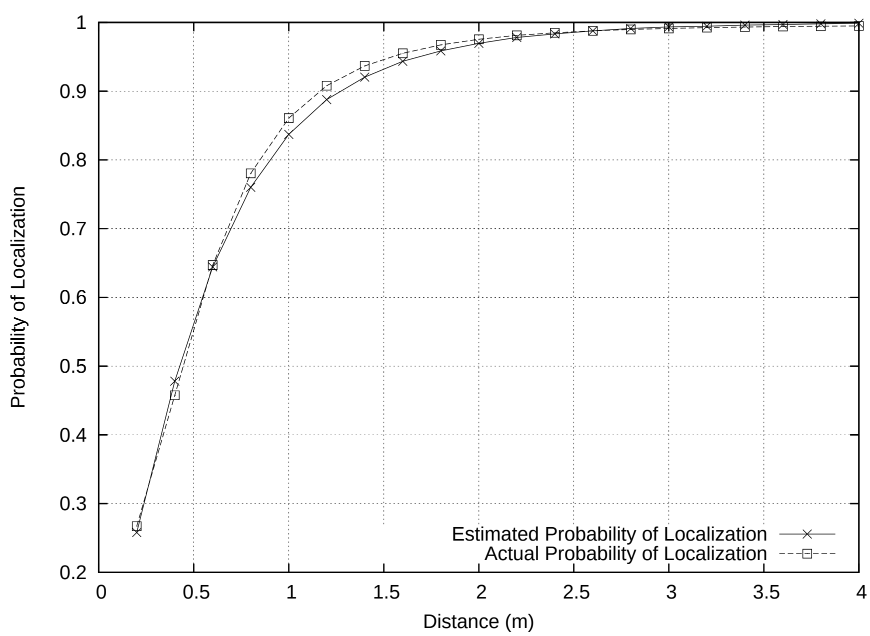

Figure 5.11: Actual probability of localization error being less than distance given by localization error estimate, compared with estimated probability - TOA.

computed positions, which can compromise the accuracy and efficiency of location dependent applications and protocols. In this chapter a means to estimate position error from localization systems was developed, which can be incorporated into location-dependant applications to improve their robustness and overall quality of service. A model for localization error variance based on the CRLB has been put forth. Coefficients which give best fits between the model and the actual location error variance using both time of arrival (TOA) and received signal strength (RSS) distance measurements were determined by a least squares estimator over repeated localization simulations. This estimated variance was then integrated into the pdf of localization error, modeled as a Gaussian random variable, and its associated cdf in order to determine the minimum distance such that localization error is less than that distance with a given probability; or alternatively, the probability that localization error is less than a given distance. Simulation results have shown that the proposed error variance model closely matches the localization MSE, especially as node density is increased due to the asymptotic optimality of the MLE used. Through extensive Monte Carlo simulations, it was determined that we can successfully estimate the upper bound on localization error with a given probability by comparing it with the actual probability of localization error being less than that upper bound. Results showed that the actual and given probabilities correlated within $p = \pm 0.1$. Similarly, we successfully estimated the probability of localization error being less than a given distance, with the estimated and actual probabilities of error less than that distance correlating well, especially when TOA measurement is used. In general, localization error can be better estimated when using TOA measurements as compared with RSS due to the reduced noise contribution in these measurements. However, although error estimates are not as accurate in RSS systems, they are likely even more useful since localization error is proportionally higher, further the necessitating the need to properly handle it. The methods in this chapter are a promising tool for helping to quantify error in localization systems, which in future work can be integrated into existing applications such as coverage and routing protocols, and sensor network queries to increase their reliability and accuracy. Additionally, future work is required to improve the proposed methods by examining sources of extrinsic error in the propagation environment, as well as to further validate the location error estimation system in a physical testbed of wireless devices.

Chapter 6

Improved Localization Scheduling with Location Error Estimation

6.1 Introduction

In this chapter the localization scheduling problem which was previously described in Chapter 4 is further investigated, whose solution employed a sleep scheduling scheme which reduces node density while maintaining acceptable localization accuracy. Minimum network coverage to maintain sufficient localization accuracy was determined experimentally, and a distributed scheduling scheme was presented which ensures this minimum node density. In this chapter, the previous localization scheduling scheme is extended by providing a more analytical method to determine the minimum node density for sufficient location estimation accuracy. We make use of a method for estimating the amount of localization error within a certain probability which was described in Chapter 5. When the estimated localization error of a node is greater than a given minimum threshold, neighbouring nodes are eligible to become reference nodes. In a similar way as the previous scheme, eligible nodes wait for a random amount of time before becoming references to avoid activation of excessive devices which are not needed for localization. Simulation results show that with the new scheme localization error and message overhead are reduced, while energy-efficiency and network lifetimes are substantially increased. Work in this chapter is based on a recently published peer-reviewed conference paper [50].

6.2 Methods

6.2.1 Problem Statement

A new definition of the localization scheduling problem is given, which is adapted from the original definition in Chapter 4 to incorporate the location error estimation method from Chapter 5.

Definition (Localization Scheduling Problem (2)): Given a network with unknown nodes $\mathcal{U}$, settled nodes $\mathcal{S}$, and beacon nodes $\mathcal{B}$, where nodes can join $\mathcal{U}$ at any time, either from leaving $\mathcal{S}$ due to node movement, or by new nodes joining the network, select a set of *reference* nodes $\mathcal{R} \subseteq \mathcal{S} \cup \mathcal{B}$, such that only nodes in $\mathcal{R}$ are used in estimating the positions $\hat{\mathbf{z}}_i$ of nodes in $i \in \mathcal{U}$, while the amount of location error $|\boldsymbol{\varepsilon_i}| = |\mathbf{z_i} - \hat{\mathbf{z}}_i|$ remains below distance D with probability greater or equal to P, where D and P are threshold constants.

In order to determine whether or not the amount of location error $|\varepsilon_i|$ is less than some constant D with a certain probability, we make use of location error estimation which was given in Chapter 5.

6.2.2 Localization Scheduling Algorithm

As with the previous scheduling scheme, the localization scheduling algorithm in this section consists of four main phases. First, information about one-hop neighbours is exchanged after running the initial localization procedure. With knowledge of one-hop neighbours, nodes can then locally compute their eligibility to become reference devices. After waiting for a random period of time, eligible reference nodes announce to their neighbours that they will become references for future localization updates, while all other devices enter into sleep mode to conserve energy. Finally, the set of active reference nodes is rotated periodically so that energy is dissipated evenly throughout the network, thus preventing coverage holes.

Reference Node Decision

In the initial phase of the proposed scheme, a DV-Hop based algorithm [126] is run so that all nodes are in $\mathcal{S} \cup \mathcal{B}$. Nodes exchange positions with their one-hop neighbours, requiring only a single message transmission per node. Once position information is known for one's neighbours, a node is able to determine if it is eligible to become a reference node using location error estimation. If there are single-hop neighbours that have location error estimates greater than the constant D with the given probability P, then a node is eligible to become a reference by the following rule.

Definition (Reference Node Eligibility Rule (2)): A settled node $i \in \mathcal{S}$ or beacon node $i \in \mathcal{B}$ is eligible to become a reference node $i \in \mathcal{R}$ if its estimated location error is greater than D with probability greater than or equal to P, or if one of its neighbours $j \in N(i)$ has estimated location error greater than D with probability greater than or equal to P, for a given distance D and probability P, $0 < P < 1$. This is expressed mathematically by,

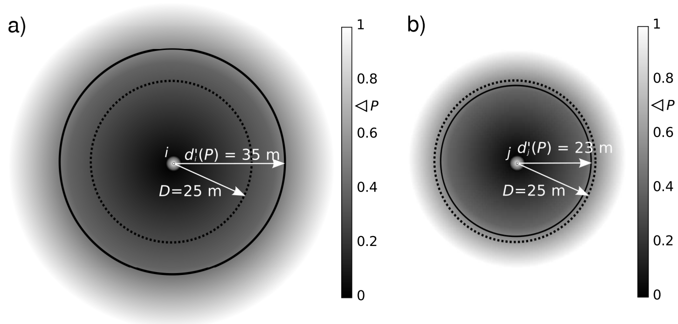

Figure 6.1: Example of eligibility rule with $D = 25$ and $P = 0.7$. a) Node i is eligible because $d'_i(0.7) = 35m > D = 25m$. b) Node j is not eligible because $d'_j(0.7) = 23m < D = 25m$.

$$i \in \mathcal{R} \Leftrightarrow (d'_i(P) > D) \vee (\exists j \in N(i) : d'_j(P) > D) \tag{6.1}$$

The location error estimates in equation (6.1) are calculated from equation (5.11), where the CRLB value given by equation (2.5) is computed using the current list of neighbouring reference nodes which node i is aware of. An example of the eligibility rule is shown in Figure 6.1, where node i is eligible because $d'_i(P) > D$ (assuming that all of i's neighbours have $d'(P) > D$ as well), and node j in not eligible since $d'_j(P) < D$. Initially there will not be any active reference nodes, and so all devices will be eligible to become references. As was done in the previous scheme, to avoid the over wake-up problem eligible nodes wait for a randomized delay time before announcing their decision to their neighbours. When this delay has passed, if nodes are still eligible they become references nodes; otherwise, they are scheduled to sleep for a period of time. The delay time is a function of a node's maximum possible location error estimate (error estimate assuming that all neighbours are active references) and remaining energy, and is given as follows.

$$delay_i = \left[\left\lceil \frac{d_i'^{max}(P)}{D} \right\rceil + \left[1 - \frac{E_r}{E_t} \right] + R \right] \times T \tag{6.2}$$

The first term in equation (6.2) looks at maximum value of the localization error estimate of i, $d_i'^{max}(P)$, using all available neighbours as reference nodes, and is normalized to the constant D. Lower error estimates result in shorter delay times, so that nodes with low location error estimates are more likely to become references. This ensures a more uniform distribution of references nodes across the network, since nodes with higher error estimates are more likely to become references regardless of delay time due to the eligibility rule. The remainder of the delay function is identical to that which was seen in equation (4.1).

Finally, to achieve accurate localization for as long as possible, we must periodically rotate the active set of reference nodes so that no devices are depleted too quickly, creating coverage holes. The reference node rotation is identical to that in Chapter 4, involving a rotation time T_r after which all nodes wake up and a new set of active reference nodes is selected. The only modification is that position information from one-hop neighbourhoods are exchanged prior to beginning a new reference node selection round so that the new eligibility rule can be recalculated.

The updated localization scheduling algorithm is given in Algorithm 6.1. The algorithm structure is similar to that in Chapter 4; therefore we will point out the differences found in this version. In the exchange of *HELLO* messages (lines 1-6), position information is exchanged between neighbours, and in the exchange of *REFERENCE* messages (lines 7-14) information regarding the current reference nodes is distributed, and decisions on eligibility are based on the new eligibility rule which involves estimating the location error. The procedure *estimateError* (lines 11, 17, 21) computes the location error estimate according to equations (2.5) and (5.11). Nodes wait for the delay given by equation (6.2) (lines 17-19), then check their eligibility to become references (lines 22, 36-40) by estimating the localziation error using the currently active set of reference nodes.

6.3 Results

Implementation and evaluations details of the proposed algorithm are carried out using the *ns-2* network simulator. We use 1000 network devices, each with a radio range of 50 m [137], deployed uniformly over a squared area of size $[0, s] \times [0, s]$, where average node density is controlled by varying s. A refinement-based localization scheme similar to that of Savarese et al. [126] is used, where twenty beacon nodes are selected at random which know their positions at all times.

To obtain values for the coefficients a, b and c from equation (5.3), 10 random topologies were generated for average node densities between 15 and 100, and the localization procedure was run with 32 random seed values on each topology. From these simulation runs, the average mean squared error on localization and the CRLB from equation (2.5) were calculated, and values for a, b and c were found using a least squares procedure to fit the CRLB to the mean squared error using equation (5.3).

The implementation follows the pseudo-code in Algorithm 6.1. The beacon nodes initiate the localization scheme so that all unknown nodes become settled and have estimated positions. The same scenario as was seen in Chapter 4 is then used; namely a single mobile node moving at a constant speed of 10 m/s requesting position updates once per minute. We then measure the number of localization messages transmitted, localization error of the mobile node, and energy expended by the network with and without localization scheduling.

Algorithm 6.1 - Localization Scheduling Algorithm (2)

▷ **Input:**
INITIATOR **or** $msg_i = HELLO(\hat{\mathbf{z}}_j)$.
▷ **Action:**
$positions_{i,j} \leftarrow msg_i.\hat{\mathbf{z}}_j$;
if $sentHello_i =$ **false then**
    $sentHello_i \leftarrow$ **true**;
    Send $HELLO(\hat{\mathbf{z}}_i)$ to $N(i)$;
[Re]Start $timer_i(0,\ delay_{max})$

▷ **Input:**
$msg_i = REFERENCE(\text{isReference},\ d'_j)$.
▷ **Action:**
$d'_{i,j} \leftarrow msg_i.d'_j$;
if msg_i.isReference **then**
    $references_i \leftarrow references_i \cup$ **sender**;
    $d'_i \leftarrow estimateError(\{positions_{i,j} : j \in references_i\})$;
    if $d'_i \leq D$ **and** $hasMinimum_i =$ **false then**
        $hasMinimum_i =$ **true**;
        Send $REFERENCE(isReference_i, d'_i)$ to $N(i)$;

▷ **Input:**
$timer_i$(ID,time) timeout.
▷ **Action:**
if $timer_i$.ID $= 0$ **then**
    $maxError_i \leftarrow estimateError(positions_i)$;
    $delay_i \leftarrow \left[\left[\frac{maxError_i}{D}\right] + \left[1 - \frac{E_r}{E_t}\right] + R\right] T$;
    [Re]Start $timer_i(1,\ delay_i)$
else if $timer_i$.ID $= 1$ **then**
    $d'_i \leftarrow estimateError(\{positions_{i,j} : j \in references_i\})$;
    if $isEligible()$ **then**
        $isReference_i \leftarrow$ **true**;
        Send $REFERENCE(isReference_i,\ d'_i)$ to $N(i)$;
    [Re]Start $timer_i(2,\ delay_{max})$
else if $timer_i$.ID $= 2$ **then**
    $\forall positions_{i,j}, \forall d'_{i,j}, references_i \leftarrow \emptyset$
    $hasMinimum_i, sentHello_i \leftarrow$ **false**;
    [Re]Start $timer_i(3,\ T_R)$
    if $isReference_i =$ **false then** go to sleep;
else if $timer_i$.ID $= 3$ **then**
    wake up;
    $isReference_i \leftarrow$ **false**; $sentHello_i \leftarrow$ **true**;
    Send $HELLO(\hat{\mathbf{z}}_i)$ to $N(i)$;
    [Re]Start $timer_i(0,\ delay_{max})$

▷ **Input:**
PROCEDURE $isEligible()$.
▷ **Action:**
if $d'_i > D$ **then return true**;
for each $j \in N(i)$ **do**
    if $d'_{i,j} > D$ **or** $d'_{i,j} =$ null **then return true**;
return false;

6.3.1 Message Overhead Comparison

The first experiment compares the messaging overhead of repeated position estimation. We compare the number of messages exchanged as a single mobile node moves through the network recomputing its position, using information broadcasted by localized neighbours. We vary the minimum location error distance, D, and the localization probability, P, as described in the eligibility rule, and fixed average node density at 100. From Figure 6.2, it is seen that as the minimum distance is decreased or the minimum probability is increased more localization messages will occur. The reason for this is that in order to have location error bounded within a smaller distance with a high probability we require more reference nodes to remain active, resulting in more messages. In the most extreme case with $D = 5$, almost all nodes become references so we have nearly 100 messages per localization.

Figure 6.3 shows the average number of messages sent per localization as average node density is varied from 10 neighbours to 100. Different values of D and P are used, and are compared with the case where no sleep scheduling is used, along with the previous localization scheduling scheme in Chapter 4 which uses the minimum number of reference neighbours for the reference node eligibility rule. In this simulation, $\chi = 15$ was used as the minimum number of reference nodes for eligibility. It is seen from Figure 6.3 that with low node density, scheduling has minimal impact on message overhead. As the density is increased, without scheduling or with using the previous localization scheduling scheme the number of messages increases linearly. With the proposed localization scheduling scheme it is obverved that node density is much better controlled and the number of messages is nearly constant.

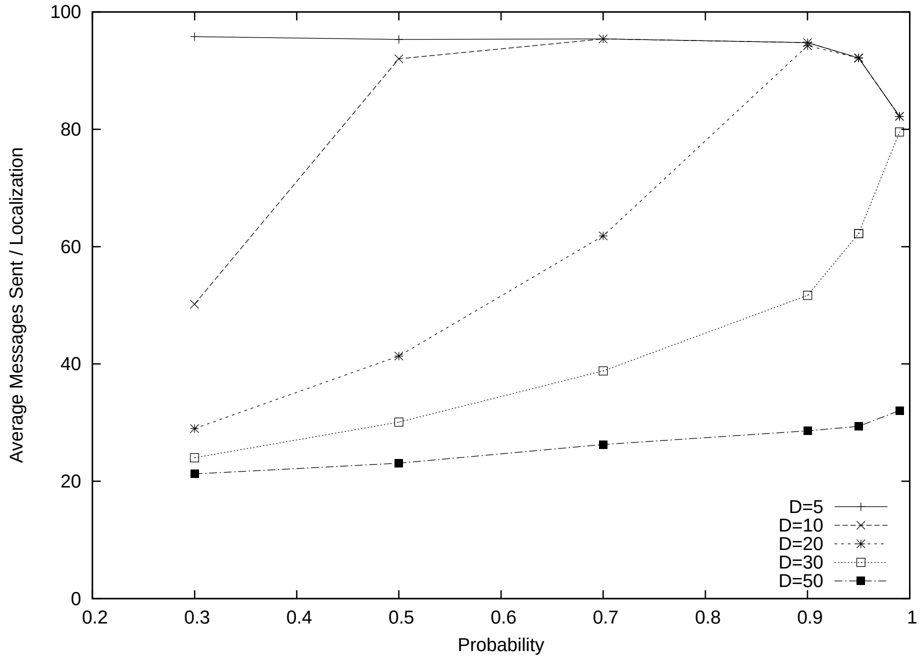

Figure 6.2: Average localization messages sent with different minimum error distances, D, and varying localization probabilities, P. Average node density is 100.

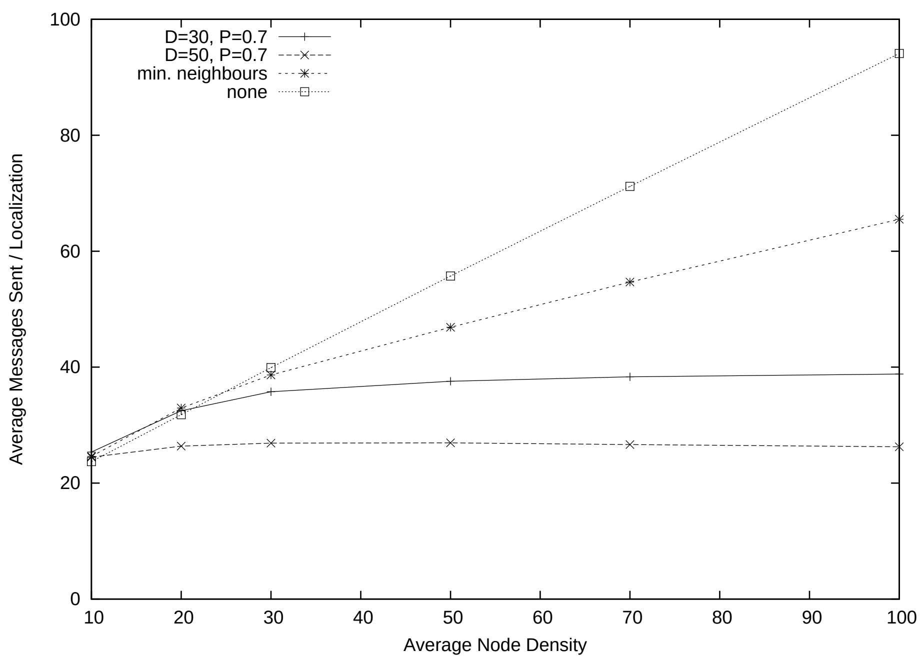

Figure 6.3: Average messages sent per localization with scheduling using location error estimation, minimum number of neighbours, and without scheduling.

6.3.2 Localization Accuracy

The average localization error over several thousand position updates of a mobile device is plotted against the localization probability P in Figure 6.4 for different minimum location error distances, D. As expected, with lower minimum error distances or higher probabilities less localization error is obtained. However, with very high values for P increased error is present, which is due to the location error estimator not working as well with higher probabilities as a result of the random nature of range estimates with RSS.

The effect on location error by varying node density is shown in Figure 6.5. With low network density, the accuracy is very similar with and without localization scheduling since nearly all nodes must remain active to maintain the minimum location error with high probability. As average node density is increased, error is increased slightly when localization scheduling is used, and is slightly higher than when the minimum neighbours scheme from Chapter 4 is used. However, the error difference is less than 10% even when the network has an average density of 100 which is marginal for many applications.

Although accuracy is better for unknown nodes initially when scheduling is not used, it comes at the cost of increased net energy usage by reference nodes. Figures 6.6 and 6.7 show localization accuracy of the mobile node over an extended period of time. With localization scheduling the moving target can be localized for much longer, and nodes run out of energy much more gradually. With less strict requirements on location error (with high D and low P) the moving target can be localized accurately for much longer than when the minimum neighbour localization scheduling scheme is used or when there is no scheduling at all.

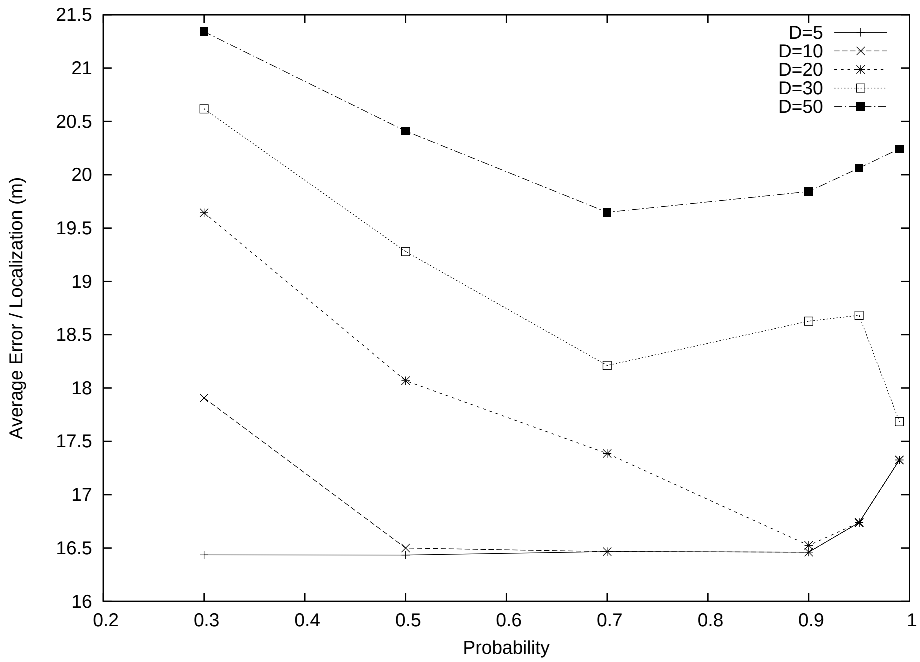

Figure 6.4: Average localization error with different minimum error distances, D, and varying localization probabilities, P. Average node density is 100.

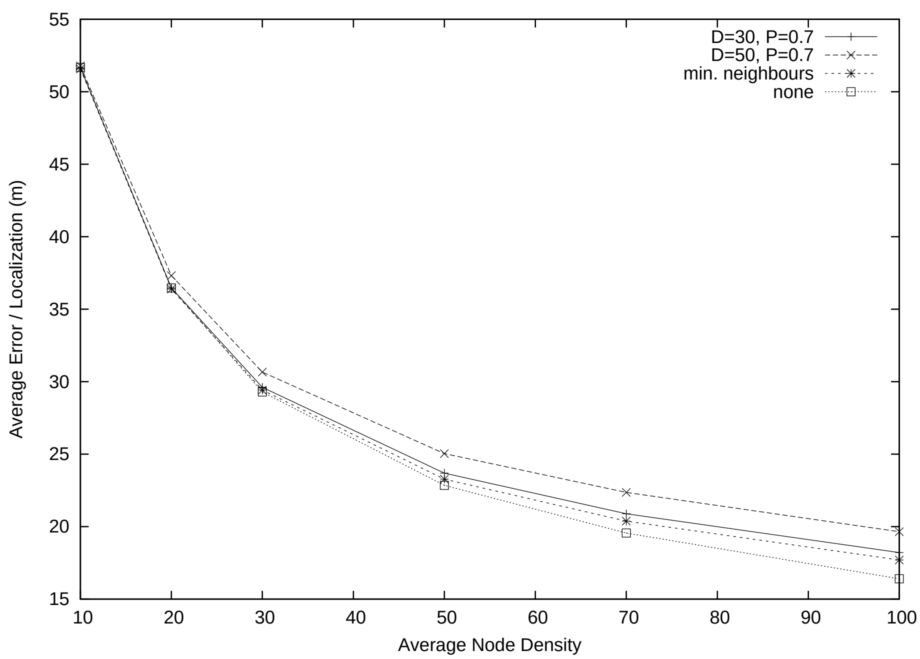

Figure 6.5: Average error per localization with scheduling using location error estimation, minimum number of neighbours, and without scheduling.

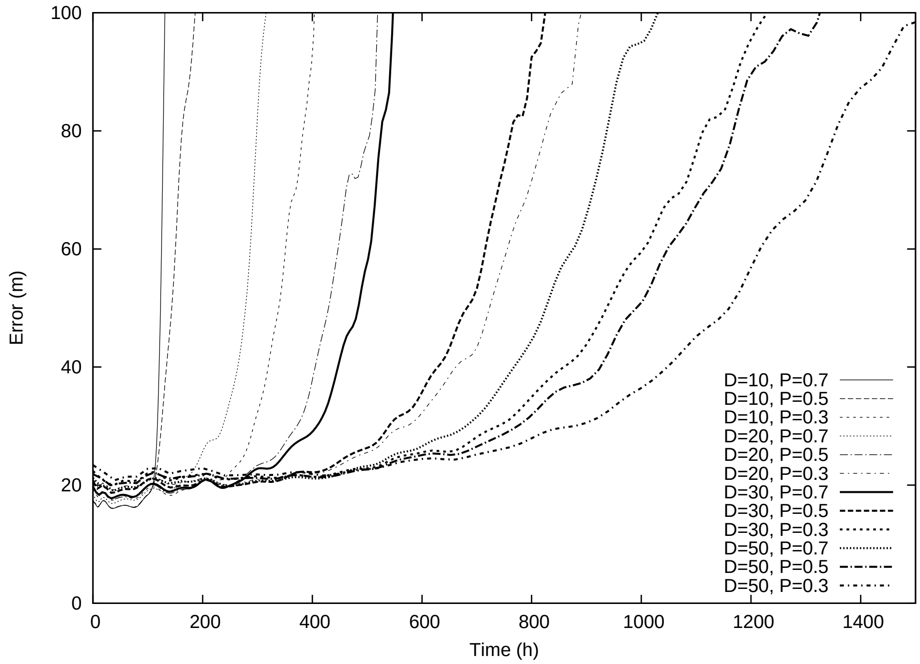

Figure 6.6: Localization error over time with with different minimum error distances, D. Localization probability, P, is 0.7, and average node density is 100.

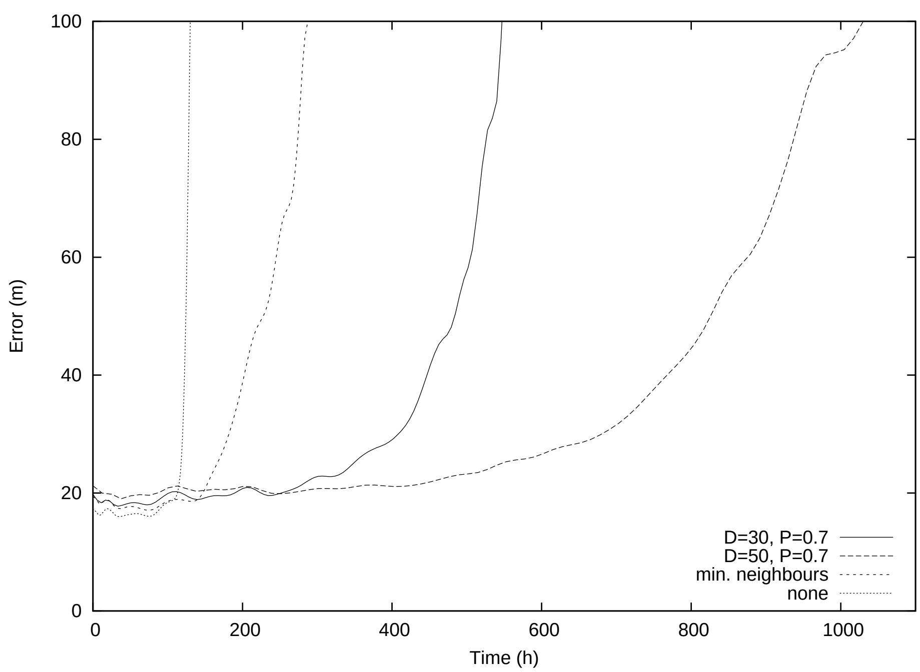

Figure 6.7: Localization error over time with scheduling using location error estimation, minimum number of neighbours, and without scheduling.

6.3.3 Network Lifetime

When nodes alternate between active and sleeping states mobile agents can be localized accurately for a much longer period of time. As seen in Figure 6.8, when the requirement on minimum location error is not tight (with high D and low P) we achieve network lifetimes which are substantially longer. In Figure 6.9, network lifetime in the proposed scheme is compared with the previous minimum neighbour localization scheduling scheme and with no sleep scheduling. Network lifetimes can exceed over 1000 hours with the new scheme while offering acceptable localization accuracy, which is several times longer than what was previously possible.

6.3.4 Localization Latency and Accuracy

Finally, we evaluate the effects of latency due to computational time required by location estimators, with and without localization scheduling. The idea is that with more data measurements the location estimator will take longer to compute, and so at high speeds these calculated positions will be obsolute before they are even available. As was seen in Figure 4.7, computational time increases linearly with increasing range measurements, which can become significant with higher movement speeds and scarce processing resources found in typical wireless devices. By limiting node density in a controlled way, we reduce the amount of information used to compute one's position to only the minimal necessary, reducing computation time and thus localization error in mobile scenarios.

We simulate the scenario of a mobile node moving at various speeds between 5 m/s and 35 m/s, updating its location once per minute. When the mobile node computes its position there will now be a delay given by Figure 4.7, which results in increasing error with computation time. Figure 6.10 shows the average error of the MLE and trilateration estimators with and without localization scheduling with an average node density of 100.

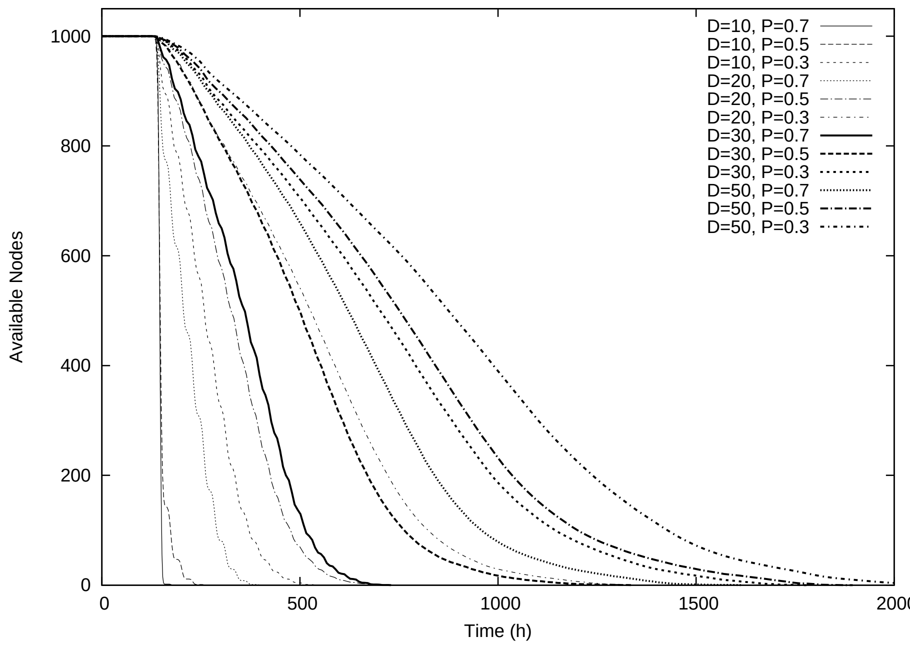

Figure 6.8: Remaining nodes with energy over time with different minimum error distances, D. Localization probability, P, is 0.7, and average node density is 100.

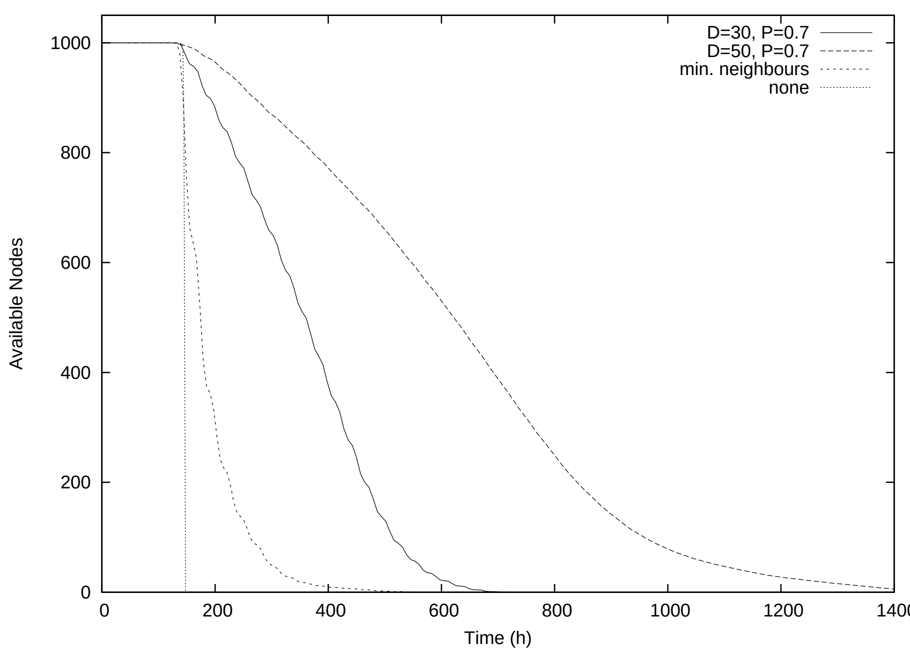

Figure 6.9: Remaining nodes with energy over time with scheduling using location error estimation, minimum number of neighbours, and without scheduling.

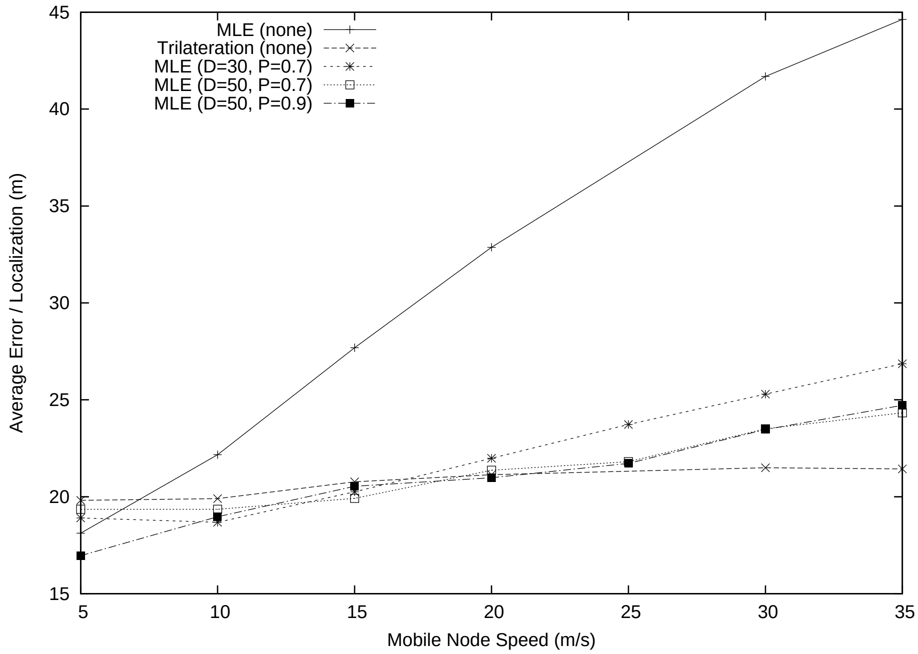

Figure 6.10: Localization error with MLE and trilateration estimators at varying speeds, with error contribution from computation latency.

Previously the more accurate MLE estimator is not practical in dense mobile networks due to accumulated error from increased computation times. However, at speeds below 20 m/s we achieve better localization accuracy than previously possible with trilateration using the MLE estimator when node density is controlled with the proposed scheme. At lower speeds, tighter error bounds (with higher values for D and lower values for P) result in lower location error, while decreasing D and increasing P results in better localization accuracy at higher speeds when computation time is more critical, since node density is further reduced.

6.4 Discussions

A scheduling scheme has been described which reduces localization messages and improves location accuracy over time by increasing network lifetimes. We make use of the method for location error estimation to ensure that sufficient reference devices are available to maintain accurate localization with high probability. Once the conditions for accurate localization are met, additional reference devices are not needed and enter sleep mode to conserve energy. Simulation results show that with increasing network density localization messages remain almost constant with the new scheme, while location accuracy is only marginally affected. Network lifetimes can be increased by over 10 times using the localization scheduling scheme, and is several times more effective than the previously proposed scheme which merely uses minimum connectivity information for scheduling decisions. As a result, unknown devices are able to estimate their positions for much longer. Furthermore, localization scheduling proves to be a viable tool for increasing localization accuracy in mobile ad hoc networks by reducing node density to reduce computational time for localization, helping to eliminate error due to latency.

Chapter 7

Coverage with Localization Error

7.1 Introduction

An important consideration in WSN is how well a region of interest is monitored by deployed sensors. Coverage protocols determine whether or not all points in a region are within sensing range of one or more devices. A prerequisite to many coverage protocols is knowledge of the geographic locations of sensors. These locations are usually obtained through the use of a localization system; however, associated with localization systems is often a significant amount of error in position estimates, which in turn can adversely affect the functioning of coverage schemes. When information is available on the inherent errors in location estimates, coverage protocols can be designed to be more robust to these errors for improved accuracy and effectiveness.

Most coverage protocols assume that devices have perfect position information available, or allow for slight location error to occur, showing a limited tolerance to location inaccuracy without explicitly handling it. A probabilistic coverage protocol was presented in [54], which ensures that an area is covered with a certain threshold probability. The scheme was shown to be robust to location inaccuracy; however the percentage of active sensors increases rapidly with increasing location error. A Voronoi diagram based sleep scheduling scheme was introduced in [31], where a node is a sleeping candidate if it is not on the coverage boundary and all of the Voronoi vertices of its one-hop neighbours are covered without it. Location estimates were assumed to be uniformly distributed in a circle located at the true positions, and the Voronoi sleep scheme was tolerant to varying degrees of location error. Finally the coverage scheme in [17] introduces the concept of 'wiggle room' to allow for minor location errors in a coverage scheme. However, no analytical method for determining the ideal amount wiggle room is discussed.

In this chapter, we investigate the problem of optimal coverage with sleep scheduling under the influence of location error present in practical WSN localization systems. Coverage and localization are two closely related problems in WSN, and by solving them together we are able to achieve higher coverage of a region of interest (ROI) using fewer devices than would be possible otherwise. The main contribution of the work in this chapter is a location error tolerant coverage scheme for node scheduling in WSN. We make use of the method for estimating the amount of localization error within a certain probability seen in Chapter 5, and ensure that coverage is maintained regardless of this estimated error. There are two approaches offered by the proposed algorithm, depending on the scenario. The optimistic approach assumes that location error effectively decreases the computed coverage level below its true amount, so nodes compensate by adjusting position estimates of their neighbours to be closer, increasing computed coverage thus resulting in fewer active devices. On the other hand, the conservative approach assumes that location error increases the computed coverage level, so nodes compensate by adjusting neighbouring position estimates to be further away, resulting in reduced computed coverage and reduced coverage holes since additional devices must remain active to cover the ROI. Simulation results show that we are able to reduce the percentage of active nodes and increase coverage, compared to schemes which do not inherently consider localization error.

7.2 Methods

7.2.1 Problem Statement

With the network model given in Chapter 2, the coverage problem is defined as follows.

Definition (Coverage): A point p is considered to be *covered* if it is less than s units away from at least one sensor in $\mathcal{N}$. A region Q is considered to be covered if every point $p \in Q$ is covered.

Definition (Coverage Problem): Given a set of nodes $\mathcal{N}$ in a region Q, where nodes $i \in \mathcal{N}$ have known positions $\mathbf{z}_i$, determine if every point $p \in Q$ is covered.

Numerous solutions to the coverage problem exist in the literature. In this work the proposed scheme is compared with the coverage protocol given by Huang et al. [62], which uses the notion of *perimeter coverage*, defined as follows.

Definition (Perimeter Coverage): Given two nodes $i, j \in \mathcal{N}$, a point p on the perimeter of the sensing range of i (i.e. $d_{i,p} = s$) is perimeter covered by j if it is within sensing range of j (i.e. $d(j, p) \leq s$). i is perimeter covered if all points on its perimeter are perimeter covered by nodes $j \in \mathcal{N}$, where $j \neq i$. It was proved in [61] that the entire area Q is covered if and only if each node in the network is perimeter covered. With this property, the optimal coverage protocol of [62] can be summarized with the following algorithm, executed by each device $i \in \mathcal{N}$, requiring only the location information of ones 2-hop neighbours.

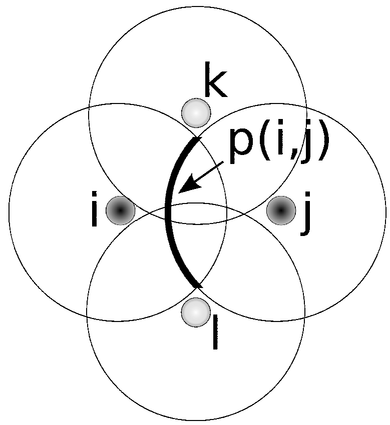

Figure 7.1: The perimeter of j in the sensing region of i, $p(i,j)$, is covered by k and l, so i is a candidate for j.

Algorithm 7.1 - Coverage Algorithm

---

1. For each neighbour j of i, let $p(i,j)$ be the perimeter of j which is within the sensing range of i. If $p(i,j)$ is covered by sensors other than i for all $j \in N(i)$, then i is a candidate.

2. If i is a candidate, wait for a random backoff time T_R. After T_R, if a sleeping request was heard, go back to 1). Otherwise broadcast a sleep request and wait for T_S.

3. Each $j \in N(i)$ sends a sleep grant to i if no other node $k \in N(j)$ has already sent a sleep request. Otherwise, send a sleep reject to i.

4. After T_S, if i receives a sleep grant from all $N(i)$, send a sleep confirm and go to sleep. Otherwise, send a withdraw message and return to 1).

An example of a candidate is shown in Figure 7.1. For brevity the details of computing perimeter coverage are not described here and the reader is referred to [62].

The vast majority of coverage protocols depend on location estimates as a prerequisite, and assume that all location information is completely accurate. The reality however, is that often large positioning errors are present in real world localization systems, especially when distance measurements from RSS are used. In this chapter we address problems caused by error in the location estimates used by coverage protocols, stated as follows.

Definition 5 (Coverage Problem with Location Error): Given a set of nodes $\mathcal{S} \cup \mathcal{B} \subseteq \mathcal{N}$ in Q, where nodes $i \in \mathcal{S}$ have estimated positions $\hat{\mathbf{z}}_i$ using a localization system, and $\boldsymbol{\varepsilon_i = \mathbf{z}_i - \hat{\mathbf{z}}_i > 0}$, determine if all points $p \in Q$ are covered.

7.2.2 Coverage With Location Error

When localization error is a factor, coverage schemes suffer from two main problems: the over wake-up problem, where more nodes remain active than are necessary to cover Q, resulting in excessive energy usage; and the problem of coverage holes in which Q is not sufficiently covered. Motivated by these issues, two approaches to the coverage problem with location error are proposed depending on the requirements of the scenario at hand: the optimistic approach which reduces active nodes, and the conservative approach which minimizes coverage holes.

7.2.3 Optimistic Approach

The primary goal of the optimistic approach to the coverage problem with location error is to reduce the number of active nodes as much as possible, while preventing coverage holes is a secondary objective. This approach is applicable for scenarios in which energy conservation is critical, while small gaps in total coverage percentage may be acceptable.

It is known that location estimates from localization systems have a certain level of error, so the main strategy of the optimistic approach is for nodes to assume that this error will cause more nodes to be active than are necessary for full coverage. Therefore, to compensate for this over wakeup nodes assume that neighbours are actually closer to each other than their estimated positions would reveal, so that the computed perimeter coverage would be higher in the first step of Algorithm 1, resulting in more candidates and thus more sleeping devices.

The distance at which nodes are assumed to be closer is given by the location error estimate $d'_i(p)$ from equation (5.11). This gives the estimated location error magnitude for a certain probability p, where p is an input parameter, and so this approach assumes that localization error causes nodes to be further apart than they really are by $d'_i(p)$.

The proposed scheme for optimistic coverage with location error begins by running the localization scheme, followed by exchanging location estimates between 1-hop neighbours in order to calculate $d'_i(p)$. Once calculated, the estimated locations and error estimates are then exchanged between 2-hop neighbourhoods. Algorithm 1 is then executed as before, but with the first step modified to use the following procedure.

Algorithm 7.2 - Optimistic Candidate Algorithm

PROCEDURE CheckIfCandidate(i):
  for each $j \in N(i)$ **do**
    for each $k \in N(j), k \neq i$ **do**
      $\theta_{j,k} \leftarrow \arctan\left(\frac{\hat{y}_j - \hat{y}_k}{\sqrt{(\hat{x}_j - \hat{x}_k)^2 + (\hat{y}_j - \hat{y}_k)^2 + (\hat{x}_j - \hat{x}_k)}}\right)$;
      $\hat{\mathbf{z}}'_k \leftarrow \hat{\mathbf{z}}_k - d'_k(p) \cdot (\sin(\theta_{j,k}),\cos(\theta_{j,k}))$;
      $Z'_j \leftarrow Z'_j \cup \hat{\mathbf{z}}'_k$;
    Calculate coverage of $p(i,j)$ using Z'_j;
  if $p(i,j)$ is covered for all $j \in N(i)$ **then**
    i is a candidate;

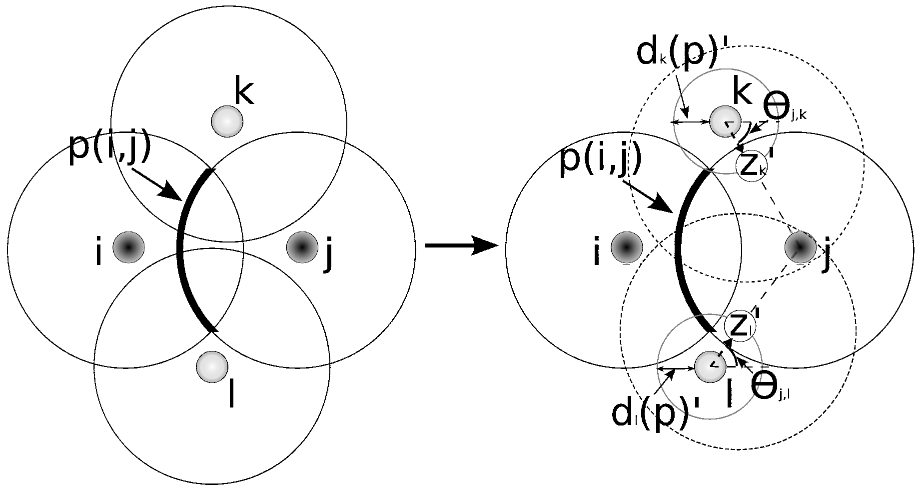

Figure 7.2: The perimeter of j in the sensing region of i, $p(i, j)$, is not originally covered by k and l, but by optimistically assuming that k and l are located at $\hat{\mathbf{z}}'_k$ and $\hat{\mathbf{z}}'_l$, respectively, $p(i, j)$ is covered, so i becomes a candidate for j.

On line 5 of Algorithm 2, the estimated position of k, $\hat{\mathbf{z}}_k$, is translated by $d'_k(p)$ units in the direction of $\hat{\mathbf{z}}_j$, which is given by the angle $\theta_{j,k}$ on line 4. The resulting translated positions, $\hat{\mathbf{z}}'_k$, are then used to calculate the perimeter coverage as usual on line 7. This is shown graphically in Figure 7.2.

7.2.4 Conservative Approach

Contrary to the optimistic approach, the conservative approach to the coverage problem with location error aims to reduce coverage holes as much as possible, while reducing active nodes is secondary. This is useful for applications in which high quality of service is critical and we cannot afford gaps in coverage, even at the cost of increased energy consumption.

The main idea of the conservative approach is that nodes assume that localization error will cause fewer nodes to become active than are necessary to cover Q. To compen-

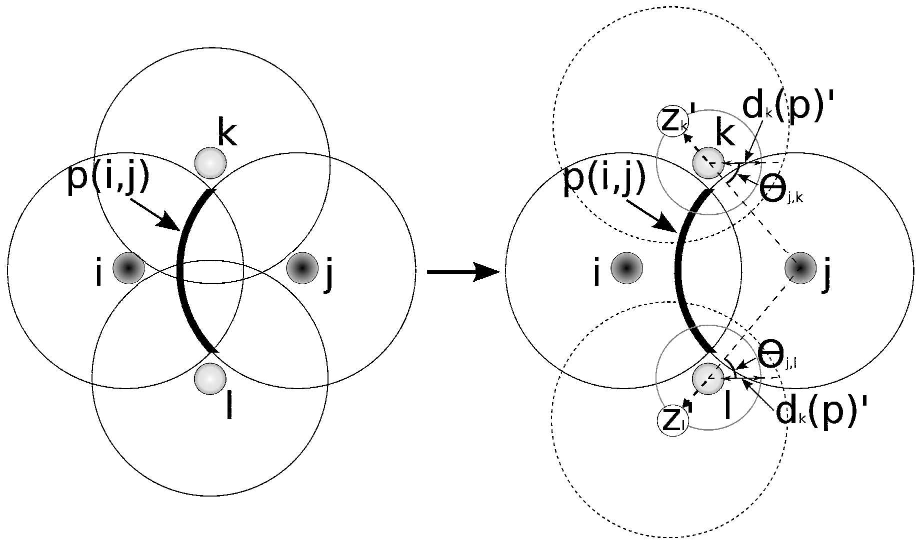

Figure 7.3: $p(i, j)$ is originally covered by k and l, but by conservatively assuming that k and l are located at $\hat{\mathbf{z}}'_k$ and $\hat{\mathbf{z}}'_l$, respectively, $p(i, j)$ is not covered, so i is no longer a candidate for j.

sate for this effect, the opposite action is taken from the optimistic approach. Distances between adjacent nodes are assumed to be further apart than estimated in order to reduce the apparent coverage level, causing additional nodes to become active, thus reducing coverage holes.

The algorithm for the conservative approach is identical to the optimistic, except that nodes are translated further away, rather than closer, by a distance of $d'_i(p)$. Therefore, we use the same algorithm listed in Algorithm 2, but change the sign on line 5 so that $\hat{\mathbf{z}}'_k = \hat{\mathbf{z}}_k + d'_k(p) \cdot (sin(\theta_{j,k}), cos(\theta_{j,k}))$. This is shown graphically in Figure 7.3.

7.3 Results

In this section simulation results are presented which evaluate the performance of the proposed coverage protocol. Implementation is done using *ns-2* and energy settings are based on the XBow IRIS XM2110CA [137]. For the localization scheme, An implementation similar to that in [126] was used. For the base coverage scheme, the protocol in [62] was implemented and modified it as described in the previous section. It should be noted that the proposed coverage algorithm should work with minor modification with any localization scheme, and any coverage scheme that requires location information. We use 200 nodes deployed randomly with a uniform distribution, each with a radio range and sensor range of 50 m, from which 20 beacon nodes are randomly selected. Average node density is varied by varying the size of the network field, Q.

The values for the coefficients a, b and c from equation (5.3) are obtained in the same way as previously seen, namely 10 random topologies were generated for average node densities between 15 and 40, and the localization procedure was run with 32 random seed values on each topology from which the least squares fitting procedure described in Chapter 5 is used to find values for a, b and c which allow the tightest fit between the localization error model of equation (5.3) with the the mean squared localization error.

We first explore the effect of varying the localization probability parameter p, given in equation (5.11), when running the coverage algorithm using both the optimistic and conservative approaches. The value of p is varied from 0.3 to 0.99, and the percentage of active nodes and percentage of coverage holes, averaged over 32 random topologies, are shown in Figures 7.4 and 7.5, respectively. As expected, there are fewer active nodes with the optimistic approach, while fewer coverage holes occur with the conservative approach. It is also noticed that with increasing the localization probability parameter, the number of active nodes decreases while coverage holes increase slightly for the conservative case, while the opposite occurs for the optimistic case. It is observed that the best trade-off between active nodes and coverage holes for the optimistic approach occurs when p is set in the mid range, from 0.5 to 0.7, while the optimal trade-off for the conservative approach occurs when p is as high as possible, namely $p = 0.99$.

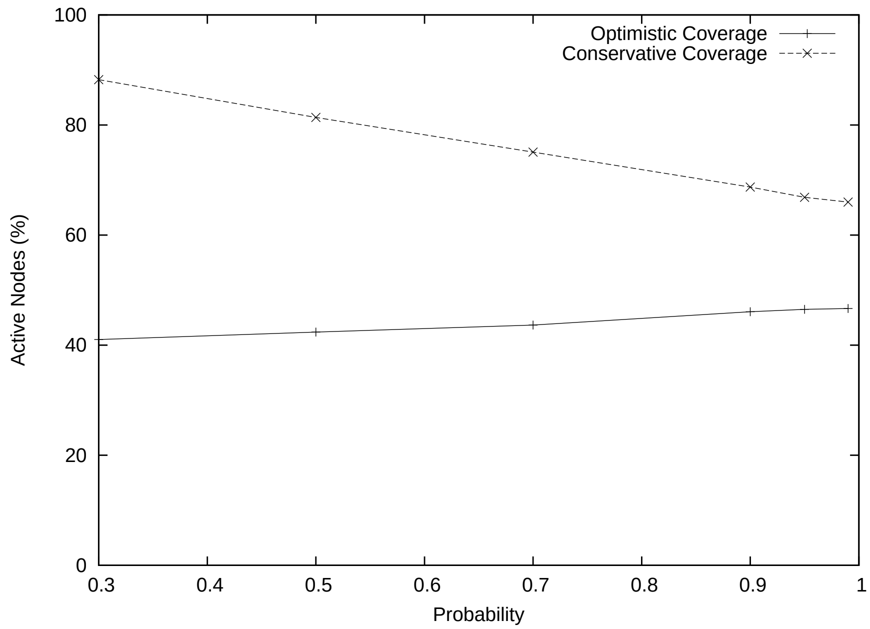

Figure 7.4: Active nodes vs. localization probability of optimistic and conservative schemes

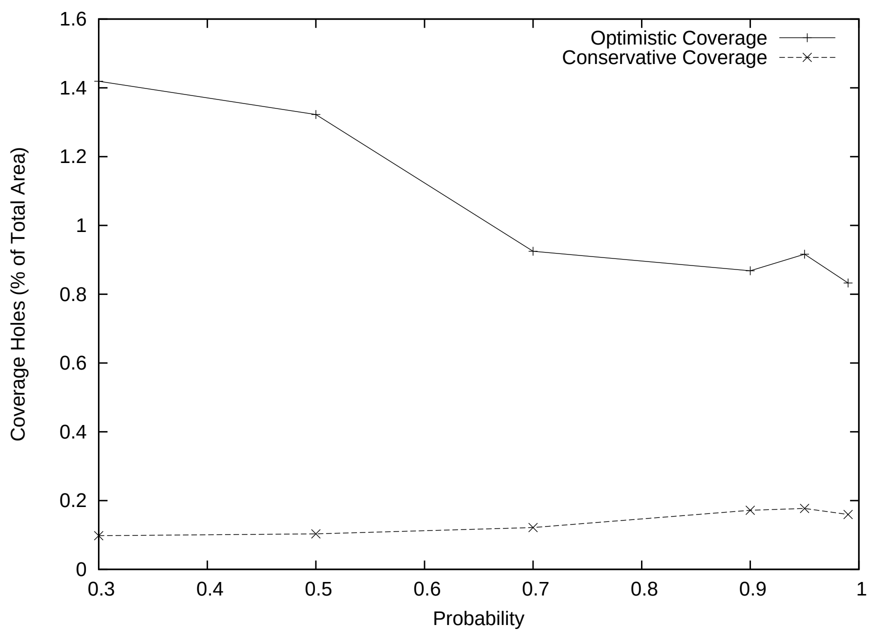

Figure 7.5: Coverage holes vs. localization probability of optimistic and conservative schemes

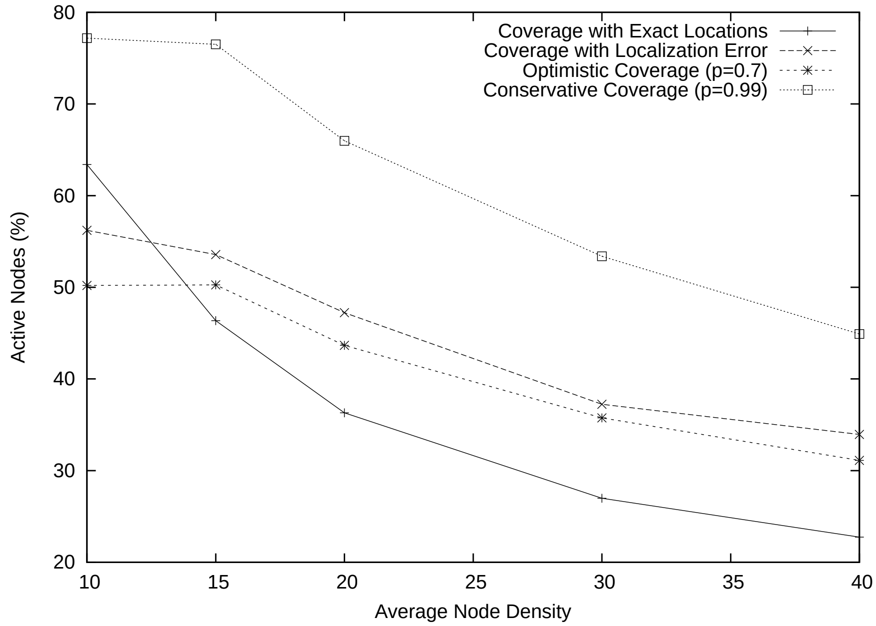

Figure 7.6: Active nodes vs. node density with different coverage schemes

We next vary average node density from 10 to 40 and compare active nodes and coverage holes between the unmodified coverage scheme without correction for localization error, and the optimistic and conservative approaches with localization error handling. We also compare the coverage scheme when exact locations are available, which serves as the best case scenario. The percentage of active nodes versus density is shown in Figure 7.6, while the percentage of coverage holes versus density is shown in Figure 7.7. It is observed that there are fewer active nodes with the optimistic approach than the standard coverage algorithm, while the percentage of coverage holes are nearly identical, especially when node density is high. On the other hand, when the conservative approach is used the number of active nodes is higher, but the percentage of coverage holes is extremely low, and is even lower than the ideal case when exact locations are known, especially for lower node densities.

Finally, we evaluate the performance of the proposed protocols over a prolonged

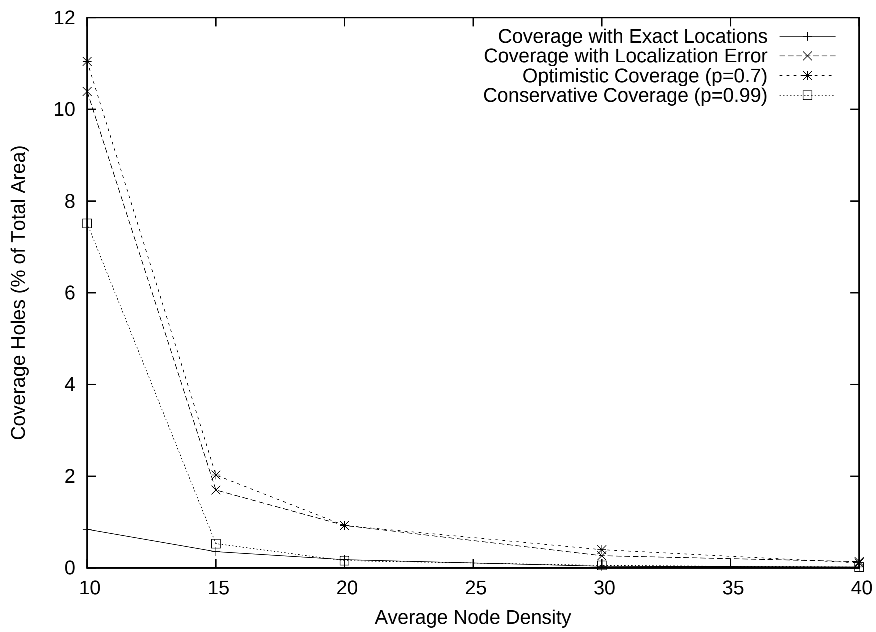

Figure 7.7: Coverage holes vs. node density with different coverage schemes

amount of time when the set of active nodes is rotated periodically. The rotation time was selected to be every 100000 seconds, after which time all devices with remaining energy will wake up and participate in another coverage election identical to the first. The percentage of devices which still have available energy over time is shown in Figure 7.8. After approximately 140 hours of operation a sudden decrease in available nodes is seen resulting from the first group of devices which run out of energy which have been active during all coverage rounds. After this point, nodes run out of energy gradually at an inversely exponential rate, with nodes running out of energy fastest with the conservative approach, while energy is expended more slowly with the optimistic approach than with the standard coverage protocol, and is improved when p is lower ($p = 0.5$).

Figures 7.9 and 7.10 show the percentage of active nodes and of coverage holes over time, respectively. It is observed from Figure 7.9 that there are more active nodes when the conservative approach is used, while fewer nodes are active with the optimistic

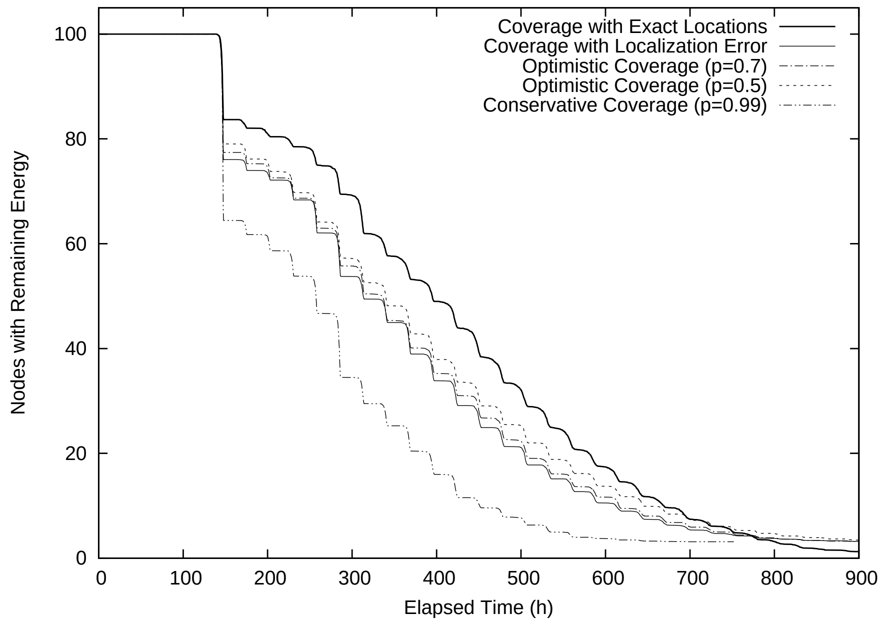

Figure 7.8: Percentage of nodes with remaining energy vs. time with different coverage schemes

approach, compared with standard coverage with no correction for localization error. As nodes begin to run out of energy one ends up with more active nodes in the optimistic approach. However, as can be seen in Figure 7.10, coverage holes remain lower for a longer period of time with the optimistic approach, while initially coverage holes are low with the conservative approach, but rapidly increase after 140 hours due to poor energy conservation.

7.4 Discussions

Coverage protocols in wireless sensor networks aim to determine if an entire region of interest is monitored by one or more sensors. In the majority of coverage protocols, nodes require accurate knowledge of their geographic locations. However, significant amounts of error are often present with localization systems, of which current coverage

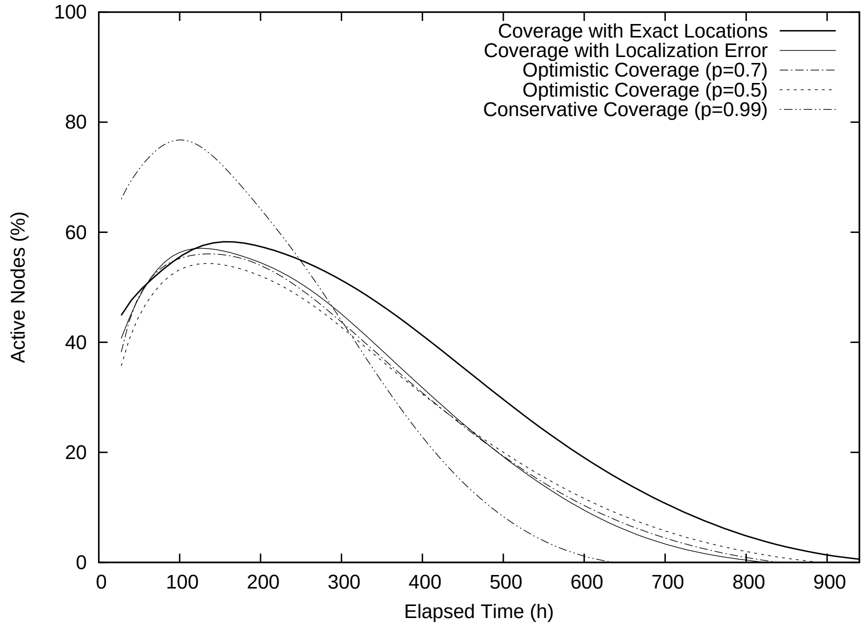

Figure 7.9: Active holes vs. time with different coverage schemes

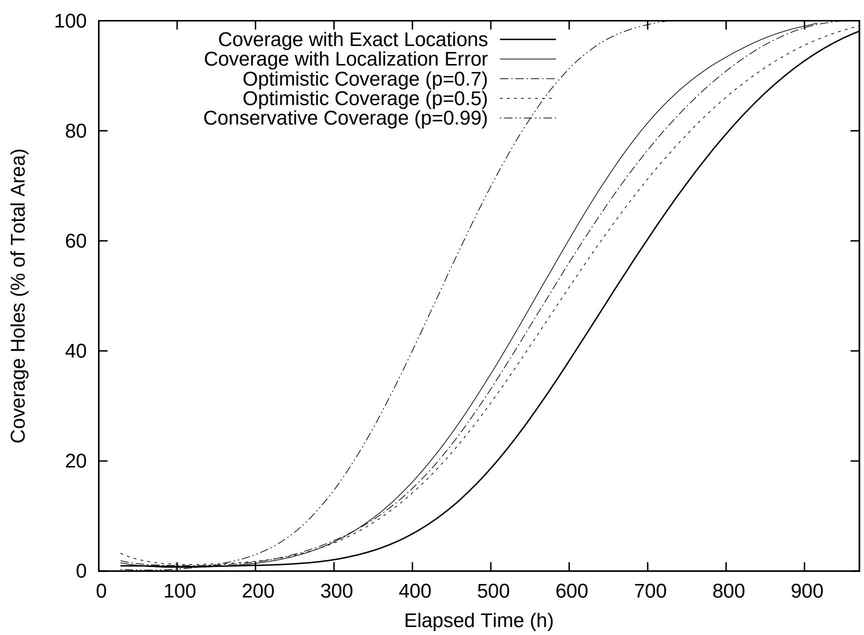

Figure 7.10: Coverage holes vs. time with different coverage schemes

schemes do not address. Two methods were proposed to deal with the over wakeup and coverage hole problems resulting from localization error in optimal coverage scheduling protocols. A technique was used to estimate the amount of location error within a given probability to find areas with high error. The optimistic approach to the coverage problem assumes that location error causes over wakeup of nodes, and manages this problem by reducing the number of active nodes. The conservative approach assumes that error generates increased coverage holes; thus more nodes become active in areas with higher location error. Simulation results show that with the optimistic approach active nodes are decreased by more than 5%, resulting in increased network lifetimes with negligible impact on coverage holes, while with the conservative approach coverage holes are greatly reduced to less than 1% with an increase in active nodes of less than 20%. Future work will explore dealing with location error for the k-coverage problem and for connectivity, and will attempt to combine aspects of the optimistic and conservative approaches to achieve the best of both schemes.

Chapter 8

Conclusions

8.1 Summary

In this thesis a number of schemes were proposed which utilize tools found in localization and coverage systems. Two solutions to the localization scheduling problem were put forth, which aim to reduce network density while maintaining high localization accuracy. The first solution relied on minimum connectivity conditions, while the second used a novel location error estimation scheme to ensure that the entire network can be localized with a high probability. The location error estimation method takes as input a minimum probability parameter and allows one to determine if a device at a given point can be localized to within certain accuracy level with that probability. In addition to the localization scheduling problem, location error estimation is applied to an optimal coverage preserving sleep scheduling scheme under the influence of positioning errors in order to avoid use of overly redundant sensors and to avoid coverage holes.

8.2 Discussions and Future Work

The main goal of this thesis was to investigate the relationship between localization and coverage to develop new solutions to these problems. This goal has been achieved, as was shown with a number of new schemes and methodologies. There are however a number of open research issues which remain to be explored.

Future work will investigate cluttered environments with numerous obstacles. In this thesis we have only concentrated on obstacle-free environments, but more sophisticated models involving NLOS and multipath propogation between devices due to obstacles will result in additional challenges, which can further ephasize the advantages of simultaneously considering coverage and localization.

Localization scheduling can be further explored in a number of ways. First of all, analysis of message collisions under the influence of high localization requests has not yet been studied. Secondly, while sleep scheduling was used in this thesis, transmission power is another parameter which can be adjusted to balance localization accuracy and energy usage. Finally, extensions of the proposed protocols to high mobility scenarios such as VANets are required, as this thesis only concentrated on the scenario of a single mobile device for simplicity.

More theoretical work is required to analyze the relationship between localization and coverage. Open questions include *with a given localization accuracy, what if anything can be directly said about the coverage level?* Also, *with a given level of coverage (or connectivity), what can be directly said about the localization accuracy?* Answers to these questions will allow for improvements to both localization and coverage by integrating results from opposing schemes.

Appendix A

Simulation Environment

A.1 Selection of Simulation Tools

There are a number of different tools which can be used to simulate the behavior of wireless networks, which can include MATLAB, OPNET, NetSim, JiST/SWANS, ns-2/ns-3 and others. For this thesis, the ns-2 networks simulator was selected [44] for the simulation of all protocols for a number of reasons, which can be summarized as follows.

- *Open source model:* ns-2 is an open source tool, meaning that it can be used free of charge, and all source code is available allowing for complete control of the system.
- *Support:* Detailed online documentation and an active online community of other academic users which are using ns-2 help to solve any problems which may arrise from using the simulation tool.
- *Previous work:* ns-2 is a well established tool by the academic community in the research of wireless networking protocols, including previous localization systems. Therefore, such prior work has already established that ns-2 can accurately simulate

real networks, and by using the same simulation environment as other research, the results presented in this thesis can be more closely compared with existing work.

Of course, ns-2 also has with it its own set of weaknesses, with the primary ones being as follows.

- *Learning curve:* ns-2 is a very large system with a great deal of complexity, and lacks much graphical user interface (GUI) support, making it a more difficult tool to learn than other systems such as OPNET and MATLAB.
- *Efficiency:* ns-2 uses a great deal of memory and computational resources, especially as networks become larger. It is therefore difficult to simulate networks with several thousands of wireless devices using ns-2. For such tasks, simulation tools such as JiST/SWANS give promising results.

In the end, by weighing the respective strengths and weakness of ns-2 it was deemed that it would be an acceptible solution for simulating wireless networks for the purposes of localization and coverage in this thesis.

A.2 Implementation Details

Implementation of the schemes presented in this thesis were done using a combination of C++ for programming the behavior of wireless nodes in ns-2, Tcl for scripting a wide variety scenarios, and Perl for performing extensive data analysis on expermal results obtained from ns-2. Core algorithms for both localization [35, 126] and coverage [62] were implemented, providing a solid base upon which to design new schemes. The scemes presented in this thesis were then implemented on top of these protocols. Extensive tests were generated with scripting languages, and were run on a 32-node cluster of quad-core

Pentium IV computers, with a total of 128 processing cores, such that an extremely high number of simulation runs could be performed for statistical averaging in a reasonable time frame.

Bibliography

[1] J.S. Abel. Optimal sensor placement for passive source localization. In *Acoustics, Speech, and Signal Processing, 1990. ICASSP-90., 1990 International Conference on*, pages 2927 –2930 vol.5, April 1990.

[2] Dawood Al-Abri and Janise McNair. On the interaction between localization and location verification for wireless sensor networks. *Computer Networks*, 52(14):2713 – 2727, 2008.

[3] N.A. Alsindi, B. Alavi, and K. Pahlavan. Measurement and modeling of ultrawideband toa-based ranging in indoor multipath environments. *Vehicular Technology, IEEE Transactions on*, 58(3):1046 –1058, 2009.

[4] Nayef Alsindi and Kaveh Pahlavan. Cooperative localization bounds for indoor ultra-wideband wireless sensor networks. *EURASIP J. Adv. Signal Process*, 2008:125:1–125:13, January 2008.

[5] D. Ampeliotis and K. Berberidis. Sorted order- k voronoi diagrams for model-independent source localization in wireless sensor networks. *Signal Processing, IEEE Transactions on*, 58(1):426 –437, 2010.

[6] J.N. Ash and R.L. Moses. On the relative and absolute positioning errors in self-localization systems. *Signal Processing, IEEE Transactions on*, 56(11):5668 –5679, 2008.

[7] Joshua N. Ash and Lee C. Potter. Sensor network localization via received signal strength measurements with directional antennas. In *in Proceedings of the 2004 Allerton Conference on Communication, Control, and Computing*, pages 1861–1870, 2004.

[8] J. Aspnes, T. Eren, D.K. Goldenberg, A.S. Morse, W. Whiteley, Y.R. Yang, B.D.O. Anderson, and P.N. Belhumeur. A theory of network localization. *Mobile Computing, IEEE Transactions on*, 5(12):1663 –1678, 2006.

[9] A. Baggio and K. Langendoen. Monte Carlo localization for mobile wireless sensor networks. *Ad Hoc Networks*, 6(5):718–733, 2008.

[10] P. Bahl and V.N. Padmanabhan. Radar: an in-building rf-based user location and tracking system. In *INFOCOM 2000. Nineteenth Annual Joint Conference of the IEEE Computer and Communications Societies. Proceedings. IEEE*, volume 2, pages 775 –784 vol.2, 2000.

[11] Pratik Biswas and Yinyu Ye. A distributed method for solving semidefinite programs arising from ad hoc wireless sensor network localization. In Panos Pardalos, William W. Hager, Shu-Jen Huang, Panos M. Pardalos, and Oleg A. Prokopyev, editors, *Multiscale Optimization Methods and Applications*, volume 82 of *Nonconvex Optimization and Its Applications*, pages 69–84. Springer US, 2006.

[12] A. Boukerche and X. Fei. Coverage protocols for detecting fully sponsored sensors in wireless sensor networks. In *Proceedings of the 3rd ACM international workshop*

on Performance evaluation of wireless ad hoc, sensor and ubiquitous networks, pages 58–65. ACM New York, NY, USA, 2006.

[13] A. Boukerche, H. Oliveira, EF Nakamura, and AAF Loureiro. Localization systems for wireless sensor networks. *Wireless Communications, IEEE*, 14(6):6–12, 2007.

[14] A. Boukerche, H.A.B.F. Oliveira, E.F. Nakamura, and A.A.F. Loureiro. A Voronoi Approach for Scalable and Robust DV-Hop Localization System for Sensor Networks. In *Computer Communications and Networks, 2007. ICCCN 2007. Proceedings of 16th International Conference on*, pages 497–502, 2007.

[15] A. Boukerche, H.A.B.F. Oliveira, E.F. Nakamura, and A.A.F. Loureiro. Vehicular ad hoc networks: a new challenge for localization-based systems. *Computer Communications*, 31(12):2838–2849, 2008.

[16] Azzedine Boukerche, Horacio A.B.F. Oliveira, Eduardo F. Nakamura, and Antonio A.F. Loureiro. Vehicular ad hoc networks: A new challenge for localization-based systems. *Computer Communications*, 31(12):2838 – 2849, 2008. Mobility Protocols for ITS/VANET.

[17] T. Brown, D. Sarioz, A.B. Noy, T. La Porta, and D. Verma. Full coverage of a region allowing inexact placement of sensors. In *First Annual Conference of the International Technology Alliance*, 2007.

[18] M. Bshara, U. Orguner, F. Gustafsson, and L. Van Biesen. Fingerprinting localization in wireless networks based on received-signal-strength measurements: A case study on wimax networks. *Vehicular Technology, IEEE Transactions on*, 59(1):283 –294, 2010.

[19] N. Bulusu, J. Heidemann, and D. Estrin. GPS-less low-cost outdoor localization for very small devices. *Personal Communications, IEEE*, 7(5):28–34, 2000.

[20] S. Capkun, M. Hamdi, and J.P. Hubaux. GPS-free Positioning in Mobile Ad Hoc Networks. *Cluster Computing*, 5(2):157–167, 2002.

[21] A. Catovic and Z. Sahinoglu. The cramer-rao bounds of hybrid toa/rss and tdoa/rss location estimation schemes. *Communications Letters, IEEE*, 8(10):626 – 628, 2004.

[22] A. Cenedese, G. Ortolan, and M. Bertinato. Low-density wireless sensor networks for localization and tracking in critical environments. *Vehicular Technology, IEEE Transactions on*, 59(6):2951 –2962, 2010.

[23] J. Chaffee and J. Abel. Gdop and the cramer-rao bound. In *Position Location and Navigation Symposium, 1994., IEEE*, pages 663 –668, April 1994.

[24] F. Chan and H.C. So. Efficient weighted multidimensional scaling for wireless sensor network localization. *Signal Processing, IEEE Transactions on*, 57(11):4548 –4553, 2009.

[25] F. Chan, H.C. So, and W.-K. Ma. A novel subspace approach for cooperative localization in wireless sensor networks using range measurements. *Signal Processing, IEEE Transactions on*, 57(1):260 –269, 2009.

[26] Y.W.E. Chan and Boon Soong Hee. Achievable error bounds on localization with wireless sensor networks. In *Wireless Communications, Networking and Mobile Computing, 2009. WiCom '09. 5th International Conference on*, pages 1 –4, 2009.

[27] G. Chandrasekaran, M.A. Ergin, Jie Yang, Song Liu, Yingying Chen, M. Gruteser, and R.P. Martin. Empirical evaluation of the limits on localization using signal

strength. In *Sensor, Mesh and Ad Hoc Communications and Networks, 2009. SECON '09. 6th Annual IEEE Communications Society Conference on*, pages 1 –9, 2009.

[28] G. Chandrasekaran, M.A. Ergin, Jie Yang, Song Liu, Yingying Chen, M. Gruteser, and R.P. Martin. Empirical evaluation of the limits on localization using signal strength. In *Sensor, Mesh and Ad Hoc Communications and Networks, 2009. SECON '09. 6th Annual IEEE Communications Society Conference on*, pages 1 –9, 2009.

[29] Cheng Chang and Anant Sahai. Cramer-rao-type bounds for localization. *EURASIP J. Appl. Signal Process.*, 2006:166–166, January 2006.

[30] B. Chen, K. Jamieson, H. Balakrishnan, and R. Morris. Span: An Energy-Efficient Coordination Algorithm for Topology Maintenance in Ad Hoc Wireless Networks. *Wireless Networks*, 8(5):481–494, 2002.

[31] Xinyu Chen, Michael R. Lyu, and Ping Guo. Voronoi-based sleeping configuration in wireless sensor networks with location error. In *ICNSC*, pages 1459–1464, 2008.

[32] Y.-C. Cheng and T.G. Robertazzi. Critical connectivity phenomena in multihop radio models. *Communications, IEEE Transactions on*, 37(7):770 –777, July 1989.

[33] Robert Connelly. Generic global rigidity. *Discrete Computational Geometry*, 33:549–563, 2005. 10.1007/s00454-004-1124-4.

[34] J.A. Costa, N. Patwari, and A.O. Hero III. Distributed weighted-multidimensional scaling for node localization in sensor networks. *ACM Transactions on Sensor Networks (TOSN)*, 2(1):39–64, 2006.

[35] D. Niculescu and B. Nath. Ad hoc positioning system (aps). *in Proceedings of GLOBECOM, San Antonio*, 2001.

[36] Antonio A. D'Amico, Umberto Mengali, and Lorenzo Taponecco. Toa estimation with the ieee 802.15.4a standard. *Wireless Communications, IEEE Transactions on*, 9(7):2238 –2247, 2010.

[37] F. Daneshgaran, M. Laddomada, and M. Mondin. Connection between system parameters and localization probability in network of randomly distributed nodes. *Wireless Communications, IEEE Transactions on*, 6(12):4383–4389, 2007.

[38] H.A.B.F. de Oliveira, E.F. Nakamura, A.A.F. Loureiro, and A. Boukerche. Localization in Time and Space for Sensor Networks. *Proceedings of the 21st International Conference on Advanced Networking and Applications*, pages 539–546, 2007.

[39] Horacio Antonio Braga Fernandes de Oliveira, Azzedine Boukerche, Eduardo Freire Nakamura, and Antonio Alfredo Ferreira Loureiro. An efficient directed localization recursion protocol for wireless sensor networks. *IEEE Transactions on Computers*, 58:677–691, 2009.

[40] G. Destino and G.T.F. De Abreu. Weighing strategy for network localization under scarce ranging information. *Wireless Communications, IEEE Transactions on*, 8(7):3668 –3678, 2009.

[41] L. Doherty, K.S.J. Pister, and L.E. Ghaoui. Convex position estimation in wireless sensor networks. *IEEE Infocom*, 3:1655–1663, 2001.

[42] M.I. Doroslovacki and E.G. Larsson. Nonuniform linear antenna arrays minimising cramer-rao bounds for joint estimation of single source range and direction of arrival. *Radar, Sonar and Navigation, IEE Proceedings* -, 152(4):225 – 231, 2005.

[43] T. Eren, O.K. Goldenberg, W. Whiteley, Y.R. Yang, A.S. Morse, B.D.O. Anderson, and P.N. Belhumeur. Rigidity, computation, and randomization in network localization. In *INFOCOM 2004. Twenty-third AnnualJoint Conference of the IEEE Computer and Communications Societies*, volume 4, pages 2673 – 2684 vol.4, 2004.

[44] Kevin Fall and Kannan Varadhan. The ns Manual. `http://www.isi.edu/nsnam/ns/doc/ns_doc.pdf`.

[45] V. Fox, J. Hightower, Lin Liao, D. Schulz, and G. Borriello. Bayesian filtering for location estimation. *Pervasive Computing, IEEE*, 2(3):24 – 33, 2003.

[46] A. Gasparri and F. Pascucci. An interlaced extended information filter for self-localization in sensor networks. *Mobile Computing, IEEE Transactions on*, 9(10):1491 –1504, 2010.

[47] J. Gribben and A. Boukerche. Coverage with Localization Error in Wireless Sensor Networks. In *Unpublished Manuscript*, 2010.

[48] J. Gribben and A. Boukerche. Probabilistic estimation of location error in wireless ad hoc networks. In *GLOBECOM 2010, 2010 IEEE Global Telecommunications Conference*, pages 1 –5, 2010.

[49] J. Gribben, A. Boukerche, and R. Pazzi. Scheduling for scalable energy-efficient localization in mobile ad hoc networks. In *Sensor Mesh and Ad Hoc Communications and Networks (SECON), 2010 7th Annual IEEE Communications Society Conference on*, pages 1 –9, 2010.

[50] Jeremy Gribben and Azzedine Boukerche. Localization scheduling in wireless ad hoc networks. In *Local Computer Networks (LCN), 2010 IEEE 35th Conference on*, pages 512 –519, 2010.

[51] Yanying Gu, A. Lo, and I. Niemegeers. A survey of indoor positioning systems for wireless personal networks. *Communications Surveys Tutorials, IEEE*, 11(1):13 –32, 2009.

[52] I. Guvenc and Chia-Chin Chong. A survey on toa based wireless localization and nlos mitigation techniques. *Communications Surveys Tutorials, IEEE*, 11(3):107 –124, 2009.

[53] Tian He, Chengdu Huang, Brian M. Blum, John A. Stankovic, and Tarek Abdelzaher. Range-free localization schemes for large scale sensor networks. In *Proceedings of the 9th annual international conference on Mobile computing and networking*, MobiCom '03, pages 81–95, New York, NY, USA, 2003. ACM.

[54] M. Hefeeda and H. Ahmadi. A probabilistic coverage protocol for wireless sensor networks. In *IEEE International Conference on Network Protocols, 2007. ICNP 2007*, pages 41–50, 2007.

[55] M. Hernandez, B. Ristic, A. Farina, and L. Timmoneri. A comparison of two crame acute;r-rao bounds for nonlinear filtering with pd¡1. *Signal Processing, IEEE Transactions on*, 52(9):2361 – 2370, 2004.

[56] M.L. Hernandez. Performance bounds for gmti tracking. In *Information Fusion, 2003. Proceedings of the Sixth International Conference of*, 2003.

[57] M.L. Hernandez, A. Farina, and B. Ristic. Pcrlb for tracking in cluttered environments: measurement sequence conditioning approach. *Aerospace and Electronic Systems, IEEE Transactions on*, 42(2):680 – 704, 2006.

[58] Jeffrey Hightower and Gaetano Borriello. Particle filters for location estimation in ubiquitous computing: A case study. In Nigel Davies, Elizabeth Mynatt, and Itiro Siio, editors, *UbiComp 2004: Ubiquitous Computing*, volume 3205 of *Lecture Notes in Computer Science*, pages 88–106. Springer Berlin / Heidelberg, 2004.

[59] A.K.M.M. Hossain and Wee-Seng Soh. Cramer-rao bound analysis of localization using signal strength difference as location fingerprint. In *INFOCOM, 2010 Proceedings IEEE*, pages 1 –9, 2010.

[60] L. Hu and D. Evans. Localization for mobile sensor networks. In *Proceedings of the 10th annual int. conference on Mobile computing and networking*, pages 45–57. ACM New York, NY, USA, 2004.

[61] C.F. Huang and Y.C. Tseng. The Coverage Problem in a Wireless Sensor Network. *Mobile Networks and Applications*, 10(4):519–528, 2005.

[62] C.F. Huang, Y.C. Tseng, and H.L. Wu. Distributed protocols for ensuring both coverage and connectivity of a wireless sensor network. *ACM Transactions on Sensor Networks (TOSN)*, 3(1), 2007.

[63] A.T. Ihler, III Fisher, J.W., R.L. Moses, and A.S. Willsky. Nonparametric belief propagation for self-localization of sensor networks. *Selected Areas in Communications, IEEE Journal on*, 23(4):809 – 819, 2005.

[64] Bill Jackson and Tibor Jordn. Connected rigidity matroids and unique realizations of graphs. *Journal of Combinatorial Theory, Series B*, 94(1):1 – 29, 2005.

[65] Donald J. Jacobs and Bruce Hendrickson. An algorithm for two-dimensional rigidity percolation: The pebble game. *Journal of Computational Physics*, 137(2):346 – 365, 1997.

[66] R. Janaswamy. Angle and time of arrival statistics for the gaussian scatter density model. *Wireless Communications, IEEE Transactions on*, 1(3):488 –497, July 2002.

[67] X. Ji and H. Zha. Sensor positioning in wireless ad-hoc sensor networks using multidimensional scaling. *INFOCOM 2004. Twenty-third AnnualJoint Conference of the IEEE Computer and Communications Societies*, 4, 2004.

[68] Lirong Jian, Zheng Yang, and Yunhao Liu. Beyond triangle inequality: Sifting noisy and outlier distance measurements for localization. In *INFOCOM, 2010 Proceedings IEEE*, pages 1 –9, 2010.

[69] G.J. Jordt, R.O. Baldwin, J.F. Raquet, and B.E. Mullins. Energy cost and error performance of range-aware, anchor-free localization algorithms. *Ad Hoc Networks*, 6(4):539–559, 2008.

[70] DB Jourdan, D. Dardari, and MZ Win. Position error bound for UWB localization in dense cluttered environments. *Aerospace and Electronic Systems, IEEE Transactions on*, 44(2):613–628, 2008.

[71] D.B. Jourdan, Jr. Deyst, J.J., M.Z. Win, and N. Roy. Monte carlo localization in dense multipath environments using uwb ranging. In *Ultra-Wideband, 2005. ICU 2005. 2005 IEEE International Conference on*, pages 314 – 319, 2005.

[72] D.B. Jourdan and N. Roy. Optimal sensor placement for agent localization. *ACM Transactions on Sensor Networks (TOSN)*, 4(3):13, 2008.

[73] K. Kaemarungsi and P. Krishnamurthy. Modeling of indoor positioning systems based on location fingerprinting. In *INFOCOM 2004. Twenty-third AnnualJoint Conference of the IEEE Computer and Communications Societies*, volume 2, pages 1012 – 1022 vol.2, 2004.

[74] A.A. Kannan, B. Fidan, and Guoqiang Mao. Analysis of flip ambiguities for robust sensor network localization. *Vehicular Technology, IEEE Transactions on*, 59(4):2057 –2070, May 2010.

[75] A.A. Kannan, Guoqiang Mao, and B. Vucetic. Simulated annealing based wireless sensor network localization with flip ambiguity mitigation. In *Vehicular Technology Conference, 2006. VTC 2006-Spring. IEEE 63rd*, volume 2, pages 1022 –1026, May 2006.

[76] L.M. Kaplan. Global node selection for localization in a distributed sensor network. *Aerospace and Electronic Systems, IEEE Transactions on*, 42(1):113 – 135, 2006.

[77] S.M. Kay. *Fundamentals of statistical signal processing: estimation theory*. Prentice-Hall Signal Processing Series, 1993.

[78] Eunchan Kim and Kiseon Kim. Distance estimation with weighted least squares for mobile beacon-based localization in wireless sensor networks. *Signal Processing Letters, IEEE*, 17(6):559 –562, 2010.

[79] L. Kleinrock and J. Silvester. Optimum transmission radii for packet radio networks or why six is a magic number. In *Proceedings of the IEEE National Telecommunications Conference*, volume 4, pages 1–4. Birimingham, Alabama, 1978.

[80] Jia-Chun Kuo and Wanjiun Liao. Wlc12-6: Estimation errors of hop-count based localization in wireless sensor networks. In *Global Telecommunications Conference, 2006. GLOBECOM '06. IEEE*, 27 2006.

[81] Jia-Chun Kuo and Wanjiun Liao. Hop count distribution of multihop paths in wireless networks with arbitrary node density: Modeling and its applications. *Vehicular Technology, IEEE Transactions on*, 56(4):2321 –2331, 2007.

[82] V. Lakafosis and M.M. Tentzeris. From single-to multihop: The status of wireless localization. *Microwave Magazine, IEEE*, 10(7):34 –41, 2009.

[83] G. Laman. On graphs and rigidity of plane skeletal structures. *Journal of Engineering Mathematics*, 4:331–340, 1970. 10.1007/BF01534980.

[84] E.G. Larsson. Cramer-rao bound analysis of distributed positioning in sensor networks. *Signal Processing Letters, IEEE*, 11(3):334 – 337, 2004.

[85] N. Levanon. Lowest gdop in 2-d scenarios. *Radar, Sonar and Navigation, IEE Proceedings -*, 147(3):149 –155, June 2000.

[86] X. Li and D.K. Hunter. Probabilistic model of triangulation. In *Proceedings of the 2008 ACM symposium on Solid and physical modeling*, pages 301–306. ACM New York, NY, USA, 2008.

[87] Xinrong Li. Collaborative localization with received-signal strength in wireless sensor networks. *Vehicular Technology, IEEE Transactions on*, 56(6):3807 –3817, 2007.

[88] D. Lieckfeldt, J. You, and D. Timmermann. Distributed Selection of References for Localization in Wireless Sensor Networks. In *Positioning, Navigation and Communication, 2008. WPNC 2008. 5th Workshop on*, pages 31–36, 27 March 2008.

[89] D. Lieckfeldt, Jiaxi You, and D. Timmermann. An algorithm for distributed beacon selection. In *Pervasive Computing and Communications, 2008. PerCom 2008. Sixth Annual IEEE International Conference on*, pages 318 –323, 2008.

[90] Dawei Liu, Moon-Chuen Lee, and Dan Wu. A node-to-node location verification method. *Industrial Electronics, IEEE Transactions on*, 57(5):1526 –1537, May 2010.

[91] Hui Liu, H. Darabi, P. Banerjee, and Jing Liu. Survey of wireless indoor positioning techniques and systems. *Systems, Man, and Cybernetics, Part C: Applications and Reviews, IEEE Transactions on*, 37(6):1067 –1080, 2007.

[92] Yunhao Liu, Zheng Yang, Xiaoping Wang, and Lirong Jian. Location, localization, and localizability. *Journal of Computer Science and Technology*, 25:274–297, 2010. 10.1007/s11390-010-9324-2.

[93] Konrad Lorincz and Matt Welsh. Motetrack: a robust, decentralized approach to rf-based location tracking. *Personal and Ubiquitous Computing*, 11:489–503, 2007. 10.1007/s00779-006-0095-2.

[94] D. Ma, M. J. Er, and B. Wang. Analysis of hop-count-based source-to-destination distance estimation in wireless sensor networks with applications in localization. *Vehicular Technology, IEEE Transactions on*, 59(6):2998 –3011, 2010.

[95] S. MacLean and S. Datta. A lower bound on range-free node localization algorithms. In *Wireless Communication Systems. 2008. ISWCS '08. IEEE International Symposium on*, pages 628 –632, 2008.

[96] H.K. Maheshwari, A.H. Kemp, and B. Peng. Localization performance comparison using optimal and sub-optimal lateration in wsns. In *Communications, 2009. APCC 2009. 15th Asia-Pacific Conference on*, pages 842 –845, 2009.

[97] A. Mainwaring, D. Culler, J. Polastre, R. Szewczyk, and J. Anderson. Wireless sensor networks for habitat monitoring. In *Proc. 1st ACM int. workshop on Wireless sensor networks and applications*, pages 88–97. ACM, 2002.

[98] Guoqiang Mao, BarIs Fidan, and Brian D.O. Anderson. Wireless sensor network localization techniques. *Computer Networks*, 51(10):2529 – 2553, 2007.

[99] Sonia Martnez and Francesco Bullo. Optimal sensor placement and motion coordination for target tracking. *Automatica*, 42(4):661 – 668, 2006.

[100] M. Mauve, A. Widmer, and H. Hartenstein. A survey on position-based routing in mobile ad hoc networks. *IEEE network*, 15(6):30–39, 2001.

[101] S. Meguerdichian, F. Koushanfar, M. Potkonjak, and M.B. Srivastava. Coverage problems in wireless ad hoc sensor networks. In *IEEE INFOCOM*, volume 3, pages 1380–1387, 2001.

[102] S. Meguerdichian, F. Koushanfar, G. Qu, and M. Potkonjak. Exposure in wireless Ad-Hoc sensor networks. In *Proceedings of the 7th annual international conference on Mobile computing and networking*, pages 139–150. ACM New York, NY, USA, 2001.

[103] Honglei Miao, Kegen Yu, and M.J. Juntti. Positioning for nlos propagation: Algorithm derivations and cramer-rao bounds. In *Acoustics, Speech and Signal Processing, 2006. ICASSP 2006 Proceedings. 2006 IEEE International Conference on*, volume 4, page IV, May 2006.

[104] L. Mihaylova, D. Angelova, D. Bull, and N. Canagarajah. Localization of mobile nodes in wireless networks with correlated in time measurement noise. *Mobile Computing, IEEE Transactions on*, 10(1):44 –53, 2011.

[105] David Moore, John Leonard, Daniela Rus, and Seth Teller. Robust distributed network localization with noisy range measurements. In *Proceedings of the 2nd international conference on Embedded networked sensor systems*, SenSys '04, pages 50–61, New York, NY, USA, 2004. ACM.

[106] R.L. Moses, D. Krishnamurthy, and R. Patterson. An auto-calibration method for unattended ground sensors. In *Acoustics, Speech, and Signal Processing, 1993. ICASSP-93., 1993 IEEE International Conference on*, volume 3, page III, 2002.

[107] Radhika Nagpal, Howard Shrobe, and Jonathan Bachrach. Organizing a global coordinate system from local information on an ad hoc sensor network. In Feng Zhao and Leonidas Guibas, editors, *Information Processing in Sensor Networks*, volume 2634 of *Lecture Notes in Computer Science*, pages 553–553. Springer Berlin / Heidelberg, 2003.

[108] Eduardo F. Nakamura, Antonio A. F. Loureiro, and Alejandro C. Frery. Information fusion for wireless sensor networks: Methods, models, and classifications. *ACM Comput. Surv.*, 39, September 2007.

[109] J. Neering, C. Fischer, M. Bordier, and N. Maizi. Optimal sensor configuration for passive position estimation. In *Position, Location and Navigation Symposium, 2008 IEEE/ION*, pages 951 –960, May 2008.

[110] M. Nicoli and D. Fontanella. Fundamental performance limits of toa-based cooperative localization. In *Communications Workshops, 2009. ICC Workshops 2009. IEEE International Conference on*, pages 1 –5, 2009.

[111] Dragoş Niculescu and Badri Nath. Error characteristics of ad hoc positioning systems (aps). In *Proceedings of the 5th ACM international symposium on Mobile ad hoc networking and computing*, MobiHoc '04, pages 20–30, New York, NY, USA, 2004. ACM.

[112] R.W. Ouyang, A.K.-S. Wong, and Chin-Tau Lea. Received signal strength-based wireless localization via semidefinite programming: Noncooperative and cooperative schemes. *Vehicular Technology, IEEE Transactions on*, 59(3):1307 –1318, 2010.

[113] L.R. Paradowski. Uncertainty ellipses and their application to interval estimation of emitter position. *Aerospace and Electronic Systems, IEEE Transactions on*, 33(1):126 –133, 1997.

[114] B.W. Parkinson and J.J. Spilker. *Global Positioning System: Theory and Applications*. Aiaa, 1996.

[115] N. Patwari, J.N. Ash, S. Kyperountas, III Hero, A.O., R.L. Moses, and N.S. Correal. Locating the nodes: cooperative localization in wireless sensor networks. *Signal Processing Magazine, IEEE*, 22(4):54 – 69, 2005.

[116] N. Patwari, A.O. Hero, M. Perkins, N.S. Correal, and R.J. O'Dea. Relative location estimation in wireless sensor networks. *IEEE Transactions on Signal Processing*, 51(8):2137–2148, 2003.

[117] N. Patwari and R.J.Y. Wang. Relative location in wireless networks. *Vehicular Technology Conference (VTC 2001)*, 2, 2001.

[118] MS Phatak, S.T. Inc, and CA San Jose. Recursive method for optimum GPS satellite selection. *Aerospace and Electronic Systems, IEEE Transactions on*, 37(2):751–754, 2001.

[119] D. Porcino and W. Hirt. Ultra-wideband radio technology: potential and challenges ahead. *Communications Magazine, IEEE*, 41(7):66 – 74, 2003.

[120] N.B. Priyantha, A. Chakraborty, and H. Balakrishnan. The Cricket location-support system. In *Conference on Mobile computing and networking (MOBICOM)*, pages 32–43. ACM, 2000.

[121] Yihong Qi and H. Kobayashi. Cramer-rao lower bound for geolocation in non-line-of-sight environment. In *Acoustics, Speech, and Signal Processing, 1993. ICASSP-93., 1993 IEEE International Conference on*, volume 3, page III, 2002.

[122] Yihong Qi, H. Kobayashi, and H. Suda. Analysis of wireless geolocation in a non-line-of-sight environment. *Wireless Communications, IEEE Transactions on*, 5(3):672 – 681, 2006.

[123] T. Rappaport. Wireless Communications: Principles and Practice. 2001.

[124] B. Ristic, S. Arulampalam, and N. Gordon. *Beyond the Kalman filter: Particle filters for tracking applications.* Artech House Publishers, 2004.

[125] H. Rowaihy, S. Eswaran, M. Johnson, D. Verma, A. Bar-Noy, T. Brown, and T. La Porta. A survey of sensor selection schemes in wireless sensor networks. In *Proceedings of SPIE*, volume 6562, page 65621A, 2007.

[126] C. Savarese, K. Langendoen, and J. Rabaey. Robust Positioning Algorithms for Distributed Ad-Hoc Wireless Sensor Networks. *USENIX Technical Annual Conference*, pages 317–328, 2002.

[127] A. Savvides, W.L. Garber, R.L. Moses, and M.B. Srivastava. An analysis of error inducing parameters in multihop sensor node localization. *IEEE Transactions on Mobile Computing*, 4(6):567–577, 2005.

[128] A. Savvides, H. Park, and M.B. Srivastava. The n-Hop Multilateration Primitive for Node Localization Problems. *Mobile Networks and Applications*, 8(4):443–451, 2003.

[129] J.B. Saxe. *Embeddability of weighted graphs in k-space is strongly NP-hard*. Carnegie-Mellon University, Dept. of Computer Science, 1980.

[130] J. Scharcanski, A.B. de Oliveira, P.G. Cavalcanti, and Y. Yari. A particle-filtering approach for vehicular tracking adaptive to occlusions. *Vehicular Technology, IEEE Transactions on*, 60(2):381 –389, 2011.

[131] R. Schubert, M. Schlingelhof, H. Cramer, and G. Wanielik. Accurate positioning for vehicular safety applications - the safespot approach. In *Vehicular Technology Conference, 2007. VTC2007-Spring. IEEE 65th*, pages 2506 –2510, 2007.

[132] Y. Shang, W. Ruml, Y. Zhang, and M. Fromherz. Localization from connectivity in sensor networks. *IEEE Transactions on parallel and distributed systems*, pages 961–974, 2004.

[133] Yuan Shen and M.Z. Win. Fundamental limits of wideband localization - part i: A general framework. *Information Theory, IEEE Transactions on*, 56(10):4956 –4980, 2010.

[134] Yuan Shen, H. Wymeersch, and M.Z. Win. Fundamental limits of wideband localization - part ii: Cooperative networks. *Information Theory, IEEE Transactions on*, 56(10):4981 –5000, 2010.

[135] F. Sottile and M.A. Spirito. Robust localization for wireless sensor networks. In *Sensor, Mesh and Ad Hoc Communications and Networks, 2008. SECON '08. 5th Annual IEEE Communications Society Conference on*, pages 46 –54, 2008.

[136] N. Swangmuang and P. Krishnamurthy. Location fingerprint analyses toward efficient indoor positioning. In *Pervasive Computing and Communications, 2008. PerCom 2008. Sixth Annual IEEE International Conference on*, pages 100 –109, 2008.

[137] Crossbow Technology. XBow IRIS XM2110CA Datasheet. September 11, 2008. November 30, 2009. <http://www.xbow.com/Products/Product_pdf_files/Wireless_pdf/IRIS_Datasheet.pdf>

[138] O. Tekdas and V. Isler. Sensor placement for triangulation-based localization. *Automation Science and Engineering, IEEE Transactions on*, 7(3):681 –685, 2010.

[139] D. Tian and N.D. Georganas. A coverage-preserving node scheduling scheme for large wireless sensor networks. In *First ACM Int. Workshop on Wireless Sensor Networks and Applications*, volume 41, 2002.

[140] D.J. Torrieri. Statistical theory of passive location systems. *Aerospace and Electronic Systems, IEEE Transactions on*, AES-20(2):183 –198, 1984.

[141] Serdar Vural and Eylem Ekici. Probability distribution of multi-hop-distance in one-dimensional sensor networks. *Computer Networks*, 51(13):3727 – 3749, 2007.

[142] Jing Wang, R. Ghosh, and Sajal Das. A survey on sensor localization. *Journal of Control Theory and Applications*, 8:2–11, 2010.

[143] X. Wang, G. Xing, Y. Zhang, C. Lu, R. Pless, and C. Gill. Integrated coverage and connectivity configuration in wireless sensor networks. In *Proceedings of the 1st international conference on Embedded networked sensor systems*, pages 28–39. ACM New York, NY, USA, 2003.

[144] Yun Wang, Xiaodong Wang, Demin Wang, and D.P. Agrawal. Range-free localization using expected hop progress in wireless sensor networks. *Parallel and Distributed Systems, IEEE Transactions on*, 20(10):1540 –1552, 2009.

[145] He-Wen Wei, Rong Peng, Qun Wan, Zhang-Xin Chen, and Shang-Fu Ye. Multidimensional scaling analysis for passive moving target localization with tdoa and fdoa measurements. *Signal Processing, IEEE Transactions on*, 58(3):1677 –1688, 2010.

[146] A.J. Weiss and J.S. Picard. Network localization with biased range measurements. *Wireless Communications, IEEE Transactions on*, 7(1):298 –304, 2008.

[147] Y. Xu, J. Heidemann, and D. Estrin. Geography-informed energy conservation for Ad Hoc routing. *Proceedings of the 7th annual international conference on Mobile computing and networking*, pages 70–84, 2001.

[148] Zheng Yang and Yunhao Liu. Quality of trilateration: Confidence-based iterative localization. *Parallel and Distributed Systems, IEEE Transactions on*, 21(5):631 –640, May 2010.

[149] Zheng Yang, Yunhao Liu, and Xiang-Yang Li. Beyond trilateration: On the localizability of wireless ad hoc networks. *Networking, IEEE/ACM Transactions on*, 18(6):1806 –1814, 2010.

[150] R. Yarlagadda, I. Ali, N. Al-Dhahir, and J. Hershey. GPS GDOP metric. In *Radar, Sonar and Navigation, IEEE Proceedings*, volume 147, pages 259–264, 2000.

[151] K. Yu and Y.J. Guo. Anchor-free localisation algorithm and performance analysis in wireless sensor networks. *Communications, IET*, 3(4):549 –560, 2009.

[152] K. Yu, Y.J. Guo, and M. Hedley. Toa-based distributed localisation with unknown internal delays and clock frequency offsets in wireless sensor networks. *Signal Processing, IET*, 3(2):106 –118, 2009.

[153] Kegen Yu. 3-d localization error analysis in wireless networks. *Wireless Communications, IEEE Transactions on*, 6(10):3472 –3481, 2007.

[154] Yingpei Zeng, Jiannong Cao, Jue Hong, Shigeng Zhang, and Li Xie. Secure localization and location verification in wireless sensor networks: a survey. *The Journal of Supercomputing*, pages 1–17, 2010.

[155] Chongming Zhang, Xi Zhou, Chuanshan Gao, and Chunmei Wang. On improving the precision of localization with gross error removal. In *Distributed Computing Systems Workshops, 2008. ICDCS '08. 28th International Conference on*, pages 144 –149, 2008.

[156] Shigeng Zhang, Jiannong Cao, Yingpei Zeng, Zhuo Li, Lijun Chen, and Daoxu Chen. On accuracy of region based localization algorithms for wireless sensor networks. *Computer Communications*, 33(12):1391 – 1403, 2010.

[157] Yuan Zhou, Choi Look Law, Yong Liang Guan, and F. Chin. Indoor elliptical localization based on asynchronous uwb range measurement. *Instrumentation and Measurement, IEEE Transactions on*, 60(1):248 –257, 2011.